Research on Construction of Electronic Tongue Combining Nanomaterials and Machine Learning Algorithms for COD Determination and Anxiolytic Herbal Medicinal Products Analysis

Qing Wang

UAB
Universitat Autònoma de Barcelona

Research on Construction of Electronic Tongue Combining Nanomaterials and Machine Learning Algorithms for COD Determination and Anxiolytic Herbal Medicinal Products Analysis

Qing Wang

Doctoral Thesis

Doctoral Studies in Chemistry

Director: Prof. Manel del Valle Zafra

Department of Chemistry

September 2023

To feel and experience,
to explore your life.

路漫漫其修远兮，

吾将上下而求索。

Declaration

Thesis submitted to aspire for the doctoral degree of Qing Wang.

Qing Wang

Director's approval:

Pro. Manel del Valle Zafra

Bellaterra, 20 September 2023

Funding support

The present thesis work has been carried out in the laboratory of the Group of Sensors and Biosensors of Chemistry Department in Universitat Autònoma de Barcelona. Researches were financially supported by the Spanish Ministry of Science and Innovation, MICINN (Madrid) through project PID2019-107102RB-C21C and PID2019-107102RB-C22 funded by MCIN/AEI/10.13039/501100011033, as well as the Generalitat of Catalunya (Project 2021SGR00006 and Project 2021SGR00124). The doctorate fellowship was supported by China Scholarship Council.

Group of Sensors and Biosensors

Universitat Autònoma de Barcelona

China Scholarship Council

Generalitat de Catalunya

Ministry of Economy and Innovation (Spain)

Acknowledgements

How time flies! Around 5 years have passed from the first day I settled down in Barcelona, a city I had never imagined that I would come to before the year 2018. The land at Barcelona opened a new chapter of my life and this city witnessed most important moments. Looking back, although it was not all joy, I am still very grateful for everything I met in this journey.

First of all, I would like to express my appreciation to my supervisor, Manel del Valle. I am grateful to him for providing me this good opportunity for PhD study. During these years, I learned a lot from him, not only research skills or academic knowledge, but also precious quality of his personal characters, kindness, responsibility, open-mindedness and inclusiveness. He is very serious and responsible on work and scientific research, and meticulous on guiding students. Working with him is an enjoyable experience. Furthermore, he is very concerned about us and willing to provide us help whenever we need. Briefly, I am really grateful for his support and understanding during these years, which means a lot to me and gives me courage and warmth to face all difficulties.

I also want to thank my colleagues, my lovely friends, Anna, Marta, Dioni, Mingyue, Munmi and Xavi. I am happy for having these years with them. Especially thanks to Anna, Marta and Dioni for accompanying me to the hospital for examination, which is very important and means a lot to my life. In addition, I would like to thank the teachers from Department of Chemical Engineering and Analytical Chemistry, Universitat de Barcelona, Jose Manuel, Núria and Clara. I am lucky for having this chance to work with them for some months and grateful for the kind advice and suggestions from them. Also, I am willing to acknowledge the help received from Diana Losantos Velasco, from the Department of Chemical, Biological and Environmental Engineering,

Universitat Autònoma de Barcelona, for the help of the determination of COD values using commercial cuvette reagents.

Also, I want to thank my boyfriend. We met and fell in love in Barcelona, where our daughter was born in the year 2020, during the coronavirus pandemic, a very tough period to people all over the world. However, she made that difficult moments become precious, sweet and warm to us. We parents, are becoming more and more mature and powerful when accompany in her side, sharing the bitter and the sweet in her growth. Then I would like to thank my parents for their endless love, support and encouragement, which make me better and stronger. I love them forever.

Most importantly, I would like to thank my motherland, China, and the China Scholarship Council for providing me this precious opportunity and fundamental financial support for study abroad.

In one word, these past five years during my PhD study are extraordinary. I really appreciate all the concerns, support and help!

Qing Wang

Bellaterra, September 2023

Summary

Owing to advantages, low cost, high sensitivity and selectivity, rapidness, easy operation and transportability, electrochemical sensors and biosensors involving nanomaterials have been accepted as an effective and promising analytical method for environment monitoring, pharmaceutical analysis, medical diagnosis, food safety etc., over the past decades. However, this difficulty of improving performance of traditional sensors, like selectivity and sensitivity, led to the concept of electronic tongues (ETs) as an alternative strategy to solve such problems. These biomimetic systems, composed of low selectivity sensor arrays, can acquire added value from the generation of the analytical information containing cross-response features.

In this thesis, three voltammetric ET arrays were constructed composed of copper-based electrodes modified with CuO nanoparticles in an electrodeposition procedure and some graphite-epoxy composite (GEC) electrodes incorporating several catalytic nanoparticles. The first ET was demonstrated the potential of evaluating wastewaters according to the difficulty of electrochemical oxidation and help estimated the accuracy of found COD values detected by prepared sensor. The second ET employed an artificial neural network (ANN) model by combining the responses obtained from five sensors and compensating the differences in the voltammetric responses to two COD standard substances, glucose and glycine. This ET showed promising application of COD determination with better performance compared with single sensor utilizing classic calibration curve method.

The third ET array, combined with principal component analysis (PCA), was able to evaluate the components in terms of contents, herb varieties for mental calming products of different forms, which indicated its potential function on product evaluation, characterization and quality control.

TABLE OF CONTENTS

ABBREVIATIONS

Abbreviations

ET	Electronic tongue
GEC	Graphite-epoxy composite
ANN	Artificial neural network
PCA	Principal component analysis
IUPAC	International Union of Pure and Applied Chemistry
EN	Electronic nose
CV	Cyclic voltammetry
LSV	Linear sweep voltammetry
SWV	Square wave voltammetry
DPV	Differential pulse voltammetry
EIS	Electrochemical impedance spectroscopy
SPE	Screen-printed electrode
AI	Artificial intelligence
ML	Machine learning
SL	Supervised learning

UL	Unsupervised learning
SSL	Semi-supervised learning
RL	Reinforcement learning
DL	Deep learning
SVM	Support vector machine
***k*-NN**	*k*-nearest neighbour
NPs	Nanoparticles
COD	Chemical oxygen demand
BOD	Biochemical oxygen demand
SS	Suspended solids
IUPAC	International Union of Pure and Applied Chemistry
FAS	Ferrous ammonium sulfate
FTIR	Fourier transform infrared
ICP-OES	Inductively coupled plasma optical emission spectrometry
WE	Working electrode
RE	Reference electrode
CE	Counter electrode
PLS	Partial least squares
OCD	Obsessive-compulsive disorder
RSD	Relative standard deviation
KHP	Potassium hydrogen phthalate
LOD	Limit of detection
RMSE	Root mean square error

CHAPTER 1 INTRODUCTION

1 Introduction

1.1 Chemical sensor and sensor array

1.1.1 Concepts and basic principles

A sensor, in simple terms, is the extended ability for human to get information by sensing stimulus. Sensors are the technological counterparts, and are widely used for monitoring different stimulus depending on certain purpose. The development of science and technology have extended the applications of sensors to many fields, such as industrial production, marine exploration, environmental monitoring, medical diagnosis, etc. Obviously, sensors are an integral part of everyday our lives. Countries all over the world attach great importance to the development of sensors' manufacture and application. Briefly, a sensor is a device that produces an output through transducer by converting the received stimulus signals. The stimulus might be acoustic, biological, chemical, electrical, optical, mechanical, thermal changes

or radiation, etc [1].

Chemical sensors are an important subclass of sensors. As the International Union of Pure and Applied Chemistry (IUPAC) proposed in 1991, a chemical sensor is "a device that transforms chemical information, ranging from the concentration of a specific sample component to total composition analysis, into an analytically useful signal" [2]. The chemical information means the chemical stimulus, which may originate from a chemical reaction of the analyte(s) or from a physical property of the system investigated [2]. From the constructure perspective, a chemical sensor is usually composed of two basic functional units: a receptor part and a transducer part. If the receptor is, e.g., DNA, antibodies, enzymes, etc.), the device is referred to as a biosensor. In some cases, some sensors may include a separator, for example, a membrane. The receptor part plays a role of transforming information into a form of energy that can be measured by the transducer. The transducer part is a device that transforms the energy into a useful and analytically measurable signal [2–4].

The principles of the chemical sensors are based on the interaction between receptor and target analytes, which are also the basics of recognition events. Then the interaction behaviour can be converted into a measurable output signal, which will be converted into a readable value by transducer. The sensing principle of chemical sensors are illustrated in Figure 1.1. It is crucial to obtain a high specificity for the target analyte in presence of interfering chemical species to decrease inaccuracy. Generally, both chemical sensors can be categorized into catalytic or affinity-based devices. Catalytic chemical sensors conduct recognition based on catalytic activity, for example, redox reactions. The affinity-based devices rely on highly specific interactions between the receptor and analyte, e.g., host-guest interactions [5]. Depending on the transducer type used in recognition events, chemical sensors can be classified into optical, gravimetric, electrochemical, etc.

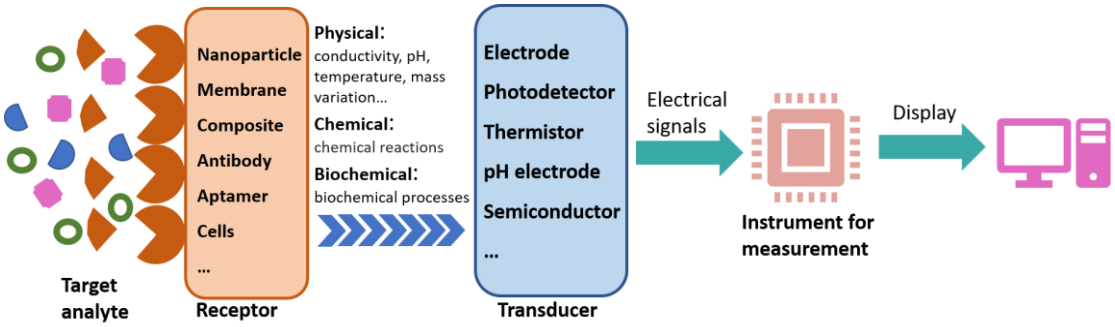

Figure 1.1 Schematic diagram illustrating principles of a chemical sensor.

Chemical sensors have attracted lot of attention because of its simplicity of the analytical procedure, fast measurements, simple sample preparation, low cost and transportability of instrumentation and promise in automatization. Generally, traditional sensors are designed based on the "lock-and-key" strategy for detecting specific analytes, but sometimes they can be affected by potential problems of interferences [6]. However, in practical applications, chemical sensors are often hindered by inadequate selectivity or specificity in multicomponent samples or media. To address this problem, on one hand, sensors should be modified with new materials or technologies to improve their performance. On the other hand, available partially selective or cross-sensitive sensors can be used in series for multicomponent analysis. This sensors in series are always called sensor arrays, which can generate complex outputs when respond to several substances in the multicomponent condition. Interpretation of such complex outputs through multivariate data analysis or pattern recognition techniques can extract lots of hidden useful information. Evidently, these sensors should have different sensitivity and selectivity patterns to produce added value from cross information [7]. The rationale for application of low-selective sensors is based on an analogy to biological organization of the olfactory and taste systems in mammals. There are millions of nonspecific receptors in nose and tongue that can respond to different substances present in the gas and liquid phases. Inspired by this, low-selective

sensor arrays can be used for producing analytically useful signals during the analysis of multicomponent matrices, such as the systems of electronic tongue (ET) and electronic nose (EN) that are used for liquids and gases analysis, respectively [8–10].

As reported from IUPAC, the application of sensor arrays consists of two main factors. Firstly, a sensor array comprises a certain number of nonspecific, low-selective chemical sensors. The second one is the application of multivariate data analysis or pattern recognition techniques, including artificial neural network (ANN), principal component analysis (PCA), etc., for processing high-dimension signals produced by the sensor arrays [10]. The mechanism of the function of a sensor array is shown in Figure 1.2 below.

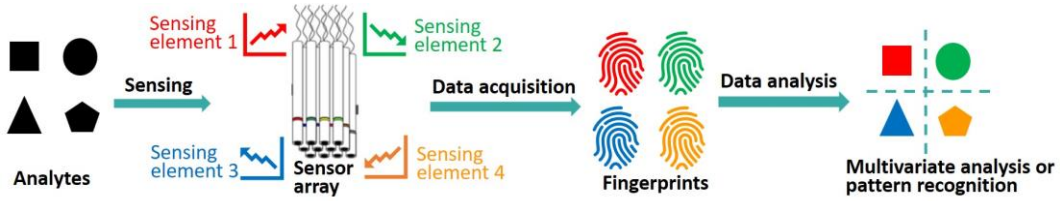

Figure 1.2 Schematic diagram illustrating the mechanism of a sensor array for multivariate analysis. Adapted from reference [6]**.**

1.1.2 Electrochemical sensors

Electrochemical sensors are frequently employed due to the fact of their advantages associated with low limit of detection, high selectivity and sensitivity, rapidness, good reproducibility, and the low-cost and transportable equipment utilized for sensing. As a category of chemical sensors, standard electrochemical sensors are also composed of two basic constituents, receptor and transducer. Particularly, the information for analysis is taken from the electrical signal produced by the interaction between the target analyte and the recognition layer. By organizing the constitution of devices, electrochemical sensors can be employed for various applications depending on the nature of the analyte, the character of the sample matrix, as well as the sensitivity or

selectivity requirements.

1.1.3 Classification of electrochemical sensors

Generally, electrochemical sensor can be divided into several categories depending on the type of the transducers, including potentiometric, amperometric, voltammetric and impedimetric devices [11].

- **Voltammetric sensors**

Voltammetry is an electroanalytical technique that collects information about one or more analytes by measuring the current signals as a function of the potential [12]. Voltammetry is a dynamic technique, which usually employs a third electrode to set the desired voltage at the sensing electrode independent of the voltage drop across the solution. Voltammetric analytical devices usually carry out in a three-electrode system and a potentiostat, as shown in Figure 1.3. A *potentiostat* is a device that controls the potential between the working and reference electrodes by adjusting the current at an auxiliary electrode. The three-electrode system consists of a reference electrode usually a calomel electrode or Ag/AgCl electrode, a counter electrode (or auxiliary electrode), generally a platinum wire, and a working electrode. The reference electrode can contribute with a known and stable electrode potential. In voltammetric principle, a time-dependent potential excitation signal to the working electrode is employed, which can change the relative potential to the fixed potential of the reference electrode. The current that flows between the working and auxiliary electrodes is changed consequently and measured for analysis. The quantification of analyte or evaluation of the redox properties can be measured at the working electrode surface, where the potential varies linearly with time in relation to the constant contribution of the reference electrode. The oxidation and reduction reaction of the analyte occurring at the working electrode surface

can result in a current flow through charge transfer on the auxiliary electrode. In general, voltammetric sensors provide information about target analytes that can be oxidized or reduced, which is a very important feature to understand the electrochemical reactivity of an analyte, the mechanisms and the kinetics of the oxidation and reduction procedures [13]. Sometimes, voltammetric sensors can even sense non-electroactive molecules indirectly, for example, via a biorecognition event or mediated enzyme electrodes [14]. Several types of information can be gathered from voltammetry technology, e.g., cyclic voltammetry (CV), linear sweep voltammetry (LSV), square wave voltammetry (SWV), and differential pulse voltammetry (DPV). In cyclic voltammetric method, the potential of the working electrode is linearly ramped up and down cyclically. A cyclic voltammogram is obtained by recording the current, derived from the oxidation or reduction of analytes at the working electrode based on the potential changes. The current intensity is proportional to the concentration of the analyte in the solution, leading to the application of this technique in analytical quantification. CV is a very generic and powerful method in the application of electrochemical characterization of trace amounts of analytes in aqueous solutions and deposits on conductive surfaces [15]. The electrochemical sensors employed in research cases presented in this thesis are used with the cyclic voltammetry technique.

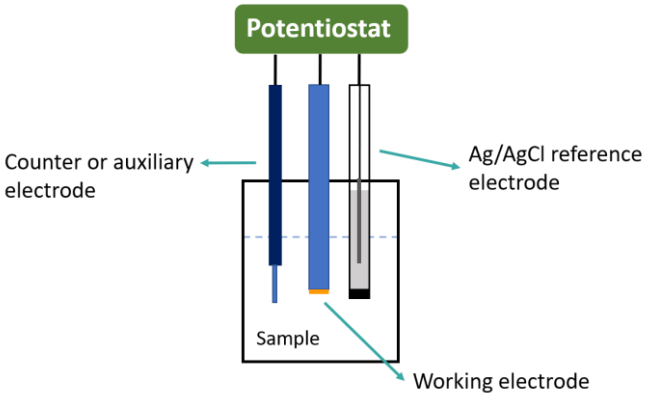

Figure 1.3 Typical three-electrode voltammetric analytical system.

- **Other electrochemical sensors**

Similar to voltammetric sensors, amperometric sensors work in a three-electrode system and a potentiostat as well. Differently, amperometric measurement is held at a constant (single-potential amperometry) or stepped potential over time (chronoamperometry). The current, which arises from the oxidation or reduction of the substances, its intensity signal is related to its concentration.

Potentiometry technology provides information about the ion activity in an electrochemical reaction and reflects the relationship between analyte concentration and the potential, which is measured at zero current intensity [16]. Potentiometric sensors measure the potential across an interface, often a membrane. The typical potentiometric analytical system consists of two electrodes, reference and indicator electrodes. The reference electrode, usually Ag/AgCl electrode, has a constant contribution to the signal, independently of the solution matrix. The indicator electrode contains a membrane that is sensitive to the target analyte, thus its potential related to the concentration of the analyte. The analyte of the sample enters the electrode membrane causing a change in membrane potential. Potentiometric electrochemical sensors are widely used in ion selectivity, clinical relevance, electronic tongues, and other fields [11].

When an electrochemical system is disturbed by perturbation of a sinusoidal voltage (or current) signal, a corresponding current (or voltage) response signal will be generated, and the impedance or admittance of the electrode can be obtained from these signals. When a sinusoidal potential over a frequency range is employed, electrochemical impedance spectroscopy (EIS) can be obtained. The resistance and capacitance of the system can be estimated by measuring the current response [17], which enables the study on material property and specific processes in monitoring changes at the surfaces of

electrodes. Impedimetric analysis is a useful tool that can be utilized in many aspects, such as characterization of different layers on the electrode surfaces, corrosion monitoring, characterization of solid electrolytes, battery performance, heavy metal ion detection, etc [18].

Conductometric sensors can be used to measure the ability of an electrolyte solution or a medium (e.g., nanowires) to conduct electrical current passing through between working electrode and counter electrodes or reference electrode [16]. The resistance of an electrolyte is gauged by use of an alternating potential in conductometric device [14]. As conductometric sensing technique is used to analyse changes in resistivity, they are considered as the subsets of impedimetric sensors [19].

1.1.4 Electronic tongues

As above mentioned, the construction and operation principles of electronic tongue (ET) and electronic nose (EN) systems were inspired by the neurophysiology of the senses of taste and smell, respectively. In sample terms of practical application, the electronic tongue acts like mammals' tongue to differentiate between distinct tastes. And the electronic nose can analyse gaseous samples like the noses' behaviour [20]. Normally, an electronic nose works with the gas phase of volatile compounds, while an electronic tongue works in the liquid phase of non-volatile compounds [21]. Electronic noses and tongues can be used to identify flavour variety and geographical origin, composition, aroma intensity, degree of freshness, and so on.

As a kind of sensor array, the ET consists of two main factors: an array of nonspecific, low-selective chemical sensors and an appropriate chemometric tool for data processing [22]. The application of nonspecific, low-selective chemical sensor array can collect the high-dimension signals and the chemometric tools, such as machine learning algorithms, artificial neural

network (ANN), principal component analysis (PCA), etc., are used to extract information. Furthermore, the stability and cross-sensitivity of sensors are of primary importance for collecting responses to as many as species reproducibly [22]. An ET system can imitate the human tongue to present a more sensitive, automated, and unbiased evaluation of tastes to samples than human, which facilitates the application of ET in many fields for qualitative and quantitative analysis in case of multicomponent samples [23]. Furthermore, this emerging tool can be utilized after transforming gas and solid materials into their liquid forms or extracts. Therefore, ET technology has been widely studied in the food and beverage analysis. They can collect information of the aroma, taste, and colour profiles through various chemical devices and use such data as input to discriminate different products by the combination of prices, geographical origins, harvest, fermentation, storage times, quality grades, and adulteration ratio, etc., with the aid of mathematical classification algorithms. Furthermore, in recent years, ETs have been reported in the application of biomedical research, national safety and environmental safety application [24].

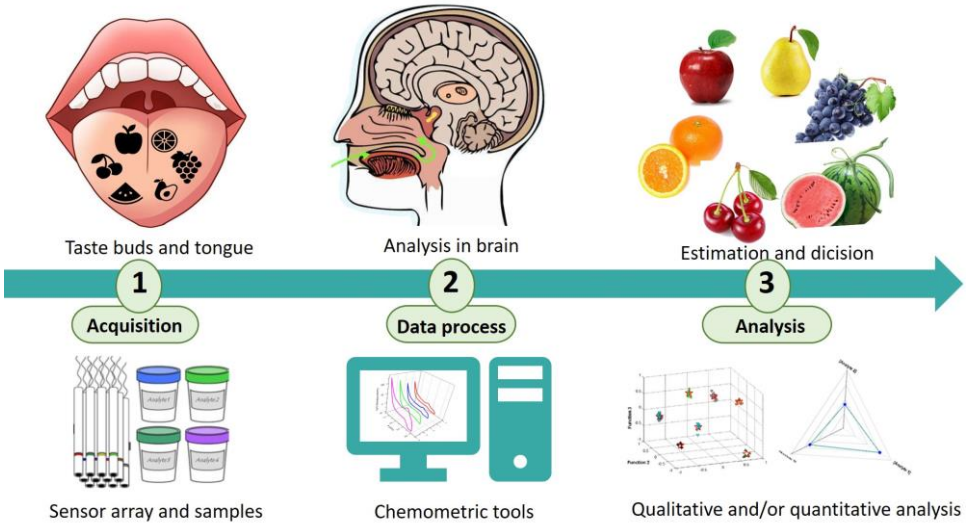

Figure 1.4 Schematic diagram illustrating the electronic tongue design inspired by gustatory system.

1.1.4.1 Voltammetric Electronic Tongue

Many kinds of sensors, from optical to mass spectrometry-based, can be employed in electronic tongue construction based on their specific principles in various fields, as summarized in Figure 1.5. But the electrochemical devices, such as potentiometric, voltammetric, impedimetric, etc., are still the most common [25]. When those of sensors considered for developing ET systems, voltammetric (bio)sensors are the most common ones [26]. In general, the experimental setup of a voltammetric ET includes several working electrodes, an auxiliary electrode and a reference electrode, as illustrated in Figure 1.6. The current is generated from the electrolysis reaction occurs on the working electrodes. The current is a function of the rate of electrolysis, which is governed by the transport of electroactive species present in the sample (i.e. diffusion coefficients and concentrations of electroactive species) [26]. Working electrodes are usually an array of noble metal ones (e.g., gold, palladium, platinum, and silver) and/or electrodes modified with some nanomaterial catalysts and coated with some membranes (e.g., polymers and epoxy-graphite). Sometime, screen-printed electrode (SPE) includes all electrodes needed for a voltammetric measurement (working, reference and auxiliary) [27].

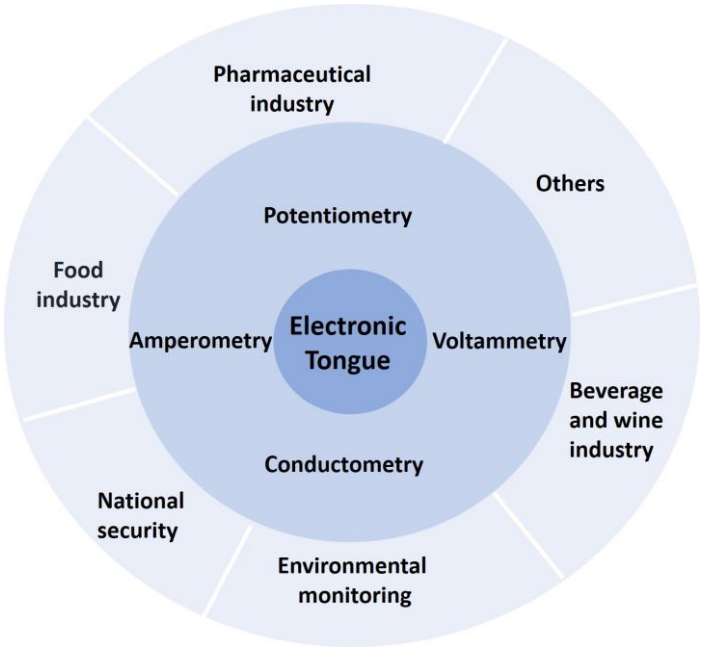

Figure 1.5 An overview diagram summarizing the classification and application of electronic tongues.

Voltammetric sensors have some advantages in multicomponent measurements because of they are assumed to be of high selectivity, high signal-to-noise ratio, high sensitivity, low limit of detection and various modes of measurement (SWV, CV, DPV, LSV, etc.) [26–29]. Moreover, it is possible to modify these electrodes to obtain sensors of various sensitivity and selectivity towards various species [21]. Therefore, there are many options or alternatives for generating voltammetric ETs, leading to their wide applications.

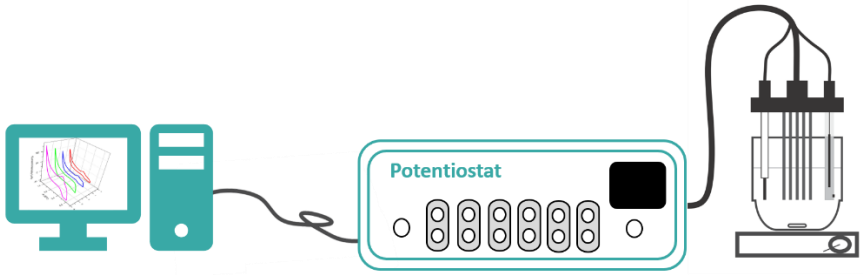

Figure 1.6 Basic principle of voltammetric electronic tongue system.

1.2 Machine learning

1.2.1 Introduction to machine learning

In recent years, the studies of artificial intelligence (AI) are soaring and widely discussed [30]. Machine learning (ML) is one group of AI technologies composed of a series of algorithms, which gives the prediction of a data based on corresponding training data's properties. It is a science of making computers learn from data and past experience and identify patterns to make prediction without being explicitly programmed. ML can be employed in many fields and considered as a powerful technology for data analysis to solve scientific problems, e.g., chemistry [31], medicine [32], economy [33] and environment [34] problems, etc. ML technology consists of several methods according to the

purpose and learning methos, including supervised learning (SL), unsupervised learning (UL), semi-supervised learning (SSL), dimensionality reduction, reinforcement learning (RL) and deep learning (DL) [30].

Figure 1.7 A general scheme for illustrating process of machine learning.

1.2.2 Supervised learning algorithms

SL is a subclass of ML, which uses labelled datasets to train algorithms to make classification or prediction, which can be used for classification and regression application. Classification works on assigning entities within test data into specific categories and attempts to label or define them. Commonly used classification algorithms are linear classifiers, such as support vector machine (SVM), *k*-nearest neighbour (*k*-NN), random forest and Naïve Bayes, etc. Regression is used to find the relationship between dependent and independent variables, e.g., linear regression, logistical regression, and polynomial regression. Some of the most commonly used learning methods are briefly explained below.

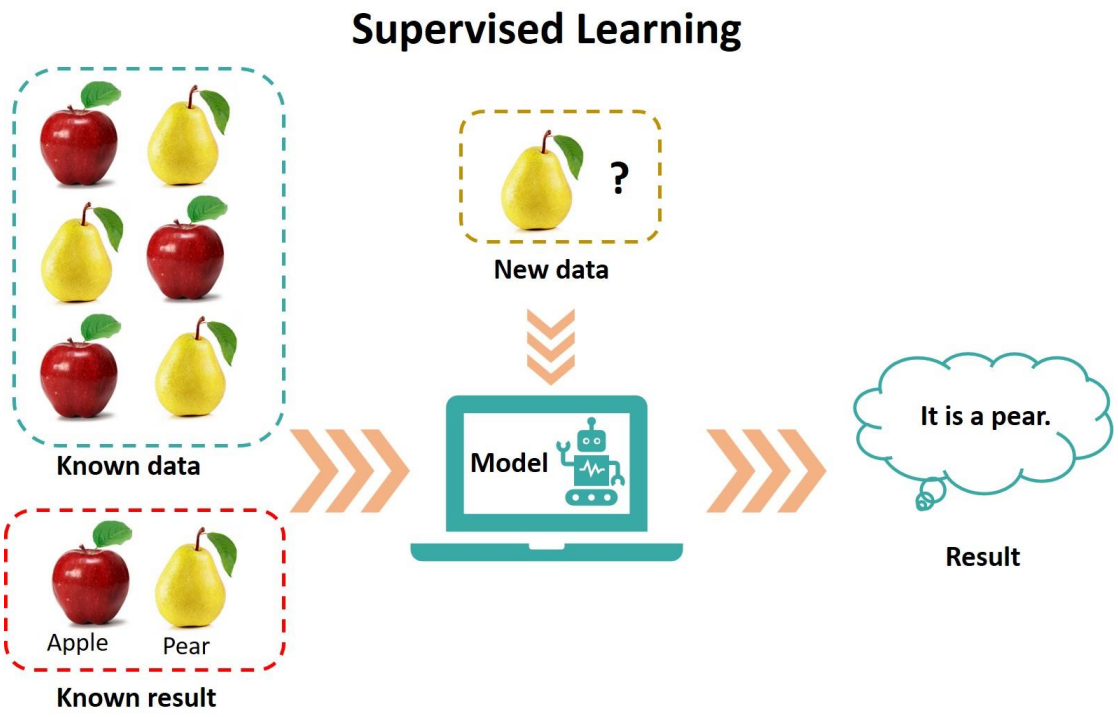

Figure 1.8 An example for showing principle of supervised learning.

- **K-Nearest Neighbour**

k-Nearest Neighbour, usually known as *k*-NN, is a non-parametric algorithm. *k*-NN can classify points of dataset based on their proximity and association to other available data. This algorithm designed based on the assumption that similar points tend to be near to each other. Therefore, it can assign a group by calculating and evaluating the distance between points. K-NN can give classification quickly with easy operation [35].

- **Naïve Bayes**

Naïve Bayes is an effective classifier that uses the conditional independence assumption. It means that each predictor has an equal effect on result and the presence of one feature does not influence that of another one in the probability of a given outcome [36]. There are three types of Naïve Bayes classifiers: Bernoulli Naïve Bayes, Gaussian Naïve Bayes and Multinomial Naïve Bayes [37].

- **Support Vector Machine (SVM)**

Support Vector Machine (SVM) is an effective and popular supervised learning model that can be used for both data classification and regression. The SVM principle is to build a hyperplane in an *n*-dimensional space (*n* means the number of features) to maximize the margin distances between data points and the hyperplane. These maximized distances can help avoid outliers effectively by creating larger distances between different classes[38].

- **Random Forest**

Random Forest is another effective and robust supervised machine learning algorithm and also can be used for both regression and classification purposes. Its principle is related to both "forest" and "trees", which generates uncorrelated decision trees and the returned outputs are subjected to the mode of class from the result of these decision trees, which can reduce variance and create more accurate predictions [39].

- **Linear Regression**

Linear Regression is typically employed for making predictions about future outcomes by finding the relationship between a dependent variable and one or more independent variables. For each type of linear regression, it works to plot a (straight) line of best fit by calculating through the method of least squares. It is known as simple linear regression and multiple linear regression in conditions when there is only one independent variable and more independent variables, respectively [40].

- **Logistic Regression**

Both linear and logistic regression models understand relationships between data inputs. Differently, logistic regression is typically used to solve binary classification problems, which means the dependent variable has binary outputs, such as "yes" and "no", "true" and "false" [41].

1.2.2.1 Artificial neural networks

Artificial Neural Networks (ANNs) are a subset of machine learning and are at the heart of deep learning algorithms [42]. Their structure and name are inspired by the way of human brain. The human brain exhibits lots of advantages over a digital computer in some tasks other than number crunching. For instance, consumer can quickly choose favourite clothes in thousands of clothes after considering all the factor, such as price, design, fabric and so on. The sets of cells in the brain, which are called neurons, are in charge of transferring information. Single neurons achieve interconnection by sending signals that containing data and information. The computations of the brain are carried out by a network of neurons, which achieve communication by sending electric pulses and passing through the neural wiring consisting of axons, synapses and dendrites, as shown in Figure 1.9.

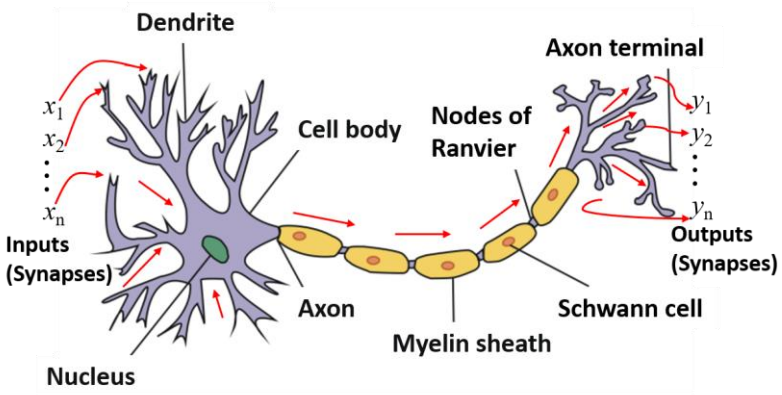

Figure 1.9 The structure and information processing of a biological neuron.

ANNs are created from the inspiration of the models of sensory processing by the brain. An ANN can be set by simulating a network of model neurons in a computer by utilizing algorithms to mimic the processes of real neurons. The created network can 'learn' to solve some problems like human does. A model neuron is illustrated in Figure 1.10, which functions as a threshold unit. It receives inputs, weighs each input and adds them up. The output of the unit is one if the total input is above a threshold, otherwise it is zero. Therefore, the

output changes from 0 to 1 when the total weighted sum of inputs is equal to the threshold [43].

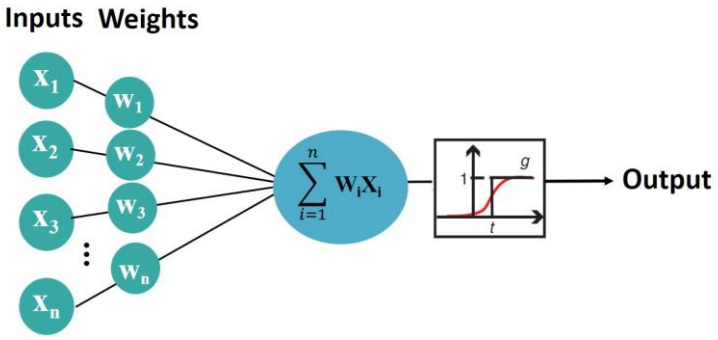

Figure 1.10 Structure and processing of a model neuron. Adapted from Figure 1 (a) of reference [43]**.**

The ANNs models can solve problems by building a simplified model of the human brain and mimicking its behaviour in learning tasks or processes. Generally, ANN models gather knowledge by defining the pattern and relationships from the obtained information to train and "learn by examples", instead of "programming processes" [44]. ANNs are capable of establishing empirical relationships between dependent and independent variables and extracting hidden information and complex knowledge from data sets. ANNs are advantageous over regression-based models in recognizing the fundamental relationship between the variables when the original information is noisy and contains some errors, which facilitates the application of ANNs in solving complicated problems [44].

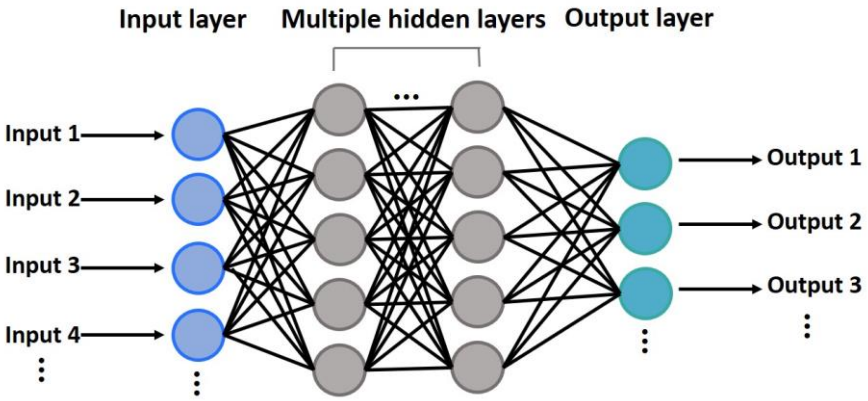

Figure 1.11 Scheme of illustrating the configuration of multi-layer ANNs.

ANNs are usually comprised of node layers, including a layer of input nodes and a layer of output nodes, which are connected by one or more layers of hidden nodes. Each node, or artificial neuron, connects to another and has an associated weight and threshold. If the value of an individual node or a set of nodes in the hidden layer is above the specified threshold value, that node is activated and data is passed to one or more nodes in next layer of the network [45]. Otherwise, no data is passed along to the next layer of the network [42]. Application of ANNs must be trained with a large number of cases (data) and is not possible for rare or extreme events, where data are insufficient to train the model.

1.2.3 Unsupervised learning algorithms

UL applies algorithms to cluster and analyse unlabelled datasets. These algorithms can extract hidden patterns and achieve grouping automatically by discovering the similarities and differences [46]. The classic UL models include principal component analysis (PCA) and *k*-means clustering.

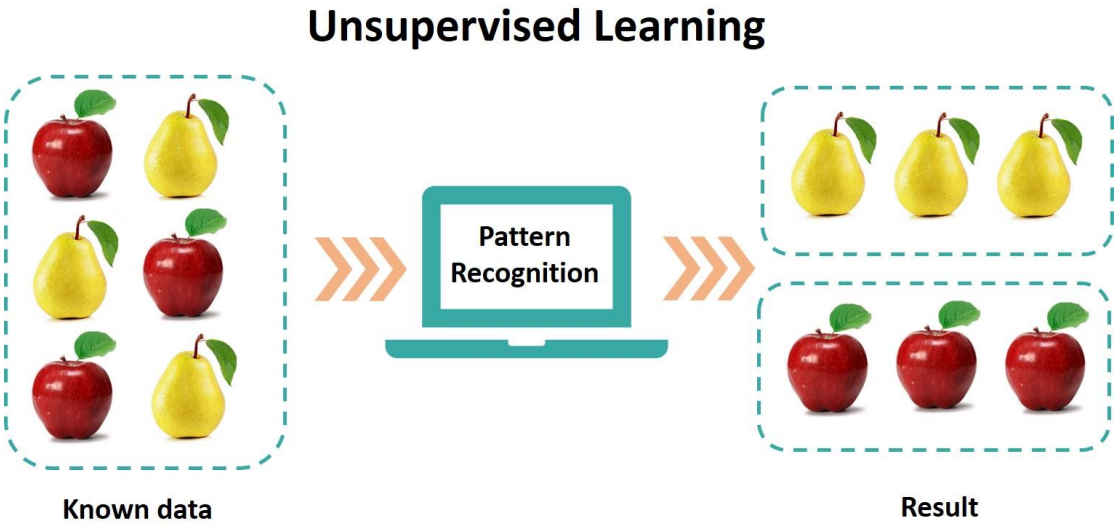

Figure 1.12 An example for illustrating principle of unsupervised learning.

❖ **Principal Component Analysis (PCA)**

Although more data usually gives more accurate results, sometimes the performance of machine learning algorithms (e.g., overfitting) can be affected. In other hands, it will be difficult to visualize datasets when there are too much features or dimensions in a given dataset. In this condition, dimensionality reduction can be used to reduce the data inputs and preserve the integrity. Principal Component Analysis (PCA) is a dimensionality reduction algorithm that reduces redundancies and compresses datasets by extracting main features. It uses a linear transformation to obtain a group of principal components and a new data representation. For example, the first principal component is the direction which maximizes the variance of the dataset. However, the second one is completely uncorrelated to the first principal component and yields a perpendicular direction to the first. When there are more dimensions, the direction of next principal component is perpendicular to the prior components [47].

- ***k*-Means clustering**

***K*-Means Clustering** is an exclusive clustering method that assigns data points into *k* groups and the *k* refers to the number of clusters based on the distance from each group's centroid. A centroid is the imaginary or real location representing the centre of the cluster. The points nearest to a given centroid will be clustered as same class. Briefly, this algorithm identifies *the* centroids to allocate every point to the closest cluster and keeps the centroids as small as possible [48].

1.3 Nanomaterials and application in electrochemical sensors

1.3.1 Introduction of nanomaterials

Nanomaterials have become one of the most exciting forefront fields and

an indispensable part of scientific research. Owing to their impressive physicochemical properties, nanomaterials have become an important bridge for many interdisciplinary researches and applications. Generally, nanomaterials refer to materials that are with at least one critical dimension of nanometre size (1-100 nm) or materials that consist of at least 50% of basic units in such size [49–52]. With material dimensions at the nanometric level, the physical and chemical properties of such materials can be modified. Nanomaterials tend to be able to give more suitable sensitivity, high adsorption and reactive properties, as well as other advantages not existing in the same corresponding bulk materials [50, 53, 54]. The development of novel functional nanomaterials accompanied with analytical and artificial intelligence technologies have promoted the advancement of electrochemical (bio)sensors, which offer some advantages such as safety, real-time, reliability, and rapid-testing. Nanoscale materials or nanomaterials are well known as and benefiting its "small scales", which aided the miniaturization of electronic sensor devices/platforms, for example the development of portable sensors. Therefore, the applications of sensors have popularized in wide range, including environmental detection and monitoring, food and medicine analysis and control, clinical and diagnostic examination, health care monitoring, biological detection, etc [55–57]. Briefly, nanomaterials are playing crucial roles in electrochemical sensing technologies for improving sensors' performance in terms of stability, specificity, sensitivity and selectivity.

1.3.2 Electrochemical application of nanoparticles

It has proven that the modification and/or functionalization of the electrochemical sensors with nanomaterials can amplify the response signals for developing sensors with high sensitivity and selectivity properties. Various nanomaterials, especially nanoparticles of different types have been employed

widely based on many kinds of analytical methods. Depending on the target analytes, reaction mechanisms, media, etc, nanoparticles can play different roles in different electrochemical sensing systems. In recent decades, nanoparticles (NPs) have been widely used in electrochemical sensors and biosensors based on their unique properties in certain systems [54,58]. The basic functions of NPs, can be mainly summarized as: enhancement of electron transfer, acting as reactant, catalysis of electrochemical reactions, immobilization of biomolecules and labelling biomolecules [59]. Sometimes even the same kind of NPs can be utilized for different applications. Because of their excellent catalytic and conductivity properties, metal nanoparticles are promising catalysts in improving electrochemical reactions by enhancing the electron transfer between analytes and electrode surfaces. Metal oxides nanoparticles also have attracted lots of efforts for a wide range of applications, such as sensors, fuel cells, batteries, actuators, as well as optical devices because of the wonderful performance in photochemical, mechanical, thermal, electrical, optical and optoelectronic properties [60].

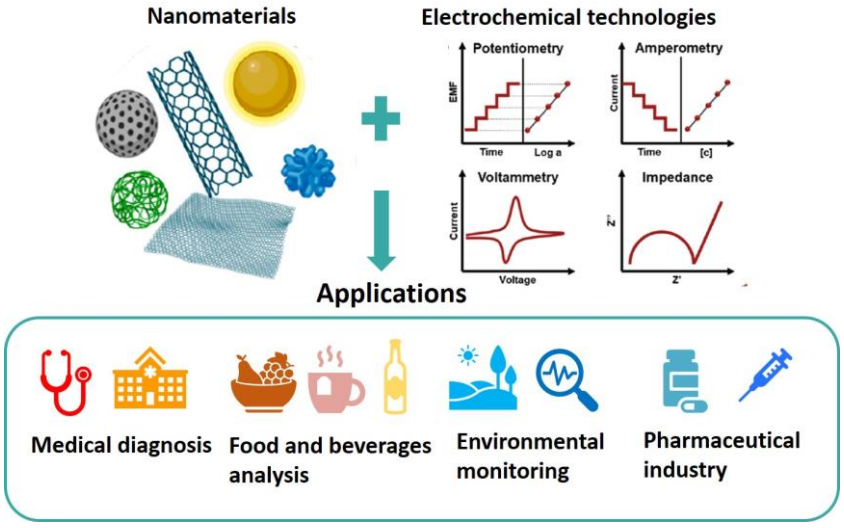

Figure 1.13 A diagram for illustrating the combination of nanomaterials and electrochemical sensors and some applications.

Generally, the modification to sensing systems start from the modification of working electrodes, apart from development of manufacturing process, the

selection of nanomaterials is an important part. In recent years, from different nanomaterials, such as nanotubes or nanocomposites, to different nanostructures, such as graphene, metal nanoparticles or nanostructured polymers, etc., lots of working electrodes were modified with these materials in different ways of manufacturing for aimed functions and applications.

1.3.3 Electrochemical anodization for nanostructure fabrication

Anodic oxidation is a commonly used approach for metals corrosion protection [61]. It can also be used to prepare an oxide layer over the surface area of the metallic substrate, which is a simple and low-cost method for modification or decoration of metal surface for specific preposes. Generally, the process and setups in the procedure of anodization are very similar to those used for electrolysis. Particularly, it is carried out in a two-electrode (or three-electrode) electrochemical cell, the metal being used as the anode and platinum (also titanium or other electrodes) as the cathode [62, 63]. In recent decades, electrochemical anodization has attracted lots of attention for fabrication of nanostructured substances via self-organized anodization owing to its ease synthesis, versatility and low cost. What's more, it is seamless between the formed anodized metal oxides nanostructures and the conductive substrate metal [64]. The tailored ordered morphology on the nanometric scale can make chemical and physical properties changed to get numerous potential applications [65]. Anodic aluminum oxide and anodic titanium oxide are most frequently studied nanostructured materials, which has achieved lots of progress in wide range of applications, such as drug releasing platforms, electrochemical sensing, renewable energy harvesting and so on [65–69].

In recent years, some of the transition metals have been tested as substrates for anodizing and some nanostructured materials, most of which are

nanoporous or nanotubular, from anodic oxidation by electrochemical procedure, i.e., Fe [70], Zn [71], Sn [72], Zr [73] etc [74].

1.3.3.1 Nanostructured anodic copper oxides

Research on nanostructured copper oxides and tailored properties have attracted lots of attention and brought high expectations to providing solutions in many fields, such as environment purification and renewable energy harvesting. Copper is a good option for fabrication of nanostructured metal oxides in self-organized anodization procedure. In general, copper can form two oxides, monovalent and bivalent oxides, i.e., cuprous oxide (Cu_2O) and cupric oxide (CuO), as well as sometimes mixtures of these two, such as Cu_3O_2 and Cu_4O_3 (tetragonal) [75].

Morphological features of nanostructured anodic oxides fabricated from electrochemical procedure are tailored by operating conditions and additives in electrolytes. The anodization of copper can improve surface area due to the morphology of formed oxides, i.e., nanowires, nanoneedles or nanorods. The stoichiometry of oxides is not fixed, Cu_2O, CuO, and $Cu(OH)_2$ co-existing in obtained samples [74]. What's more, the chemical composition of the formed nanostructures can be adjusted by changing experimental conditions during anodization and post-treatment methods [74]. Due to these features, the anodization of copper has attracted lots of interest in the fundamental research and application, particularly as catalysts owing to the properties of CuO and Cu_2O and improved surface areas, as a promising method in terms of fabrication and doping of high-aspect ratio nanostructures and morphology control. It does not require numerous steps or expensive equipment and time-efficient and easy to scale-up because of self-organization [74].

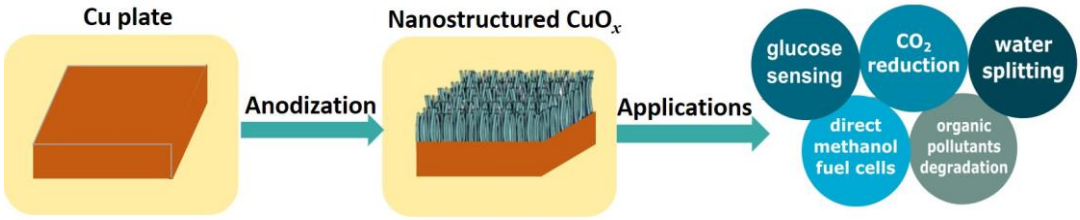

Figure 1.14 The diagram illustrating the fabrication of anodic copper nanostructure (nanowires) and the fields of application.

Metal oxides of nanostructure fabricated in anodization procedure usually made of nanopores or nanotubes. Note that, copper oxides offer more than one type of nanostructure morphology, among which, the most interesting ones are nanowires and nanoneedles with high aspect ratios and surface-to-bulk atom ratios [76]. To grow nanostructured oxides on copper, electrochemically voltametric methods, such as LSV or CV, are supposed to be the most facile one, which gives satisfactory nanostructures, usually nanoneedles morphology, and related information on reactions occurred on the electrode [63, 77].

Copper can be oxidized to Cu(I) and form metastable CuOH firstly on the copper surface and then it can transform into Cu_2O, see equations (1) and (2). At the same time, two electrons can be taken away from one copper atom, forming Cu(II) substances directly at greater potentials, such as CuO and $Cu(OH)_2$ (water insoluble), as shown equations (3) and (4) [78]. In addition, Cu(I) species can also be taken one electron and oxidized into Cu(II) species. Furthermore, Cu(III) species can also be formed with copper at a greater oxidation state when sufficiently high potentials applied, in copper oxides-based sensing reaction. Therefore, CuO and $Cu(OH)_2$ may also transform into soluble species, such as $Cu(OH)_4^-$, as shown equation (5) and (6).

$$Cu - e^- + OH^- \rightarrow Cu(OH) \quad (1)$$

$$2Cu(OH) \rightarrow Cu_2O + H_2O \quad (2)$$

$$Cu - 2e^- + 2OH^- \rightarrow CuO + H_2O \quad (3)$$

$$Cu - 2e^- + 2OH^- \rightarrow Cu(OH)_2 \quad (4)$$

$$CuO - e^- + H_2O + 2OH^- \rightarrow Cu(OH)_4^- \quad (5)$$

$$Cu(OH)_2 - e^- + 2OH^- \rightarrow Cu(OH)_4^- \qquad (6)$$

1.3.3.2 Anodic copper oxides in electrochemical sensing

Cu-derived nanostructures formed by anodization procedure have wide utilization as catalysts in photochemical or electrochemical analysis. The Cu substrate can offer a conductive path for the photo-generated electrons and prevent their recombination with photo-holes to maintain photocatalytic activity and stability. In addition, Cu-derived materials have obtained wide acceptance as a powerful electrocatalyst for oxidation of organic compounds because of the efficient catalytic activity, which might be related to the formation and chemisorption of strong oxidant hydroxyl radicals (·OH) on the electrode surface [79]. Therefore, anodic copper oxides can also be applied into modification of electrochemical sensors and have been accepted as outstanding electrodes in organic compounds analysis, such as glucose sensing, as well as chemical oxygen demand (COD) determination in wastewater. Electrodes modified with Cu-derived nanostructured have been explored for many years as a good choice for electrochemical sugars oxidation benefiting from the low cost and good chemical activity [80]. In recent decades, anodic copper oxides were reported in the application of electrochemical sensors for COD determination in wastewater [81, 82]. The application of anodic copper oxide into will be expressed in detail in section 1.4.4.2.

1.3.4 Application of nanomaterials in environmental monitoring

The efforts on the research of nanomaterials over the past decades have promoted the development of analytical techniques in fields such as food and beverage analysis, national safety, pharmaceutical analysis, medical diagnosis, as well as environmental monitoring [54]. Owing to the advantages, such as

easy operation, low cost, rapidness, smooth manufacture and transportability, electrochemical devices incorporating nanomaterials have achieved lots of advances and accepted widely as a promising analytical method in these fields [83, 84]. Benefitting from the properties of nanomaterials, miniaturization and portability are about to become reality. In addition, the high surface-to-volume ratios and facility of surface functionalization make nanomaterials highly sensitive in surface chemistry, which contributed to the achievement of extremely low limits of detection [85]. Therefore, the integration of nanomaterials has promoted the activity, sensitivity and selectivity of electrochemical sensors in trace analysis. The application of nanomaterials into electrochemical sensors in pollution detection, such as nutrients, heavy metals, and organic matters has proven to be successful and promising as easy and quick tools [54, 83, 86]. Furthermore, and the combination of sensors used in the sensor arrays, such as electronic tongue and electronic nose, which can provide more global and generic final information by multivariate analysis, has expanded the application of sensors and nanomaterials.

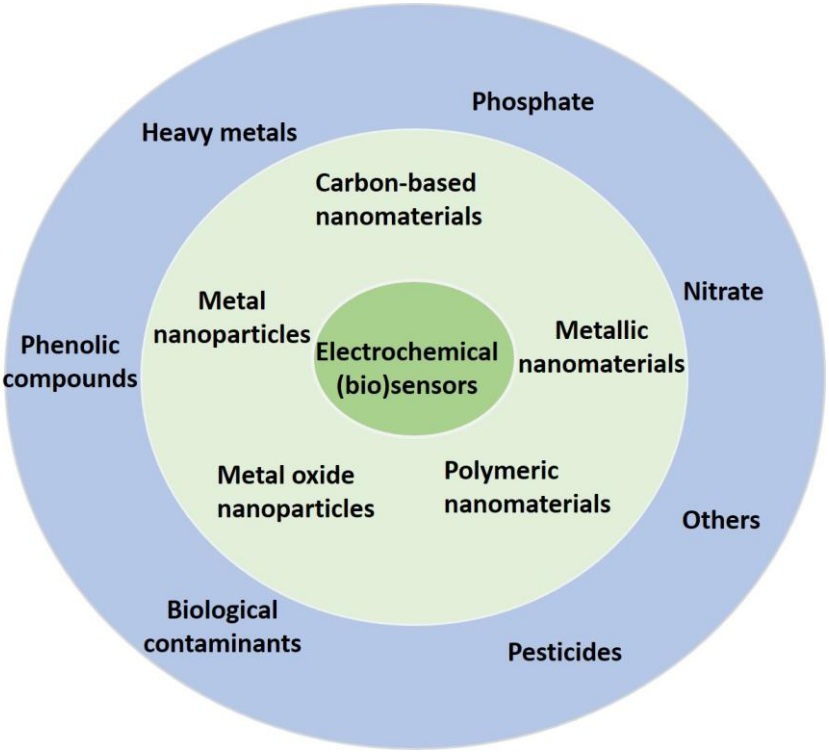

Figure 1.15 A diagram summarizing the application of nanomaterials in electrochemical (bio)sensors for environmental monitoring.

1.4 Organic pollution of wastewater

1.4.1 Water pollution

As the vital component of biological cells and bodies, water is crucial to all lives in the world. A continuous supply of water provides this essential thing for the survival of humanity and the rest of living beings. Accompanied with the increasing population, the demand of fresh water is soaring. As reported, demand of freshwater for global use has increased six-fold in the past 100 years [87]. The Organisation for Economic Co-operation and Development (OECD) projected that global water demand would increase by 55% between 2000 and 2050 [88]. However, as reported on a research done by World Health Organization and United Nations International Children's Emergency Fund (WHO/UNICEF), 1 in 4 people or 2 billion people around the world lack safe drinking water [89]. Meanwhile, the development of economy and society is making requests of drinking water with higher criteria and standards. However, along with the rapidly increasing population, industrialization and urbanization globally plus the variability in rainfall patterns, the demand of fresh water is surging, which has aggravated the issue of water security [90].

Figure 1.16 The photos showing some utilizations of fresh water.

However, fresh and clean water supply is under threat by overuse and pollution. The activities of human always need to use water, which can always produce wastewater. Meanwhile, the improvement of water use is growing resulted from the increasing population and industry development, which is exacerbating the wastewater problems globally, such as the increased quantity of wastewater and overall pollution load [91]. The behaviours of people's life, agriculture and industry, as well as the lack of awareness of protecting fresh water, can bring lots of effects on it. In many countries, some are even developed countries, the majority of wastewater was released to water systems directly without proper treatment, which lead to lots of impacts on ecosystems, human and animal health, economy and freshwater resources in the world. Drinking contaminated, sometimes even toxic water, can cause some water-borne diseases to humanity and animals, such as cholera, diarrhoeal diseases, shigella, hepatitis A and E, etc, that related to the ingestion of drinking water [92, 93]. As estimated by the United Nations Educational, Scientific and Cultural Organization (UNESCO), approximately 829,000 people die from diarrhoea as a result of unsafe drinking water, sanitation and hand hygiene each year [94]. Even in high-income countries, water-borne illness can also be a

concern and attracted lot of attention, which exacerbated the global burden of disease control[3]. In addition, unsafe drinking water and poor hygiene can cause gastrointestinal illness that inhibits nutrient absorption and malnutrition, particularly effecting health and growth for children [87]. Therefore, it is urgent and important to develop technologies to facilitate safe drinking water worldwide [95].

In simple terms, wastewater refers to the water that contains some pollutants, making it not suitable for either drinking directly or domestic cleaning use or irrigation [96]. The formation of wastewater is usually in the procedure of domestic, industrial, agricultural and commercial use that make the fresh water's composition changed [97]. Depending on the source and levels of pollution, wastewater can contain different pollutants. Wastewater always contain some contaminants, such as organic, inorganic, pathogens and microbial contaminants, as well as suspended particles, etc. Some contaminants are hazardous, which can result in serious problems to aquatic ecosystems and further affect animals and humanity through food chain and environment. Some common contaminants were summarized in Table 1.

Owing to soaring demand to high-quality life, industries such as pharmaceutical industry, painting industry, food industry, distillery industry, etc, always need lots of organic compounds in manufacturing procedure, which contributed organic pollutants to their wastewater produced. Organic pollutants are a common group of compounds making water contaminated. Dyes, petroleum, humic substances, surfactants, phenolic compounds, pesticides, and pharmaceuticals are main organic pollutants in wastewater[98]. Some of these organic pollutants can act as endocrine disruptors, for example, bisphenol A, dioxins, and fire retardants, which can cause impacts on human bodes both to adults, children and unborn babies by passing to them through mothers' bodies [99]. Sometimes can cause neurodegenerative

disorder, rectal and immunodeficiency diseases and sexual health problems by mimicking the influence of reproductive hormones [99].

Table 1. Major sources of pollutants in wastewater and their effects

Pollutant	Primary sources	Influence	Constituents of concern	References
Organic matter	Industrial and agricultural wastewater and domestic sewage.	Depletes oxygen dissolved in water for degradation. Some toxic organic pollutants, like pesticides, can kill aquatic life.	BOD, COD, DOC (Dissovled Organic Carbon), DO (Dissolved Oxygen)	[99–102]
Nutrients	Agricultural runoff and inefficient nutrient removal during industrial and domestic wastewater treatment.	Eutrophication. Over-growth of algae, degradation of water quality, loss of biodiversity, hypoxia and fish kill.	Total N (organic + inorganic), total P, COD	[100–102]
Pathogens, microbial contaminants	Human, livestock, and natural sources. Contaminated drinking water and inadequate health-care and domestic wastewater treatment.	Spread of infectious diseases (e.g., diarrheal disease and intestinal parasites). Increased childhood mortality in developing countries	Shigella, salmonella, cryptosporidium, fecal coliform (Coliform), escherichia coli (mammal feces – E. coli)	[96, 103–105]

Salinity	Agricultural and various industrial fields such as food processing, leather manufacturing, paper and pulp production, pharmaceutical, etc.	Impacts on agricultural crops, deterioration of water quality and natural environment, soil infertility and on ecological systems.	Electrical conductivity, chloride, major cations (Ca, Mg, etc.), anions	[106–109]
Heavy metals	Industry and mining activities	Persist in freshwater environments, especially sediments for long periods. Can be remobilized by change in redox state. Can accumulate in fish and shellfish tissue and be toxic to aquatic organisms and humans through food chain.	Pb, Cd, Zn, Cu, Ni, Cr, Hg, As.	[110–113]
others	Silt and suspended particles, exotic species from shipping or anthropogenic origin, radioactivity, fluoride and selenium contaminants, etc.	Reduces water quality and affect aquatic ecosystems. Impacts on environment, animals and humanity through food chain.	Total suspended solids, turbidity. Any non-native species, plant or animal, that disrupts aquatic ecosystems and the contents of other contaminants.	[114–117]

1.4.2 Sources of organic pollutants

➢ Industrial activities

The discharge of untreated or partially treated industrial wastewaters to natural water bodies is a considerable source of pollution and contaminants that may have risks of causing a variety of adverse effects on the environment and human health. Generally, industrial production consumes a large amount of water and simultaneously produces considerable wastewaters containing suspended solids (SS), inorganic and organic pollutants, featured as high toxicity, high values of biochemical oxygen demand (BOD) as well as chemical oxygen demand (COD) values [118–120].

Industries, such as nuclear industry, iron and steel industry, printing and dyeing industry, shoes and clothes industry, food and drink production, etc, contribute a lot in developing economy and improve life quality but simultaneously cause much pollution to the environment and water. Decided by their producing procedures and products, these industries can't avoid releasing lots of chemicals, including organic and inorganic substances or solvents, which are harmful to environment or even toxic. Sewage release without adequate treatment can cause water pollution [121]. Therefore, the discharge of sewage to aquatic ecosystems should be treated previously and reach the standards proposed by the regions or countries. Meanwhile, with the acceleration of urbanization globally, wastewater caused by industrial production is increasing gradually [122].

➢ Domestic activities

Accelerated urbanization all over the world brings many benefits to peoples as well as many challenges, one of which is the dramatically increased

generation and discharge of domestic wastewater. As reported, over 80% of domestic wastewater globally was discharged into water bodies without adequate treatment [123]. In general, domestic wastewater refers to the wastewater produced from household activities, such as washing clothes and utensils, domestic hygiene, defecation, micturition, cleaning home and vehicles, and other wastes formed in daily life [124]. The pollutants contributed by domestic wastes can increase levels of BOD and COD in discharged water bodies, accompanied with the impacts of altering the pH, inorganic constituents, hardness, and pathogen load of the water [125]. Domestic wastewater usually consists of synthetic detergents, soaps, fats, lignin, carbohydrates, proteins, and natural or synthetic chemicals from the processing industries [123]. In addition to some organic and inorganic, domestic wastewater may contain millions of intestinal bacteria and a minority of other pathogenic organisms, which can cause diseases like typhoid, gastroenteritis, cholera, hepatitis, bacterial dysentery, and amoebic dysentery [123, 124].

➢ Agricultural activities

In addition, agricultural activities can also bring pollution to water because of the utilization of pesticides, phosphate fertilizer and nitrogen fertilizers, as well as the organic farm wastes [126]. What's more, agriculture irrigation using polluted wastewater that untreated or partially treated is common in water-scarce regions of developing countries, which expand the pollution range and insert pollutants to agricultural products. Pesticides are indispensable in agricultural activities for controlling weeds and insects, as well as improving agricultural products harvest. Thus, they have made a significant contribution to alleviating hunger and an abundant supply of high-quality food. Pesticides that are used aiming at killing pests and control weeds usually use chemical ingredients, which can also be toxic to other organisms, including non-target

plants, birds and beneficial insects, as well as crops and animals. Moreover, pesticide moves away from the target plants can bring contamination to air, water and soil, resulting in environmental pollution [127].

- **Health-care wastes**

Hospitals are playing pivotal roles in guaranteeing the well-being of humanity in protecting people's lives and providing services to tackle the complex health problems. With the growth of human population and the improving demand on health care, the medication and health care activities in the hospital are expanding correspondingly [128]. As defined by WHO, the term health-care waste, refers to all the waste generated within health-care facilities, research centres and laboratories related to medical procedures. And the health-care wastewater is defined as any water that has been polluted during the provision of health-care services [129].

Health-care wastewater is characterized as high levels of BOD, COD, ammonia, and nitrogen content, which might contain chemicals, pharmaceuticals and contagious biological agents, and might even contain radioisotopes [129]. Sometimes, some microorganisms, for example, antibiotic-resistant bacteria, antibiotic-resistant genes, persistent viruses, etc, also could be found, which imposes a significant threat to the human health and environment [130–132]. The ratio of BOD and COD values of wastewater is used as the biodegradability index [133]. The biodegradability index of health-care wastewater is also lower than that of domestic wastewater, which indicates that it is difficult to treat by conventional biological systems.

1.4.3 Chemical Oxygen Demand (COD)

As defined by International Union of Pure and Applied Chemistry (IUPAC), Chemical Oxygen Demand (COD) is "a measure of the amount of

oxygen, divided by the volume of the system, required to oxidize the organic (and inorganic) matter in wastewater using a chemically oxidizing agent. In practice, it is usually expressed in milligrams O_2 per litre" [134]. According to this definition, COD is calculated as the oxygen equivalent that used for oxidizing all the reducing substances by high oxidants in aqueous solutions, usually with a unit of mg/L O_2, as expressed by equation (7) below. Therefore, it can reflect the degree of contamination in water by reducing substances. There is usually a variety of reducing substances in contaminated water, such as organic matters, nitrites, sulfides, and ferrites, but the majority group is organic matters. Therefore, COD is often used as a measure to the content of organic pollutants in water samples. Briefly, the larger the COD value is, the more serious the water is polluted by organic matters.

$$C_nH_aO_bN_c + (n + a/4 - b/2 - 3/4c)\ O_2 \rightarrow n\ CO_2 + (a/2 - 3/2c)\ H_2O + c\ NH_3 \qquad (7)$$

Therefore, COD is also used as one of the comprehensive parameters for indicating and evaluating the quality of water samples, e.g., lakes, rivers or wastewater, in terms of organic contamination [96]. COD can be determined to different values in different methods because of the different oxidation to reducing substances. Using potassium permanganate or potassium dichromate under acidic condition to conduct oxidation and determination is a commonly used method. The strong oxidizing agent potassium permanganate ($KMnO_4$) has been used for many years in COD measurement. However, its effectiveness at oxidizing organic matters can vary widely to different compounds. The limit of its oxidation capacity renders it a relatively poor oxidant for determining COD. Therefore, potassium dichromate ($K_2Cr_2O_7$) become a better choice because it is relatively cheap, easy to purify, and importantly it can oxidize a wide range of organic compounds and shows good reproducibility. Sometimes, the determinations from $KMnO_4$ are called *oxygen consumption* and the detected results are called *oxygen demand* from $K_2Cr_2O_7$.

1.4.3.1 Traditional method of COD determination

The traditional standard method of chemical oxygen demand measurement is represented by the international standard ISO6060 "Determination of the chemical oxygen demand" [135]. This method shows high oxidation rate, good reproducibility, accuracy and reliability, and been universally recognized and used as standard for COD detection in many countries [136]. The detection procedure is carried out in sulfuric acid medium providing an acidic environment. There are two main steps in standard method, including digestion step and titration step. In digestion step, $K_2Cr_2O_7$ is used as oxidant, silver sulfate as catalyst, mercury sulfate as masking agent of chloride ions. The acidity of sulfuric acid used as digestion reaction liquid is 9 mol/L. Digestion reaction is carried out by boiling reflux for 2 hours at 148°C ± 2°C. After the digestion procedure, the excess $K_2Cr_2O_7$ is titrated with ferrous ammonium sulfate (FAS) solution using ferroin as an indicator. The consumption of FAS solution is equivalent to the unreacted $K_2Cr_2O_7$ added originally. The COD value of the water sample can be calculated according to the subtraction of unreacted $K_2Cr_2O_7$ from the total amount that originally added.

In digestion step, oxidizing agent must be in excess to ensure that all organic compounds can be oxidized completely. When $K_2Cr_2O_7$ is used as the oxidant, it is titrated with FAS once oxidation is complete until all of the excess oxidant has been reduced to Cr^{3+}. The reaction of organic compounds with $K_2Cr_2O_7$ under acidic conditions is shown in equation (8). In this equation, $d=2n/3 + a/6 – b/3 – c/2$. As an oxidizing agent, $K_2Cr_2O_7$ does not make organic nitrogen oxidized into nitrate, so nitrification is not included in the standard COD test [137].

$$C_nH_aO_bN_c + d\ Cr_2O_7^{2-} + (8d + c)\ H^+ \rightarrow n\ CO_2 + (a/2 + 4d - 3/2c)\ H_2O + c\ NH_4^+ + 2d\ Cr^{3+} \quad (8)$$

As the definition shows, the COD values detected from traditional methods can count the oxidation to some reduced inorganic ions, which can affect the evaluation to organic contents. Because of the common existence and high concentration in wastewater, chloride can cause serious interference in COD values when used for monitoring organic pollutants [137]. The chemical reaction between chloride and dichromate was illustrated in equation (9). To eliminate this interference, mercuric sulfate can be added prior to other reagents to form a poorly ionized mercuric chloride complex. In addition to chloride, there are also a small amount of other inorganic compounds that can cause possible interference, such as nitrite, ferrous iron and sulfides, which can be overcome by adding sulfamic acid [136, 137].

$$Cl^- + Cr_2O_7^{2-} + 14\ H^+ \rightarrow 3\ Cl_2 + 2\ Cr^{3+} + 7\ H_2O \quad (9)$$

1.4.3.2 Electrochemical sensors for COD detection

According to the above section, although the traditional COD detection is well established and standardized, this procedure is time-consuming and expensive as well as the involvement of some corrosive and highly toxic reagents. Above all, the final back-titration procedure confers a poor reproducibility and it demands qualified personnel, which made the method hard to automate. For the purpose of circumventing these drawbacks, lots of efforts have been put in developing rapid, easy-operation and environmentally friendly methods for COD determination. As summarized by Wang et al., alternatives for COD detection can be classified into three categories [138]. The first category involves modification based on traditional methods, which focused on reducing digestion time, finding alternatives as oxidizing or masking reagents, and seeking to use spectrophotometry instead of titration [79,

138]. The second category refers to the methods of direct or indirect determination of COD by spectroscopy technologies[138], e.g., near-infrared spectroscopy [139], fluorescence spectroscopy [140], fourier transform infrared (FTIR) spectroscopy [141], as well as inductively coupled plasma optical emission spectrometry (ICP-OES) [142], etc. The third category mainly involves catalytic reactions based on such as electrochemical [143], photocatalytic [144] and photoelectrochemical techniques [145]. Photocatalytic and photoelectrochemical methods are simple and rapid without secondary pollution. However, the use of ultraviolet light raises complexity of the device and operation, as well as increases the cost for COD determination. In addition to lower environmental impact, in situ and real-time measurement are very important for monitoring water quality. Therefore, such equipment should be simple, cheap, reliable, sensitive and easy to be automatized [79]. Compared to the others mentioned above, electrochemical sensors have good potential for in situ and real-time COD analysis due to advantages of simple operation, small size, high sensitivity and good reproducibility, lack of complex pre-treatments and rapid electrical signal responses [138, 146–148].

1.4.3.3 Principles of COD detection by electrochemical sensors

In electrochemical methods, organic substances are oxidized on surfaces of working electrodes (or sensors). An electro-catalysis-based redox reaction occurs at the electrode surface after organic compounds of a certain concentration are adsorbed on the interface, which can result in the gain or loss of electrons. The amount of gained or lost electrons during a redox reaction can be evaluated by measuring the current intensity at the macro level. Therefore, a quantitative relationship can be established between the electrical signal (e.g., current intensity) and the concentration of organic pollutants [148, 149]. Based

on the chemical properties of different organic compounds, the electrode can identify and evaluate different pollutants qualitatively and quantitatively based on electrodes' properties and differences of electrical signals, such as different intensities or positions of current peaks. The equipment of electrochemical sensing system for COD analysis was illustrated in Figure 1.17. The electrochemical device is a typical three-electrode system composed of a working electrode (WE), a reference electrode (RE) and a counter electrode (CE).

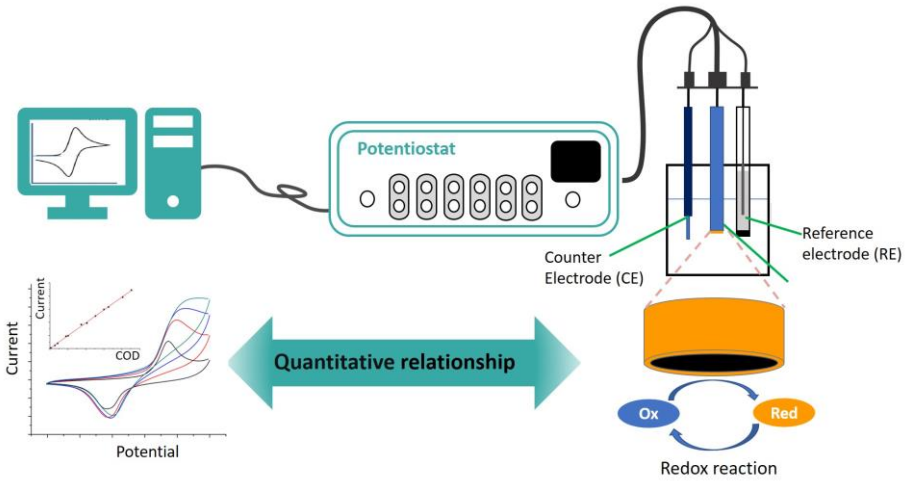

Figure 1.17 Basic principles of COD detection by electrochemical sensing systems

1.4.3.4 Application of copper-derived materials for COD detection in wastewater

Despite of those advantages of electrochemical methods for COD determination, it is not possible to achieve direct oxidation of organic pollutants utilizing carbon-based or metal sensors because of the reason that the high potential required would be outside the potential window of the electrochemical device, whose limit is defined by the oxidation of water at positive potential [79]. Many electrochemical sensors have been reported good performance for COD sensors construction, such as Cu, PbO_2, Ni, Rh_2O_3, CoO and Ni Cu alloy [143, 150–154]. The mechanism and catalytic activity of these fabricated electrodes were accepted to be related to the formation of hydroxyl radicals (·OH) on the electrodes' surfaces, which is a strong oxidant [155].

Whereas, the performance of a COD sensor can be affected a lot by the material itself and its structure in terms of reaction mechanism and reaction products, as well as the efficiency of electrochemical oxidation, which can further influence the accuracy of the result. In this sense, copper-derived material has attracted lots of attention in organic pollution analysis as it is widely accepted to be a powerful electrocatalyst in alkaline media for oxidation of some organic compounds, such as carbohydrates and amino acids [82, 147, 152, 156–158].

Nanostructured copper (oxide) materials have attracted lot of attention on the synthesis and application on many fields [159–161]. Cu and CuO (or Cu_2O) nanoparticles have reported a wide application for sensor fabrication in molecule detection, such as glucose, catechol, dopamine and other phenolic compounds, etc, which makes Cu-derived nanostructures are suitable for COD determination as the same organic target analytes. The procedure of the electrocatalytic behaviour for the oxidation of organic compounds was proposed, as shown below in equation (10) and (11). The catalytic performance can be affected by the hydroxide concentration and CuO. The Cu(III) species act as the electron-transfer mediator, which contribute to the good performance of copper electrodes in alkaline medium in oxidation process to organic compounds. Hydroxide ions can neutralize the protons appeared in the formation of active sites CuO(OH) through discharge of water.

$$Cu^{II}O + OH^- \rightarrow Cu^{III}OOH\cdot + e^- \quad \text{(electronic step) (10)}$$

$$Cu^{III}OOH\cdot + \text{organic (reduced)} \rightarrow Cu^{II}O + \text{organic(oxidized)} + H_2O \quad \text{(chemical step) (11)}$$

Cu-derived nanostructure modified electrode surface with highly developed surface area in controllable manner can be also obtained by anodization process. Growth of oxide/hydroxide layers on copper surface can be controlled by changing conditions, such as: species and concentration in electrolyte, electrochemical condition, pH or temperature. Silva and co-workers

reported a surface modified copper-based electrode for COD detection in 2008 by anodization technique [162]. This electrode was fabricated utilizing a copper rod, wrapped by epoxy resin and a glass cylinder. The anodic copper oxide was formed in CV cycling the potential between −1.0 and +0.70 V vs. Ag/AgCl in 0.1 mol/L NaOH solution for 15 min. The analytical linear range of 53.0~2801.4 mg/L O_2 with detection limit of 20.3 mg/L O_2 was achieved in the test of COD detection using 0.1 mol/L NaOH as the medium. Carchi and co-workers presented a work of modification of Cu electrode by filming with Nafion and anodic CuO for COD determination [81]. In this research, two copper-based electrodes were fabricated and coated with a layer of CuO nanomaterials in an electrochemical procedure in 0.1 mol/L NaOH solution, cycling (50 cycles) potential between −1.0 and +0.80 V vs. Ag/AgCl. This obtained COD sensor presented an analytical linear range of 50~1000 mg/L, with a detection limit of 2.11 mg/L (n = 6) O_2 in 0.1 mol/L NaOH medium.

In this thesis, anodization technique was employed for growing copper oxide nanostructures on copper plate substrate for analysis of organic pollutants in wastewater with use of the electronic tongue principles.

1.4.4 Electronic tongue for water analysis

As mentioned above, it is not easy to make all organic pollutants oxidized to carbon dioxide and water through electrochemical procedure. Current approaches for COD determination are based on oxidation of organic pollutants and corresponding changes of chemical, physics chemistry and electrochemical properties. However, wastewaters, especially industrial waste usually contains diverse organic compounds with complex structures, natures or concentration, which may result in low accuracy of detected COD values [163]. In practical COD test based on electrochemical measurements, a calibration curve showing the relationship between the COD values and

electrical signals is always required. However, sometimes these signals do not always reflect the COD values because of the complexity and diversity of organic pollution. Basically, the COD value can be estimated from the calibration curve only when the sample contains a single species. In this sense, electrochemical sensor array can be a promising tool for COD analysis because of the advantage of specifically identify and quantify certain compounds or groups of compounds, which can give more information about the organic pollutants [164]. Therefore, electrochemical sensor arrays, such as electronic tongues, emerge as promising tools for monitoring of water resources and provide more generic and global information [165]. The principle of the application of electronic tongue in water or wastewater analysis can be divided into four steps: sensor array preparation, electrochemical measurement (data collection), model building and analysis, as illustrated in Figure 1.18. Campos and co-workers proposed a voltammetric electronic tongue system for parameters prediction in a bioreactor pilot wastewater treatment plant [166]. The electronic tongue array was composed of a set of 8 metallic electrodes (Au, Pt, Rh, Ir, Ag, Ni, Co and Cu). A training/validation procedure was conducted in the electronic tongue research with a set of 28 samples for training and a set of 11 samples for validation. Then partial least squares (PLS) analysis was applied to obtain a correlation between the signals and the water quality parameters, such as soluble COD, soluble BOD, ammonia, orthophosphate, sulphate, acetic acid and alkalinity. It was demonstrated that the electronic tongue showed relatively better predictive power for the determination and evaluation of the general contamination status.

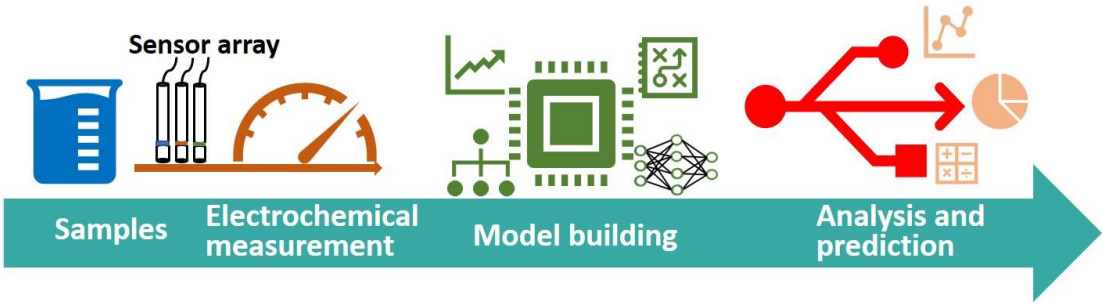

Figure 1.18 Principle of water analysis using electronic tongue technology.

1.5 Anxiolytic herbal medicinal products and protocol for quality control

1.5.1 Mental anxiety disorders

As reported by World Health Organization, there are more and more people suffering from mental health disorders, particularly in low-income countries where lots of people with high life burden and more people are reaching the age with high occurrence [167]. Generally, Mental health disorders consists of anxiety disorders and depressive disorders. Anxiety disorders can cause health problems in terms of fear and anxiety, which can occur in different types, e.g., social anxiety disorder, generalized anxiety disorder, panic disorder phobias, post-traumatic stress disorder (PTSD) and obsessive-compulsive disorder (OCD) [167]. Social anxiety disorder (13% lifetime prevalence), Generalized anxiety disorder (6.2% lifetime prevalence), and panic disorder (5.2% lifetime prevalence) are common anxiety disorders seen in primary care [168]. The symptoms tend to be chronic and the degrees can be mild, moderate and severe. Patients may suffer different symptoms according to different degrees, mainly including high blood pressure, palpitations, elevated heart rate, shortness of breath, sweating, fatigue, tension, irritability, insomnia, dizziness and restless. These symptoms can cause very negative influence to patients, aggravate the burden of patients' life and further cause impacts to society.

Patients would progress to depression and sometimes committee suicide without adequate treatment [169].

1.5.2 Herbal plants for anxiety disorders treatment

In addition to psychotherapy, pharmacotherapy is also a first-line treatment to anxiety disorders. Pharmacological therapy includes selective serotonin and norepinephrine reuptake inhibitors, selective serotonin reuptake inhibitors, pregabalin, buspirone, tricyclic antidepressants, monoamine oxidase inhibitors and benzodiazepines [169, 170]. However, such therapies with synthetic anxiolytics or antidepressants were reported to present certain adverse effects, including seizure, nausea, restlessness, addiction, headache, sexual dysfunction, fatigue, increased or decreased appetite, weight gain, weight loss and so on [171, 172]. These symptoms were reduced in cases where herbal medicines were used for treatment [171–173]. Some herbs and products derived from them that are dietary supplements or over-the-counter medicines are commonly used in the Western world for the above anxiety disorders treatment. The application of herbs is supported by the European Medicines Agency herbal monograph[169]. Lots of interest has been attracted by plant-derived natural products owing to their considerable beneficial effects. Flavonoids are natural polyphenol-like compounds, which can be found in some medicinal herbs [174]. Their positive therapeutic effects on anxiety and depression disorders have been demonstrated by preclinical studies [174, 175]. Some anxiolytic herbs, as introduced as following, were researched on their products' discrimination and authentication in this thesis.

- **Valerian:**

Valerian (*Valeriana officinalis* L.) is the species that has been studied a lot for its effects on different types of nervous alterations, including insomnia and anxiety. Valerian has a rhizome and a root with many secondary roots and

stolons, which is an important pharmaceutical source. It was confirmed that aqueous ethanol extracts of valerian root contain iridoids, flavonoids, etc [169]. The principal active compound of valerian was considered as the valerenic acid [170]. Studies indicated that valerian significantly reduced anxiety and various other psychiatric symptoms, such as insomnia or OCD, etc [176]. Various medicinal products made of valerian can be found for patients who are pursuing sense of relax, anxiolytic effect or improvement of sleeping quality and time.

Figure 1.19 Images of fresh valerian flower (A), plant and root (B) and loose valerian root product (C).

- **Chamomile**:

Chamomile (*Matricaria chamomilla* L.) has long been used as a medicinal plant to treat different pathologies and ailments around the world [177]. Aqueous standardized extract of chamomile flowers were reported to contain about 1.2% apigenin and 0.5% essential oils; quercetin, glucosides and various acetylated derivatives were also included [178]. Studies demonstrated that chamomile has good effects on treating patients with symptoms of anxiety disorders of different levels, as well as enhancing sleeping quality [179]. In addition, chamomile can also be used as an antidepressant in anxious patients with depression [180]. Teas, extracts and oils made from chamomile are used as a sedative, mild analgesic and sleep medication for its soothing qualities. Briefly, chamomile is an effective complementary treatment for anxiety and depression disorders and help decrease the related negative symptoms such as

insomnia.

(A) (B)

Figure 1.20 Images of fresh chamomile flowers (A) and loose chamomile flowers product (B).

- **Passionflower:**

Passionflower (*Passiflora incarnata* L.), also known as maypop, is commonly used in contemporary Western phytotherapy. It is a plant that has been used to treat insomnia traditionally [181]. In addition, it was tested without side effects in some preclinical experiments for treating anxiety disorders problems in clinical practices. The aqueous extract of passionflower contains many flavonoids, such as apigenin, chrysin, quercetin and so on [182]. It is widely accepted that passionflower's anxiolytic effects are associated with the phenolic substances, primarily from flavonoids. Different clinical trials have confirmed the anxiolytic and sedative effects of the aerial parts of this plant. Passionflower are now widely used for preparing anxiolytic pharmaceutical or health care products.

(A) (B)

Figure 1.21 Images of fresh passionflower aerial part (A) and loose passionflower product (B).

- **Lavender:**

Species of *Lavandula angustifolia* Mill., commonly known as English Lavender, is usually used in perfumes and in aromatherapy because its fragrance has a purported calming effect. Lavender flowers can also be used for the relief of mild symptoms of stress and exhaustion to aid sleep according to the European Medicines Agency monograph [183]. As reported, lavender flowers contain essential oil, tannins, phenolcarboxylic acids, flavonoids, coumarin derivatives, etc [184]. Its anxiolytic properties have also been demonstrated in pharmacological studies and some clinical trials [185]. Lavender oils and tea made of lavender flowers can be used as oral supplements for sleeping aids based on the property of calming nervous states in traditional and ancient medicinal uses. In addition, such products work for treatments of wounds, lice infestation, migraines, panic attacks and some heart problems, cold, bites, cramps and congestion.

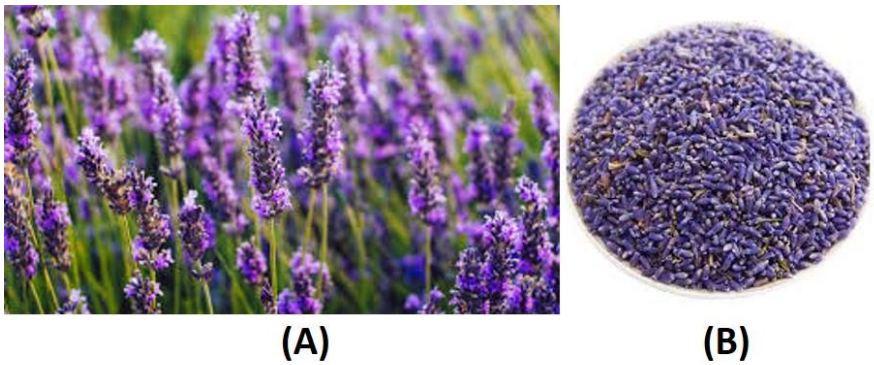

Figure 1.22 Images of fresh lavender flowers (A) and loose lavender flowers product (B).

1.5.3 Quality control of herbal medicinal products

Herbal medicines have already existed for centuries worldwide. Due to the advantages of lower toxicity, relatively low costs, increasing availability of

high-quality herbal drugs, the lower side-effect and the popular natural properties, the demand for medicinal products is showing an increasing tendency in recent years [186]. As reported by Globe Newswire, the global market for herbal medicines was estimated at US$110.2 billion in the year 2020 and is projected to reach US$178.4 billion by year 2026 [186]. In Europe, the consumption and demand of herbal drugs in pharmaceuticals are increasing as well. The European herbal medicine market will reach US$35.8 billion by 2026, predicted by Globe Newswire. This will make Europe become the second-largest market for herbal medicine worldwide, after Asia-Pacific [186].

Herbal medicinal products usually refer to products, e.g., tablets, powder, extracts, capsules, and tea forms, containing ingredients made from plants or natural resources. They are considered as safe and ideal alternatives with few or no side-effects to improve health and organ function. Although herbal medicinal products are considered natural remedies, it does not mean that they are always beneficial and safe. For instance, specific particularities can exist depending on the natural origins of the raw materials, the production processes and quality control, as well as the complex character of the products [187]. In addition, their purity must be an important factor since these plants may be exposed to various environmental influences [187]. Therefore, quality control is crucial in the entire process of production of medicinal drugs, from raw materials to products. To produce herbal medicine or health-care products, the first step is to identify the herb species correctly. Therefore, it is foundational to research and develop approaches for accurate and efficient herbal authentication. In the past, selection of herbs was relied on experienced herbalists according to morphologies, smell, colour and taste [188]. Nevertheless, such traditional methods could be too subjective and inefficient. Advanced technologies need to be invented to provide much more precise information and be suitable to complex systems along with the increasing

demand of multitudinous herbal products. The existence of multiple preparations for the same type of herb (e.g., tablet, infusion, drop) increases the difficulty in their quality control, which facilitates the possibility of frauds and tampering [189]. In addition, the quality of products is also related to their price establishment. When different parts of the plant may be used to obtain the infusions or other forms, activity and quality of the preparation may well be highly dependent on the proportions used. Therefore, higher proportions of the most active part should be much better valued than others. In a word, the identification, characterization and authentication of herbal medicinal products is a subject in terms of safety and the development of herbal medicinal products market.

Reference

[1] F. Regan, Sensors | Overview☆, in: P. Worsfold, C. Poole, A. Townshend, M. Miró (Eds.), Encyclopedia of Analytical Science (Third Edition), Academic Press, Oxford, 2019: pp. 172–178. https://doi.org/10.1016/B978-0-12-409547-2.14540-8.

[2] A. Hulanicki, S. Glab, F. Ingman, Chemical sensors: definitions and classification, Pure and Applied Chemistry. 63 (1991) 1247–1250. https://doi.org/10.1351/pac199163091247.

[3] L. Eddaif, A. Shaban, Chapter 2 - Fundamentals of sensor technology, in: A. Barhoum, Z. Altintas (Eds.), Advanced Sensor Technology, Elsevier, 2023: pp. 17–49. https://doi.org/10.1016/B978-0-323-90222-9.00003-0.

[4] H. Bi, X. Han, 10 - Chemical sensors for environmental pollutant determination, in: K. Mitsubayashi, O. Niwa, Y. Ueno (Eds.), Chemical, Gas, and Biosensors for Internet of Things and Related Applications, Elsevier, 2019: pp. 147–160. https://doi.org/10.1016/B978-0-12-815409-0.00010-3.

[5] J. Baranwal, B. Barse, G. Gatto, G. Broncova, A. Kumar, Electrochemical Sensors and Their Applications: A Review, Chemosensors. 10 (2022) 363. https://doi.org/10.3390/chemosensors10090363.

[6] T. Li, X. Zhu, X. Hai, S. Bi, X. Zhang, Recent Progress in Sensor Arrays: From Construction Principles of Sensing Elements to Applications, ACS Sens. (2023). https://doi.org/10.1021/acssensors.2c02596.

[7] M. Bonet-San-Emeterio, X. Cetó, M. del Valle, Voltammetric electronic tongues, in: Electron. Tongues Fundam. Recent Adv., IOP Publishing, 2021. https://doi.org/10.1088/978-0-7503-3687-1ch4.

[8] F. Röck, N. Barsan, U. Weimar, Electronic Nose: Current Status and Future Trends, Chemical Reviews. 108 (2008) 705–25. https://doi.org/10.1021/cr068121q.

[9] A. Rudnitskaya, Sensors | Biomimetic Sensor Arrays, in: P. Worsfold, C. Poole, A. Townshend, M. Miró (Eds.), Encyclopedia of Analytical Science (Third Edition), Academic Press, Oxford, 2019: pp. 154–160. https://doi.org/10.1016/B978-0-12-409547-2.13935-6.

[10] N. Seddaoui, A. Amine, Chapter 19 - Recent advances in sensor and biosensor technologies for adulteration detection, in: A. Barhoum, Z. Altintas (Eds.), Adv. Sens. Technol., Elsevier, 2023: pp. 699–739. https://doi.org/10.1016/B978-0-323-90222-9.00017-0.

[11] D.W. Kimmel, G. LeBlanc, M.E. Meschievitz, D.E. Cliffel, Electrochemical Sensors and Biosensors, Anal. Chem. 84 (2012) 685–707. https://doi.org/10.1021/ac202878q.

[12] B.J. Venton, D.J. DiScenza, Chapter 3 - Voltammetry, in: B. Patel (Ed.),

Electrochem. Bioanal., Elsevier, 2020: pp. 27–50. https://doi.org/10.1016/B978-0-12-821203-5.00004-X.

[13] F. Scholz, Voltammetric techniques of analysis: the essentials, ChemTexts. 1 (2015) 17. https://doi.org/10.1007/s40828-015-0016-y.

[14] C. Dincer, R. Bruch, E. Costa-Rama, M.T. Fernández-Abedul, A. Merkoçi, A. Manz, G.A. Urban, F. Güder, Disposable Sensors in Diagnostics, Food, and Environmental Monitoring, Adv Mater. 31 (2019) e1806739. https://doi.org/10.1002/adma.201806739.

[15] B.E. Rapp, Electrochemical Methods for Biomass and Biocorrosion Monitoring, in: K. Wandelt (Ed.), Encyclopedia of Interfacial Chemistry, Elsevier, Oxford, 2018: pp. 166–172. https://doi.org/10.1016/B978-0-12-409547-2.13507-3.

[16] D. Grieshaber, R. MacKenzie, J. Vörös, E. Reimhult, Electrochemical Biosensors - Sensor Principles and Architectures, Sensors. 8 (2008) 1400–1458. https://doi.org/10.3390/s80314000.

[17] E. Randviir, C. Banks, Electrochemical impedance spectroscopy: An overview of bioanalytical applications, Analytical Methods. 5 (2013) 1098–1115. https://doi.org/10.1039/c3ay26476a.

[18] S. Wang, J. Zhang, O. Gharbi, V. Vivier, M. Gao, M.E. Orazem, Electrochemical impedance spectroscopy, Nat Rev Methods Primers. 1 (2021) 1–21. https://doi.org/10.1038/s43586-021-00039-w.

[19] N.K. Bakirhan, B. Uslu, S.A. Ozkan, Chapter 3 - Sensitive and Selective Assay of Antimicrobials on Nanostructured Materials by Electrochemical Techniques, in: A. Ficai, A.M. Grumezescu (Eds.), Nanostructures Antimicrob. Ther., Elsevier, 2017: pp. 55–83. https://doi.org/10.1016/B978-0-323-46152-8.00003-2.

[20] C.M.G. Ribeiro, C. de M. Strunkis, P.V.S. Campos, M.O. Salles, Sensing Materials: Electronic Nose and Tongue Materials, in: R. Narayan (Ed.), Encyclopedia of Sensors and Biosensors (First Edition), Elsevier, Oxford, 2023: pp. 231–253. https://doi.org/10.1016/B978-0-12-822548-6.00035-2.

[21] P. Ciosek, W. Wróblewski, Sensor arrays for liquid sensing – electronic tongue systems, Analyst. 132 (2007) 963–978. https://doi.org/10.1039/B705107G.

[22] Y. Vlasov, A. Legin, A. Rudnitskaya, C.D. Natale, A. D'Amico, Nonspecific sensor arrays ("electronic tongue") for chemical analysis of liquids (IUPAC Technical Report), Pure and Applied Chemistry. 77 (2005) 1965–1983. https://doi.org/10.1351/pac200577111965.

[23] S.M.T. Gharibzahedi, F.J. Barba, J. Zhou, M. Wang, Z. Altintas, Electronic Sensor Technologies in Monitoring Quality of Tea: A Review, Biosensors (Basel). 12 (2022) 356. https://doi.org/10.3390/bios12050356.

[24] M. Podrażka, E. Bączyńska, M. Kundys, P.S. Jeleń, E. Witkowska Nery, Electronic Tongue—A Tool for All Tastes?, Biosensors. 8 (2018) 3. https://doi.org/10.3390/bios8010003.

[25] L. Bagnasco, M.E. Cosulich, G. Speranza, L. Medini, P. Oliveri, S. Lanteri, Application of a voltammetric electronic tongue and near infrared spectroscopy for a rapid umami taste assessment, Food Chemistry. 157 (2014) 421–428. https://doi.org/10.1016/j.foodchem.2014.02.044.

[26] X. Cetó, S. Pérez, B. Prieto-Simón, Fundamentals and application of voltammetric electronic tongues in quantitative analysis, TrAC Trends in Analytical Chemistry. 157 (2022) 116765. https://doi.org/10.1016/j.trac.2022.116765.

[27] L. Wang, Q. Niu, Y. Hui, H. Jin, Discrimination of Rice with Different Pretreatment Methods by Using a Voltammetric Electronic Tongue, Sensors. 15 (2015) 17767–17785. https://doi.org/10.3390/s150717767.

[28] F. Winquist, Voltammetric electronic tongues – basic principles and applications, Microchim Acta. 163 (2008) 3–10. https://doi.org/10.1007/s00604-007-0929-2.

[29] C. Pérez-Ràfols, N. Serrano, C. Ariño, M. Esteban, J.M. Díaz-Cruz, Voltammetric Electronic Tongues in Food Analysis, Sensors (Basel). 19 (2019) 4261. https://doi.org/10.3390/s19194261.

[30] R.I. Mukhamediev, Y. Popova, Y. Kuchin, E. Zaitseva, A. Kalimoldayev, A. Symagulov, V. Levashenko, F. Abdoldina, V. Gopejenko, K. Yakunin, E. Muhamedijeva, M. Yelis, Review of Artificial Intelligence and Machine Learning Technologies: Classification, Restrictions, Opportunities and Challenges, Mathematics. 10 (2022) 2552. https://doi.org/10.3390/math10152552.

[31] N. Artrith, K.T. Butler, F.-X. Coudert, S. Han, O. Isayev, A. Jain, A. Walsh, Best practices in machine learning for chemistry, Nat Chem. 13 (2021) 505–508. https://doi.org/10.1038/s41557-021-00716-z.

[32] J.A. Cruz, D.S. Wishart, Applications of Machine Learning in Cancer Prediction and Prognosis, Cancer Inform. 2 (2006) 117693510600200030. https://doi.org/10.1177/117693510600200030.

[33] M.S. Mahdavinejad, M. Rezvan, M. Barekatain, P. Adibi, P. Barnaghi, A.P. Sheth, Machine learning for internet of things data analysis: a survey, Digital Communications and Networks. 4 (2018) 161–175. https://doi.org/10.1016/j.dcan.2017.10.002.

[34] F. Recknagel, Applications of machine learning to ecological modelling, Ecological Modelling. 146 (2001) 303–310. https://doi.org/10.1016/S0304-3800(01)00316-7.

[35] M. Ali, L.T. Jung, A.-H. Abdel-Aty, M.Y. Abubakar, M. Elhoseny, I. Ali, Semantic-k-NN algorithm: An enhanced version of traditional k-NN algorithm, Expert Systems with Applications. 151 (2020) 113374. https://doi.org/10.1016/j.eswa.2020.113374.

[36] G.A. Ruz, P. Araya-Díaz, P.A. Henríquez, Facial biotype classification for orthodontic treatment planning using an alternative learning algorithm for tree augmented Naive Bayes, BMC Medical Informatics and Decision Making. 22 (2022) 316. https://doi.org/10.1186/s12911-022-02062-7.

[37] What is Supervised Learning? | IBM, (n.d.). https://www.ibm.com/topics/supervised-learning (accessed June 8, 2023).

[38] L. Nguyen, T.-H. Nguyen Vo, Q.H. Trinh, B.H. Nguyen, P.-U. Nguyen-Hoang, L. Le, B.P. Nguyen, iANP-EC: Identifying Anticancer Natural Products Using Ensemble Learning Incorporated with Evolutionary Computation, J. Chem. Inf. Model. 62 (2022) 5080–5089. https://doi.org/10.1021/acs.jcim.1c00920.

[39] J.-L. Solorio-Ramírez, R. Jiménez-Cruz, Y. Villuendas-Rey, C. Yáñez-Márquez, Random Forest Algorithm for the Classification of Spectral Data of Astronomical Objects, Algorithms. 16 (2023) 293. https://doi.org/10.3390/a16060293.

[40] K. Kumari, S. Yadav, Linear regression analysis study, Journal of the Practice of Cardiovascular Sciences. 4 (2018) 33. https://doi.org/10.4103/jpcs.jpcs_8_18.

[41] J. Peng, K. Lee, G. Ingersoll, An Introduction to Logistic Regression Analysis and Reporting, Journal of Educational Research - J EDUC RES. 96 (2002) 3–14. https://doi.org/10.1080/00220670209598786.

[42] What are Neural Networks? | IBM, (n.d.). https://www.ibm.com/topics/neural-networks (accessed June 13, 2023).
[43] A. Krogh, What are artificial neural networks?, Nat Biotechnol. 26 (2008) 195–197. https://doi.org/10.1038/nbt1386.
[44] A. Malekian, N. Chitsaz, Chapter 4 - Concepts, procedures, and applications of artificial neural network models in streamflow forecasting, in: P. Sharma, D. Machiwal (Eds.), Advances in Streamflow Forecasting, Elsevier, 2021: pp. 115–147. https://doi.org/10.1016/B978-0-12-820673-7.00003-2.
[45] R. Sadiq, M.J. Rodriguez, H.R. Mian, Empirical Models to Predict Disinfection By-Products (DBPs) in Drinking Water: An Updated Review☆, in: J. Nriagu (Ed.), Encyclopedia of Environmental Health (Second Edition), Elsevier, Oxford, 2019: pp. 324–338. https://doi.org/10.1016/B978-0-12-409548-9.11193-5.
[46] What is Unsupervised Learning? | IBM, (n.d.). https://www.ibm.com/topics/unsupervised-learning (accessed June 8, 2023).
[47] I.T. Jolliffe, J. Cadima, Principal component analysis: a review and recent developments, Philosophical Transactions of the Royal Society A: Mathematical, Physical and Engineering Sciences. 374 (2016) 20150202. https://doi.org/10.1098/rsta.2015.0202.
[48] A.M. Ikotun, A.E. Ezugwu, L. Abualigah, B. Abuhaija, J. Heming, K-means clustering algorithms: A comprehensive review, variants analysis, and advances in the era of big data, Information Sciences. 622 (2023) 178–210. https://doi.org/10.1016/j.ins.2022.11.139.
[49] I. Tzouvadaki, T. Prodromakis, Large-scale nano-biosensing technologies, Frontiers in Nanotechnology. 5 (2023). https://www.frontiersin.org/articles/10.3389/fnano.2023.1127363 (accessed April 4, 2023).
[50] A. Curulli, Nanomaterials in Electrochemical Sensing Area: Applications and Challenges in Food Analysis, Molecules. 25 (2020) 5759. https://doi.org/10.3390/molecules25235759.
[51] N. Verma, N. Kumar, Synthesis and Biomedical Applications of Copper Oxide Nanoparticles: An Expanding Horizon, ACS Biomater. Sci. Eng. 5 (2019) 1170–1188. https://doi.org/10.1021/acsbiomaterials.8b01092.
[52] C. Contado, Nanomaterials in consumer products: a challenging analytical problem, Frontiers in Chemistry. 3 (2015). https://www.frontiersin.org/articles/10.3389/fchem.2015.00048 (accessed April 4, 2023).
[53] A. Chen, S. Chatterjee, Nanomaterials based electrochemical sensors for biomedical applications, Chem. Soc. Rev. 42 (2013) 5425–5438. https://doi.org/10.1039/C3CS35518G.
[54] M. Ramya, P. Senthil Kumar, G. Rangasamy, V. Uma shankar, G. Rajesh, K. Nirmala, A. Saravanan, A. Krishnapandi, A recent advancement on the applications of nanomaterials in electrochemical sensors and biosensors, Chemosphere. 308 (2022) 136416. https://doi.org/10.1016/j.chemosphere.2022.136416.
[55] I.M. Handrea-Dragan, I. Botiz, A.-S. Tatar, S. Boca, Patterning at the micro/nano-scale: Polymeric scaffolds for medical diagnostic and cell-surface interaction applications, Colloids Surf B Biointerfaces. 218 (2022) 112730. https://doi.org/10.1016/j.colsurfb.2022.112730.
[56] H. Kaur, S.S. Siwal, G. Chauhan, A.K. Saini, A. Kumari, V.K. Thakur, Recent

advances in electrochemical-based sensors amplified with carbon-based nanomaterials (CNMs) for sensing pharmaceutical and food pollutants, Chemosphere. 304 (2022) 135182. https://doi.org/10.1016/j.chemosphere.2022.135182.

[57] P. Huang, X. Wang, X. Liang, J. Yang, C. Zhang, D. Kong, W. Wang, Nano-, micro-, and macroscale drug delivery systems for cancer immunotherapy, Acta Biomater. 85 (2019) 1–26. https://doi.org/10.1016/j.actbio.2018.12.028.

[58] H.A. Potes-Lesoinne, F. Ramirez-Alvarez, V.H. Perez-Gonzalez, S.O. Martinez-Chapa, R.C. Gallo-Villanueva, Nanomaterials for electrochemical detection of pollutants in water: A review, Electrophoresis. 43 (2022) 249–262. https://doi.org/10.1002/elps.202100204.

[59] X. Luo, A. Morrin, A.J. Killard, M.R. Smyth, Application of Nanoparticles in Electrochemical Sensors and Biosensors, Electroanalysis. 18 (2006) 319–326. https://doi.org/10.1002/elan.200503415.

[60] Y. Yoon, P.L. Truong, D. Lee, S.H. Ko, Metal-Oxide Nanomaterials Synthesis and Applications in Flexible and Wearable Sensors, ACS Nanosci. Au. 2 (2022) 64–92. https://doi.org/10.1021/acsnanoscienceau.1c00029.

[61] D. Giziński, A. Brudzisz, J.S. Santos, F. Trivinho-Strixino, W.J. Stępniowski, T. Czujko, Nanostructured Anodic Copper Oxides as Catalysts in Electrochemical and Photoelectrochemical Reactions, Catalysts. 10 (2020) 1338. https://doi.org/10.3390/catal10111338.

[62] G.D. Sulka, Chapter one - Introduction to anodization of metals, in: G.D. Sulka (Ed.), Nanostructured Anodic Metal Oxides, Elsevier, 2020: pp. 1–34. https://doi.org/10.1016/B978-0-12-816706-9.00001-7.

[63] Y. Wan, Y. Zhang, X. Wang, Q. Wang, Electrochemical formation and reduction of copper oxide nanostructures in alkaline media, Electrochemistry Communications. 36 (2013) 99–102. https://doi.org/10.1016/j.elecom.2013.09.026.

[64] Z. Li, Y. Chen, Y. Xin, Z. Zhang, Sensitive electrochemical nonenzymatic glucose sensing based on anodized CuO nanowires on three-dimensional porous copper foam, Scientific Reports. 5 (2015) 16115. https://doi.org/10.1038/srep16115.

[65] A.M. Md Jani, D. Losic, N.H. Voelcker, Nanoporous anodic aluminium oxide: Advances in surface engineering and emerging applications, Progress in Materials Science. 58 (2013) 636–704. https://doi.org/10.1016/j.pmatsci.2013.01.002.

[66] D. Kowalski, D. Kim, P. Schmuki, TiO2 nanotubes, nanochannels and mesosponge: Self-organized formation and applications, Nano Today. 8 (2013) 235–264. https://doi.org/10.1016/j.nantod.2013.04.010.

[67] E. Wierzbicka, G.D. Sulka, Fabrication of highly ordered nanoporous thin Au films and their application for electrochemical determination of epinephrine, Sensors and Actuators B: Chemical. 222 (2016) 270–279. https://doi.org/10.1016/j.snb.2015.08.066.

[68] C.S. Law, A. Santos, T. Kumeria, D. Losic, Engineered Therapeutic-Releasing Nanoporous Anodic Alumina-Aluminum Wires with Extended Release of Therapeutics, ACS Appl. Mater. Interfaces. 7 (2015) 3846–3853. https://doi.org/10.1021/am5091963.

[69] X. Feng, K. Shankar, M. Paulose, C.A. Grimes, Tantalum-Doped Titanium Dioxide Nanowire Arrays for Dye-Sensitized Solar Cells with High Open-Circuit Voltage, Angewandte Chemie. 121 (2009) 8239–8242.

https://doi.org/10.1002/ange.200903114.
[70] T. Ohta, H. Masegi, K. Noda, Photocatalytic decomposition of gaseous methanol over anodized iron oxide nanotube arrays in high vacuum, Materials Research Bulletin. 99 (2018) 367–376. https://doi.org/10.1016/j.materresbull.2017.11.027.
[71] J. Park, K. Kim, J. Choi, Formation of ZnO nanowires during short durations of potentiostatic and galvanostatic anodization, Current Applied Physics. 13 (2013) 1370–1375. https://doi.org/10.1016/j.cap.2013.04.015.
[72] L. Zaraska, K. Gawlak, M. Gurgul, D.K. Chlebda, R.P. Socha, G.D. Sulka, Controlled synthesis of nanoporous tin oxide layers with various pore diameters and their photoelectrochemical properties, Electrochimica Acta. 254 (2017) 238–245. https://doi.org/10.1016/j.electacta.2017.09.113.
[73] M. Pisarek, J. Krajczewski, E. Wierzbicka, M. Hołdyński, G.D. Sulka, R. Nowakowski, A. Kudelski, M. Janik-Czachor, Influence of the silver deposition method on the activity of platforms for chemometric surface-enhanced Raman scattering measurements: Silver films on ZrO2 nanopore arrays, Spectrochimica Acta Part A: Molecular and Biomolecular Spectroscopy. 182 (2017) 124–129. https://doi.org/10.1016/j.saa.2017.04.005.
[74] W.J. Stepniowski, W.Z. Misiolek, Review of Fabrication Methods, Physical Properties, and Applications of Nanostructured Copper Oxides Formed via Electrochemical Oxidation, Nanomaterials. 8 (2018) 379. https://doi.org/10.3390/nano8060379.
[75] A.S. Zoolfakar, R.A. Rani, A.J. Morfa, A.P. O'Mullane, K. Kalantar-zadeh, Nanostructured copper oxide semiconductors: a perspective on materials, synthesis methods and applications, J. Mater. Chem. C. 2 (2014) 5247–5270. https://doi.org/10.1039/C4TC00345D.
[76] W.J. Stepniowski, W.Z. Misiolek, Chapter thirteen - Nanostructured anodic films grown on copper: a review of fabrication techniques and applications, in: G.D. Sulka (Ed.), Nanostructured Anodic Metal Oxides, Elsevier, 2020: pp. 415–452. https://doi.org/10.1016/B978-0-12-816706-9.00013-3.
[77] S.D. Giri, A. Sarkar, Electrochemical Study of Bulk and Monolayer Copper in Alkaline Solution, J. Electrochem. Soc. 163 (2016) H252. https://doi.org/10.1149/2.0071605jes.
[78] J. Ambrose, R.G. Barradas, D.W. Shoesmith, Investigations of copper in aqueous alkaline solutions by cyclic voltammetry, Journal of Electroanalytical Chemistry and Interfacial Electrochemistry. 47 (1973) 47–64. https://doi.org/10.1016/S0022-0728(73)80344-4.
[79] M. Gutiérrez-Capitán, A. Baldi, R. Gómez, V. García, C. Jiménez-Jorquera, C. Fernández-Sánchez, Electrochemical Nanocomposite-Derived Sensor for the Analysis of Chemical Oxygen Demand in Urban Wastewaters, Anal. Chem. 87 (2015) 2152–2160. https://doi.org/10.1021/ac503329a.
[80] N. Torto, T. Ruzgas, L. Gorton, Electrochemical oxidation of mono- and disaccharides at fresh as well as oxidized copper electrodes in alkaline media, Journal of Electroanalytical Chemistry. 464 (1999) 252–258. https://doi.org/10.1016/S0022-0728(99)00041-8.
[81] T. Carchi, B. Lapo, J. Alvarado, P.J. Espinoza-Montero, J. Llorca, L. Fernández, A Nafion Film Cover to Enhance the Analytical Performance of the CuO/Cu Electrochemical Sensor for Determination of Chemical Oxygen Demand, Sensors. 19 (2019) 669. https://doi.org/10.3390/s19030669.
[82] C.R. Silva, C.D.C. Conceição, V.G. Bonifácio, O.F. Filho, M.F.S. Teixeira,

Determination of the chemical oxygen demand (COD) using a copper electrode: a clean alternative method, J Solid State Electrochem. 13 (2009) 665–669. https://doi.org/COD.

[83] N. Baig, I. Kammakakam, W. Falath, Nanomaterials: a review of synthesis methods, properties, recent progress, and challenges, Mater. Adv. 2 (2021) 1821–1871. https://doi.org/10.1039/D0MA00807A.

[84] W. Chen, S. Liu, Y. Fu, H. Yan, L. Qin, C. Lai, C. Zhang, H. Ye, W. Chen, F. Qin, F. Xu, X. Huo, H. Qin, Recent advances in photoelectrocatalysis for environmental applications: Sensing, pollutants removal and microbial inactivation, Coordination Chemistry Reviews. 454 (2022) 214341. https://doi.org/10.1016/j.ccr.2021.214341.

[85] V.S. Manikandan, B. Adhikari, A. Chen, Nanomaterial based electrochemical sensors for the safety and quality control of food and beverages, Analyst. 143 (2018) 4537–4554. https://doi.org/10.1039/C8AN00497H.

[86] T. Bahru, E. Ajebe, A Review on Nanotechnology: Analytical Techniques Use and Applications, International Research Journal of Pure and Applied Chemistry. (2019) 1–10. https://doi.org/10.9734/irjpac/2019/v19i430117.

[87] L. Lin, H. Yang, X. Xu, Effects of Water Pollution on Human Health and Disease Heterogeneity: A Review, Frontiers in Environmental Science. 10 (2022). https://www.frontiersin.org/articles/10.3389/fenvs.2022.880246 (accessed April 14, 2023).

[88] Green growth and water - OECD, (n.d.). https://www.oecd.org/greengrowth/water-and-green-growth.htm (accessed April 14, 2023).

[89] nina, Progress on household drinking water, sanitation and hygiene, 2000-2020: Five years into the SDGs, UNICEF DATA. (2021). https://data.unicef.org/resources/progress-on-household-drinking-water-sanitation-and-hygiene-2000-2020/ (accessed April 14, 2023).

[90] M. Irannezhad, B. Ahmadi, J. Liu, D. Chen, J.H. Matthews, Global water security: A shining star in the dark sky of achieving the sustainable development goals, Sustainable Horizons. 1 (2022) 100005. https://doi.org/10.1016/j.horiz.2021.100005.

[91] The United Nations world water development report, 2017: Wastewater: the untapped resource - UNESCO Digital Library, (n.d.). https://unesdoc.unesco.org/ark:/48223/pf0000247153 (accessed April 27, 2023).

[92] H.M. Murphy, K.D.M. Pintar, E.A. McBean, M.K. Thomas, A systematic review of waterborne disease burden methodologies from developed countries, J Water Health. 12 (2014) 634–655. https://doi.org/10.2166/wh.2014.049.

[93] G. Cissé, Food-borne and water-borne diseases under climate change in low- and middle-income countries: Further efforts needed for reducing environmental health exposure risks, Acta Trop. 194 (2019) 181–188. https://doi.org/10.1016/j.actatropica.2019.03.012.

[94] U.D.-G. authorCorporate:UNESCO World Water Assessment Programme, United Nations world water development report 4: managing water under uncertainty and risk, (2012). https://unesdoc.unesco.org/ark:/48223/pf0000217175?posInSet=5&queryId=N-EXPLORE-50221b72-65f3-4475-84fe-2d1b943ef96a (accessed April 13, 2023).

[95] A.A. Lanrewaju, A.M. Enitan-Folami, S. Sabiu, F.M. Swalaha, A review on disinfection methods for inactivation of waterborne viruses, Frontiers in Microbiology. 13 (2022).

https://www.frontiersin.org/articles/10.3389/fmicb.2022.991856 (accessed April 14, 2023).

[96] F.M. Wilhelm, Pollution of Aquatic Ecosystems I, in: G.E. Likens (Ed.), Encyclopedia of Inland Waters, Academic Press, Oxford, 2009: pp. 110–119. https://doi.org/10.1016/B978-012370626-3.00222-2.

[97] C. Tuser, What is Wastewater?, Wastewater Digest. (2021). https://www.wwdmag.com/wastewater-treatment/wastewater-treatment/article/10938418/what-is-wastewater (accessed May 8, 2023).

[98] S. Chowdhury, N. Khan, G.-H. Kim, J. Harris, P. Longhurst, N.S. Bolan, Chapter 22 - Zeolite for Nutrient Stripping From Farm Effluents, in: M.N.V. Prasad, K. Shih (Eds.), Environmental Materials and Waste, Academic Press, 2016: pp. 569–589. https://doi.org/10.1016/B978-0-12-803837-6.00022-6.

[99] A. Ojha, D. Tiwary, Chapter 16 - Organic pollutants in water and its health risk assessment through consumption, in: A. Ahamad, S.I. Siddiqui, P. Singh (Eds.), Contamination of Water, Academic Press, 2021: pp. 237–250. https://doi.org/10.1016/B978-0-12-824058-8.00039-6.

[100] Y.V. Nancharaiah, S. Venkata Mohan, P.N.L. Lens, Recent advances in nutrient removal and recovery in biological and bioelectrochemical systems, Bioresour Technol. 215 (2016) 173–185. https://doi.org/10.1016/j.biortech.2016.03.129.

[101] C.M. Manaia, J. Rocha, N. Scaccia, R. Marano, E. Radu, F. Biancullo, F. Cerqueira, G. Fortunato, I.C. Iakovides, I. Zammit, I. Kampouris, I. Vaz-Moreira, O.C. Nunes, Antibiotic resistance in wastewater treatment plants: Tackling the black box, Environ Int. 115 (2018) 312–324. https://doi.org/10.1016/j.envint.2018.03.044.

[102] J. De Vrieze, D. Smet, J. Klok, J. Colsen, L.T. Angenent, S.E. Vlaeminck, Thermophilic sludge digestion improves energy balance and nutrient recovery potential in full-scale municipal wastewater treatment plants, Bioresour Technol. 218 (2016) 1237–1245. https://doi.org/10.1016/j.biortech.2016.06.119.

[103] K.A. Gilbride, D.-Y. Lee, L.A. Beaudette, Molecular techniques in wastewater: Understanding microbial communities, detecting pathogens, and real-time process control, J Microbiol Methods. 66 (2006) 1–20. https://doi.org/10.1016/j.mimet.2006.02.016.

[104] U. Stottmeister, A. Wiessner, P. Kuschk, U. Kappelmeyer, M. Kästner, O. Bederski, R.A. Müller, H. Moormann, Effects of plants and microorganisms in constructed wetlands for wastewater treatment, Biotechnol Adv. 22 (2003) 93–117. https://doi.org/10.1016/j.biotechadv.2003.08.010.

[105] T. Mackuľak, K. Cverenkárová, A. Vojs Staňová, M. Fehér, M. Tamáš, A.B. Škulcová, M. Gál, M. Naumowicz, V. Špalková, L. Bírošová, Hospital Wastewater-Source of Specific Micropollutants, Antibiotic-Resistant Microorganisms, Viruses, and Their Elimination, Antibiotics (Basel). 10 (2021) 1070. https://doi.org/10.3390/antibiotics10091070.

[106] T.N.-D. Cao, X.-T. Bui, L.-T. Le, B.-T. Dang, D.P.-H. Tran, T.-K.-Q. Vo, H.-T. Tran, T.-B. Nguyen, H. Mukhtar, S.-Y. Pan, S. Varjani, H.H. Ngo, T.-D.-H. Vo, An overview of deploying membrane bioreactors in saline wastewater treatment from perspectives of microbial and treatment performance, Bioresour Technol. 363 (2022) 127831. https://doi.org/10.1016/j.biortech.2022.127831.

[107] D. Marathe, A. Singh, K. Raghunathan, P. Thawale, K. Kumari, Current available treatment technologies for saline wastewater and land-based treatment as an emerging environment-friendly technology: A review, Water Environ Res.

93 (2021) 2461–2504. https://doi.org/10.1002/wer.1633.
[108] X. Tan, I. Acquah, H. Liu, W. Li, S. Tan, A critical review on saline wastewater treatment by membrane bioreactor (MBR) from a microbial perspective, Chemosphere. 220 (2019) 1150–1162. https://doi.org/10.1016/j.chemosphere.2019.01.027.
[109] J. Li, P. Qi, Z. Qiang, H. Dong, D. Gao, D. Wang, Is anammox a promising treatment process for nitrogen removal from nitrogen-rich saline wastewater?, Bioresour Technol. 270 (2018) 722–731. https://doi.org/10.1016/j.biortech.2018.08.115.
[110] M. Kumar, M. Nandi, K. Pakshirajan, Recent advances in heavy metal recovery from wastewater by biogenic sulfide precipitation, J Environ Manage. 278 (2021) 111555. https://doi.org/10.1016/j.jenvman.2020.111555.
[111] M. Hejna, E. Onelli, A. Moscatelli, M. Bellotto, C. Cristiani, N. Stroppa, L. Rossi, Heavy-Metal Phytoremediation from Livestock Wastewater and Exploitation of Exhausted Biomass, Int J Environ Res Public Health. 18 (2021) 2239. https://doi.org/10.3390/ijerph18052239.
[112] H. Znad, M.R. Awual, S. Martini, The Utilization of Algae and Seaweed Biomass for Bioremediation of Heavy Metal-Contaminated Wastewater, Molecules. 27 (2022) 1275. https://doi.org/10.3390/molecules27041275.
[113] H. Li, J. Watson, Y. Zhang, H. Lu, Z. Liu, Environment-enhancing process for algal wastewater treatment, heavy metal control and hydrothermal biofuel production: A critical review, Bioresour Technol. 298 (2020) 122421. https://doi.org/10.1016/j.biortech.2019.122421.
[114] M.M. Damtie, Y.C. Woo, B. Kim, R.H. Hailemariam, K.-D. Park, H.K. Shon, C. Park, J.-S. Choi, Removal of fluoride in membrane-based water and wastewater treatment technologies: Performance review, J Environ Manage. 251 (2019) 109524. https://doi.org/10.1016/j.jenvman.2019.109524.
[115] A.D. Lemly, Symptoms and implications of selenium toxicity in fish: the Belews Lake case example, Aquat Toxicol. 57 (2002) 39–49. https://doi.org/10.1016/s0166-445x(01)00264-8.
[116] C.F. Okey-Onyesolu, O.D. Onukwuli, M.I. Ejimofor, C.C. Okoye, Kinetics and mechanistic analysis of particles decontamination from abattoir wastewater (ABW) using novel Fish Bone Chito-protein (FBC), Heliyon. 6 (2020) e04468. https://doi.org/10.1016/j.heliyon.2020.e04468.
[117] S. Li, Q. Zhu, J. Luo, Y. Shu, K. Guo, J. Xie, F. Xiao, S. He, Application Progress of Deinococcus radiodurans in Biological Treatment of Radioactive Uranium-Containing Wastewater, Indian J Microbiol. 61 (2021) 417–426. https://doi.org/10.1007/s12088-021-00969-9.
[118] J. Lalwani, A. Gupta, S. Thatikonda, C. Subrahmanyam, An industrial insight on treatment strategies of the pharmaceutical industry effluent with varying qualitative characteristics, Journal of Environmental Chemical Engineering. 8 (2020) 104190. https://doi.org/10.1016/j.jece.2020.104190.
[119] I.K. Konstantinou, T.A. Albanis, TiO2-assisted photocatalytic degradation of azo dyes in aqueous solution: kinetic and mechanistic investigations: A review, Applied Catalysis B: Environmental. 49 (2004) 1–14. https://doi.org/10.1016/j.apcatb.2003.11.010.
[120] M. Antonopoulou, Homogeneous and Heterogeneous Photocatalysis for the Treatment of Pharmaceutical Industry Wastewaters: A Review, Toxics. 10 (2022) 539. https://doi.org/10.3390/toxics10090539.
[121] P. Chowdhary, R. Bharagava, S. Mishra, N. Khan, Role of Industries in Water

Scarcity and Its Adverse Effects on Environment and Human Health, in: 2020: pp. 235–256. https://doi.org/10.1007/978-981-13-5889-0_12.

[122] H. Wu, Z. Gai, Y. Guo, Y. Li, Y. Hao, Z.-N. Lu, Does environmental pollution inhibit urbanization in China? A new perspective through residents' medical and health costs, Environ Res. 182 (2020) 109128. https://doi.org/10.1016/j.envres.2020.109128.

[123] S. Agarwal, S. Darbar, S. Saha, Chapter 25 - Challenges in management of domestic wastewater for sustainable development, in: A.L. Srivastav, S. Madhav, A.K. Bhardwaj, E. Valsami-Jones (Eds.), Current Directions in Water Scarcity Research, Elsevier, 2022: pp. 531–552. https://doi.org/10.1016/B978-0-323-91838-1.00019-1.

[124] B. Koul, D. Yadav, S. Singh, M. Kumar, M. Song, Insights into the Domestic Wastewater Treatment (DWWT) Regimes: A Review, Water. 14 (2022) 3542. https://doi.org/10.3390/w14213542.

[125] M. Salehi, Global water shortage and potable water safety; Today's concern and tomorrow's crisis, Environment International. 158 (2022) 106936. https://doi.org/10.1016/j.envint.2021.106936.

[126] K. Parris, Impact of Agriculture on Water Pollution in OECD Countries: Recent Trends and Future Prospects, International Journal of Water Resources Development. 27 (2011) 33–52. https://doi.org/10.1080/07900627.2010.531898.

[127] M. Tudi, H. Daniel Ruan, L. Wang, J. Lyu, R. Sadler, D. Connell, C. Chu, D.T. Phung, Agriculture Development, Pesticide Application and Its Impact on the Environment, International Journal of Environmental Research and Public Health. 18 (2021) 1112. https://doi.org/10.3390/ijerph18031112.

[128] A. Kumari, N.S. Maurya, B. Tiwari, 15 - Hospital wastewater treatment scenario around the globe, in: R.D. Tyagi, B. Sellamuthu, B. Tiwari, S. Yan, P. Drogui, X. Zhang, A. Pandey (Eds.), Current Developments in Biotechnology and Bioengineering, Elsevier, 2020: pp. 549–570. https://doi.org/10.1016/B978-0-12-819722-6.00015-8.

[129] Safe management of wastes from health-care activities, 2nd ed., (n.d.). https://www.who.int/publications-detail-redirect/9789241548564 (accessed May 2, 2023).

[130] J. Berto, G.C. Rochenbach, M.A.B. Barreiros, A.X.R. Corrêa, S. Peluso-Silva, C.M. Radetski, Physico-chemical, microbiological and ecotoxicological evaluation of a septic tank/Fenton reaction combination for the treatment of hospital wastewaters, Ecotoxicology and Environmental Safety. 72 (2009) 1076–1081. https://doi.org/10.1016/j.ecoenv.2008.12.002.

[131] P. Kajitvichyanukul, N. Suntronvipart, Evaluation of biodegradability and oxidation degree of hospital wastewater using photo-Fenton process as the pretreatment method, Journal of Hazardous Materials. 138 (2006) 384–391. https://doi.org/10.1016/j.jhazmat.2006.05.064.

[132] M.L. Petrovich, A. Zilberman, A. Kaplan, G.R. Eliraz, Y. Wang, K. Langenfeld, M. Duhaime, K. Wigginton, R. Poretsky, D. Avisar, G.F. Wells, Microbial and Viral Communities and Their Antibiotic Resistance Genes Throughout a Hospital Wastewater Treatment System, Front Microbiol. 11 (2020) 153. https://doi.org/10.3389/fmicb.2020.00153.

[133] Y. Sun, Z. Chen, G. Wu, Q. Wu, F. Zhang, Z. Niu, H.-Y. Hu, Characteristics of water quality of municipal wastewater treatment plants in China: implications for resources utilization and management, Journal of Cleaner Production. 131

(2016) 1–9. https://doi.org/10.1016/j.jclepro.2016.05.068.
[134] T.I.U. of P. and A. Chemistry (IUPAC), IUPAC - chemical oxygen demand (C01031), (n.d.). https://doi.org/10.1351/goldbook.C01031.
[135] ISO 6060:1989 - Water quality — Determination of the chemical oxygen demand, (n.d.). https://www.iso.org/standard/12260.html (accessed May 5, 2023).
[136] D. Wu, Y. Hu, Y. Liu, A Review of Detection Techniques for Chemical Oxygen Demand in Wastewater, American Journal of Biochemistry and Biotechnology. 18 (2022) 23–32. https://doi.org/10.3844/ajbbsp.2022.23.32.
[137] C.N. Sawyer, P.L. McCarty, G.F. Parkin, Chemistry for Environmental Engineering and Science, McGraw-Hill Education, 2003.
[138] College of Sciences, Northeastern University, Shenyang 110819, China, Y. Ge, Electrochemical Determination of Chemical Oxygen Demand Using Ti/TiO2 Electrode, Int. J. Electrochem. Sci. (2016) 9812–9821. https://doi.org/10.20964/2016.12.05.
[139] M.C. Sarraguça, A. Paulo, M.M. Alves, A.M.A. Dias, J.A. Lopes, E.C. Ferreira, Quantitative monitoring of an activated sludge reactor using on-line UV-visible and near-infrared spectroscopy, Anal Bioanal Chem. 395 (2009) 1159–1166. https://doi.org/10.1007/s00216-009-3042-z.
[140] J.N. Louvet, B. Homeky, M. Casellas, M.N. Pons, C. Dagot, Monitoring of slaughterhouse wastewater biodegradation in a SBR using fluorescence and UV–Visible absorbance, Chemosphere. 91 (2013) 648–655. https://doi.org/10.1016/j.chemosphere.2013.01.011.
[141] T. Pan, Q. Ji, Y. Han, P. Li, FTIR/ATR spectroscopy analysis of COD in wastewater based on combination optimization of SG smoothing modes and PLS factor, Key Engineering Materials. 474–476 (2011) 1797–1801. https://doi.org/10.4028/www.scientific.net/KEM.474-476.1797.
[142] C.A. Almeida, P. González, M. Mallea, L.D. Martinez, R.A. Gil, Determination of chemical oxygen demand by a flow injection method based on microwave digestion and chromium speciation coupled to inductively coupled plasma optical emission spectrometry, Talanta. 97 (2012) 273–278. https://doi.org/10.1016/j.talanta.2012.04.030.
[143] J. Wang, C. Wu, K. Wu, Q. Cheng, Y. Zhou, Electrochemical sensing chemical oxygen demand based on the catalytic activity of cobalt oxide film, Analytica Chimica Acta. 736 (2012) 55–61. https://doi.org/10.1016/j.aca.2012.05.046.
[144] Y.-C. Kim, S. Sasaki, K. Yano, K. Ikebukuro, K. Hashimoto, I. Karube, A Flow Method with Photocatalytic Oxidation of Dissolved Organic Matter Using a Solid-Phase (TiO2) Reactor Followed by Amperometric Detection of Consumed Oxygen, Anal. Chem. 74 (2002) 3858–3864. https://doi.org/10.1021/ac015678r.
[145] N.A. Alves, A. Olean-Oliveira, C.X. Cardoso, M.F.S. Teixeira, Photochemiresistor Sensor Development Based on a Bismuth Vanadate Type Semiconductor for Determination of Chemical Oxygen Demand, ACS Appl. Mater. Interfaces. 12 (2020) 18723–18729. https://doi.org/10.1021/acsami.0c04259.
[146] C. Ma, F. Tan, H. Zhao, S. Chen, X. Quan, Sensitive amperometric determination of chemical oxygen demand using Ti/Sb–SnO2/PbO2 composite electrode, Sensors and Actuators B: Chemical. 155 (2011) 114–119. https://doi.org/10.1016/j.snb.2010.11.033.
[147] B.G. Jeong, S.M. Yoon, C.H. Choi, K.K. Kwon, M.S. Hyun, D.H. Yi, H.S. Park, M. Kim, H.J. Kim, Performance of an electrochemical COD (chemical oxygen

demand) sensor with an electrode-surface grinding unit, J. Environ. Monit. 9 (2007) 1352–1357. https://doi.org/10.1039/B713393F.

[148] Y. Liu, Q. Xue, C. Chang, R. Wang, Z. Liu, L. He, Recent progress regarding electrochemical sensors for the detection of typical pollutants in water environments, ANAL. SCI. 38 (2022) 55–70. https://doi.org/10.2116/analsci.21SAR12.

[149] T. Liu, Q. Xue, J. Jia, F. Liu, S. Zou, R. Tang, T. Chen, J. Li, Y. Qian, New insights into the effect of pH on the mechanism of ofloxacin electrochemical detection in aqueous solution, Phys. Chem. Chem. Phys. 21 (2019) 16282–16287. https://doi.org/10.1039/C9CP03486B.

[150] J. Li, L. Li, L. Zheng, Y. Xian, L. Jin, Rh2O3/Ti electrode preparation using laser anneal and its application to the determination of chemical oxygen demand, Meas. Sci. Technol. 17 (2006) 1995. https://doi.org/10.1088/0957-0233/17/7/044.

[151] S. Ai, M. Gao, Y. Yang, J. Li, L. Jin, Electrocatalytic Sensor for the Determination of Chemical Oxygen Demand Using a Lead Dioxide Modified Electrode, Electroanalysis. 16 (2004) 404–409. https://doi.org/10.1002/elan.200302839.

[152] Y. Diksy, I. Rahmawati, P.K. Jiwanti, T.A. Ivandini, Nano-Cu Modified Cu and Nano-Cu Modified Graphite Electrodes for Chemical Oxygen Demand Sensors, ANAL. SCI. 36 (2020) 1323–1327. https://doi.org/10.2116/analsci.20P069.

[153] T. Jing, Y. Zhou, Q. Hao, Y. Zhou, S. Mei, A nano-nickel electrochemical sensor for sensitive determination of chemical oxygen demand, Anal. Methods. 4 (2012) 1155–1159. https://doi.org/10.1039/C2AY05631C.

[154] Y. Zhou, T. Jing, Q. Hao, Y. Zhou, S. Mei, A sensitive and environmentally friendly method for determination of chemical oxygen demand using NiCu alloy electrode, Electrochimica Acta. 74 (2012) 165–170. https://doi.org/10.1016/j.electacta.2012.04.048.

[155] C. Comninellis, Electrocatalysis in the electrochemical conversion/combustion of organic pollutants for waste water treatment, Electrochimica Acta. 39 (1994) 1857–1862. https://doi.org/10.1016/0013-4686(94)85175-1.

[156] X. Huang, Y. Zhu, W. Yang, A. Jiang, X. Jin, Y. Zhang, L. Yan, G. Zhang, Z. Liu, A Self-Supported CuO/Cu Nanowire Electrode as Highly Efficient Sensor for COD Measurement, Molecules. 24 (2019) 3132. https://doi.org/10.3390/molecules24173132.

[157] H.H. Hassan, I.H.A. Badr, H.T.M. Abdel-Fatah, E.M.S. Elfeky, A.M. Abdel-Aziz, Low cost chemical oxygen demand sensor based on electrodeposited nano-copper film, Arabian Journal of Chemistry. 11 (2018) 171–180. https://doi.org/10.1016/j.arabjc.2015.07.001.

[158] W. Duan, M. Gunes, A. Baldi, M. Gich, C. Fernández-Sánchez, Compact fluidic electrochemical sensor platform for on-line monitoring of chemical oxygen demand in urban wastewater, Chemical Engineering Journal. 449 (2022) 137837. https://doi.org/10.1016/j.cej.2022.137837.

[159] R.A. de Jesus, Í.M. Oliveira, V.R.S. Nascimento, L.F.R. Ferreira, R.T. Figueiredo, Chapter 18 - Porous nanostructured metal oxides as potential scaffolds for drug delivery, in: S. Das, S. Thomas, P.P. Das (Eds.), Novel Platforms for Drug Delivery Applications, Woodhead Publishing, 2023: pp. 437–457. https://doi.org/10.1016/B978-0-323-91376-8.00018-5.

[160] A.A. Adegoke, T.A. Stenström, Chapter 17 - Metal oxide nanoparticles in removing residual pharmaceutical products and pathogens from water and

wastewater, in: A.M. Grumezescu (Ed.), Nanoparticles in Pharmacotherapy, William Andrew Publishing, 2019: pp. 561–589. https://doi.org/10.1016/B978-0-12-816504-1.00016-8.

[161] Cu and Cu-Based Nanoparticles: Synthesis and Applications in Catalysis | Chemical Reviews, (n.d.). https://pubs.acs.org/doi/10.1021/acs.chemrev.5b00482 (accessed August 27, 2023).

[162] C.R. Silva, C.D.C. Conceição, V.G. Bonifácio, O.F. Filho, M.F.S. Teixeira, Determination of the chemical oxygen demand (COD) using a copper electrode: a clean alternative method, J Solid State Electrochem. 13 (2009) 665–669. https://doi.org/10.1007/s10008-008-0580-9.

[163] S. Garcia-Segura, E. Brillas, Applied photoelectrocatalysis on the degradation of organic pollutants in wastewaters, Journal of Photochemistry and Photobiology C: Photochemistry Reviews. 31 (2017) 1–35. https://doi.org/10.1016/j.jphotochemrev.2017.01.005.

[164] E. Tønning, S. Sapelnikova, J. Christensen, C. Carlsson, M. Winther-Nielsen, E. Dock, R. Solna, P. Skladal, L. Nørgaard, T. Ruzgas, J. Emnéus, Chemometric exploration of an amperometric biosensor array for fast determination of wastewater quality, Biosens Bioelectron. 21 (2005) 608–617. https://doi.org/10.1016/j.bios.2004.12.023.

[165] X. Cetó, M. del Valle, Electronic tongue applications for wastewater and soil analysis, IScience. 25 (2022) 104304. https://doi.org/10.1016/j.isci.2022.104304.

[166] I. Campos, M. Alcañiz, D. Aguado, R. Barat, J. Ferrer, L. Gil, M. Marrakchi, R. Martínez-Mañez, J. Soto, J.-L. Vivancos, A voltammetric electronic tongue as tool for water quality monitoring in wastewater treatment plants, Water Research. 46 (2012) 2605–2614. https://doi.org/10.1016/j.watres.2012.02.029.

[167] World Health Organization, Depression and other common mental disorders: global health estimates, World Health Organization, 2017. https://apps.who.int/iris/handle/10665/254610 (accessed March 7, 2023).

[168] K.L. Szuhany, N.M. Simon, Anxiety Disorders: A Review, JAMA. 328 (2022) 2431–2445. https://doi.org/10.1001/jama.2022.22744.

[169] M. Kenda, N. Kočevar Glavač, M. Nagy, M. Sollner Dolenc, Medicinal Plants Used for Anxiety, Depression, or Stress Treatment: An Update, Molecules. 27 (2022) 6021. https://doi.org/10.3390/molecules27186021.

[170] S. Borrás, I. Martínez-Solís, J.L. Ríos, Medicinal Plants for Insomnia Related to Anxiety: An Updated Review, Planta Med. 87 (2021) 738–753. https://doi.org/10.1055/a-1510-9826.

[171] K.S. Yeung, M. Hernandez, J.J. Mao, I. Haviland, J. Gubili, Herbal medicine for depression and anxiety: A systematic review with assessment of potential psycho-oncologic relevance, Phytotherapy Research. 32 (2018) 865–891. https://doi.org/10.1002/ptr.6033.

[172] B. Bandelow, S. Michaelis, D. Wedekind, Treatment of anxiety disorders, Dialogues in Clinical Neuroscience. 19 (2017) 93–107. https://doi.org/10.31887/DCNS.2017.19.2/bbandelow.

[173] S.B. Sartori, N. Singewald, Novel pharmacological targets in drug development for the treatment of anxiety and anxiety-related disorders, Pharmacology & Therapeutics. 204 (2019) 107402. https://doi.org/10.1016/j.pharmthera.2019.107402.

[174] Y.-H. Ko, S.-K. Kim, S.-Y. Lee, C.-G. Jang, Flavonoids as therapeutic candidates for emotional disorders such as anxiety and depression, Arch Pharm

Res. 43 (2020) 1128–1143. https://doi.org/10.1007/s12272-020-01292-5.
[175] J.F. Rodríguez-Landa, L.J. German-Ponciano, A. Puga-Olguín, O.J. Olmos-Vázquez, Pharmacological, Neurochemical, and Behavioral Mechanisms Underlying the Anxiolytic- and Antidepressant-like Effects of Flavonoid Chrysin, Molecules. 27 (2022) 3551. https://doi.org/10.3390/molecules27113551.
[176] D. Roh, J.H. Jung, K.H. Yoon, C.H. Lee, L.Y. Kang, S.-K. Lee, K. Shin, D.H. Kim, Valerian extract alters functional brain connectivity: A randomized double-blind placebo-controlled trial, Phytother Res. 33 (2019) 939–948. https://doi.org/10.1002/ptr.6286.
[177] J.K. Srivastava, E. Shankar, S. Gupta, Chamomile: A herbal medicine of the past with bright future, Mol Med Report. 3 (2010) 895–901. https://doi.org/10.3892/mmr.2010.377.
[178] V. Svehliková, R.N. Bennett, F.A. Mellon, P.W. Needs, S. Piacente, P.A. Kroon, Y. Bao, Isolation, identification and stability of acylated derivatives of apigenin 7-O-glucoside from chamomile (Chamomilla recutita [L.] Rauschert), Phytochemistry. 65 (2004) 2323–2332. https://doi.org/10.1016/j.phytochem.2004.07.011.
[179] J.D. Amsterdam, Y. Li, I. Soeller, K. Rockwell, J.J. Mao, J. Shults, A randomized, double-blind, placebo-controlled trial of oral Matricaria recutita (chamomile) extract therapy for generalized anxiety disorder, J Clin Psychopharmacol. 29 (2009) 378–382. https://doi.org/10.1097/JCP.0b013e3181ac935c.
[180] S.-M. Chang, C.-H. Chen, Effects of an intervention with drinking chamomile tea on sleep quality and depression in sleep disturbed postnatal women: a randomized controlled trial, J Adv Nurs. 72 (2016) 306–315. https://doi.org/10.1111/jan.12836.
[181] M. Kim, H.-S. Lim, H.-H. Lee, T.-H. Kim, Role Identification of Passiflora Incarnata Linnaeus: A Mini Review, Journal of Menopausal Medicine. 23 (2017) 156–159. https://doi.org/10.6118/jmm.2017.23.3.156.
[182] K. Dhawan, S. Dhawan, A. Sharma, Passiflora: a review update, Journal of Ethnopharmacology. 94 (2004) 1–23. https://doi.org/10.1016/j.jep.2004.02.023.
[183] S.S. Denner, Lavandula angustifolia Miller: English lavender, Holist Nurs Pract. 23 (2009) 57–64. https://doi.org/10.1097/01.HNP.0000343210.56710.fc.
[184] D. Radu (Lupoae), P. Alexe, N. Stănciuc, Overview on the potential role of phytochemicals from lavender as functional ingredients, The Annals of the University Dunarea de Jos of Galati. Fascicle VI - Food Technology. 44 (2020) 173–188. https://doi.org/10.35219/foodtechnology.2020.2.11.
[185] The effect of lavender on stress in individuals: A systematic review and meta-analysis | Elsevier Enhanced Reader, (n.d.). https://doi.org/10.1016/j.ctim.2022.102832.
[186] ReportLinker, Global Herbal Medicines Market to Reach US$178.4 Billion by the Year 2026, GlobeNewswire News Room. (2022). https://www.globenewswire.com/news-release/2022/02/24/2391072/0/en/Global-Herbal-Medicines-Market-to-Reach-US-178-4-Billion-by-the-Year-2026.html (accessed June 13, 2023).
[187] B. Steinhoff, Challenges in the quality of herbal medicinal products with a specific focus on contaminants, Phytochem Anal. 32 (2021) 117–123. https://doi.org/10.1002/pca.2879.
[188] W. Lam, W. Cai, Y. Li, Z. Xu, J. Yang, Editorial: Quality control for efficacy

and safety of herbal medicinal products, Frontiers in Pharmacology. 14 (2023). https://www.frontiersin.org/articles/10.3389/fphar.2023.1162698 (accessed August 27, 2023).

[189] C. Pérez-Ràfols, N. Serrano, J.M. Díaz-Cruz, Authentication of soothing herbs by UV–vis spectroscopic and chromatographic data fusion strategy, Chemometrics and Intelligent Laboratory Systems. 235 (2023) 104783. https://doi.org/10.1016/j.chemolab.2023.104783.

CHAPTER 2 OBJECTIVES

2 Objectives

The general objective of the thesis is to fabricate some electrochemical sensors using metallic nanomaterials as modifiers to constitute ET arrays for the purpose of particular applications. Those prepared sensors would be utilized to build several electronic tongue arrays for qualitative and quantitative analysis. For this aim, some chemometric tools, e.g., PCA and ANN, as well as several supervised machine learning classifiers, *k*-NN, Naïve Bayes, random forest and SVM, would be approached for extracting information. The specific objectives were related to two research topics:

1. To fabricate electrochemical sensors using different substrates, i.e., graphite-epoxy composite (GEC) or Cu block, approaches or nanoscale modifiers. To establish ET arrays for COD determination and qualitatively evaluation of organic pollution in wastewater.

- ♦ To fabricate metal copper-based electrodes and modify their surfaces by forming CuO nanostructure through an

electrochemical anodization procedure;

- To construct some electrodes using GEC as substrate incorporating some nanoparticles (NPs) as electro-catalysts, such as Cu, CuO, Ni and Ni Cu alloy NPs;
- To optimize the measuring condition, such as measuring medium, to improve the efficiency of electrochemical oxidation.
- To test cyclic voltammetric responses of prepared electrodes to different COD standard substances and evaluate their potential for building the ET array.
- To get a classic calibration equation showing the relationship between COD values and current intensity for individual sensor using standard substance.
- To prepared samples with two or more standard substances to simulate wastewater conditions to build PCA or ANN models for organic pollution evaluation qualitatively and quantitatively
- To apply ET array into analyzing and evaluating real wastewater or spiked wastewater samples to test the practicability.

2. To build an ET array using GEC-based electrodes modified with some electro-catalysts for various forms of herbal anxiolytic products analysis. Collected anxiolytic products were composed of five forms, e.g., dried plant, tea bag, extracted liquid, tablet and capsule, and four target herb varieties, including chamomile, valerian, passionflower and lavender.

- To fabricate some GEC sensors using various nanoparticles, such as Cu, CuO, Ni, TiO_2 and Ni Cu alloy, as well as a bare GEC electrode;
- To optimize the measuring condition;

- To test electrochemical responses of these sensors to different herb varieties and choose electrodes for ET array;
- To use CV data collected by the ET array to extract information for authentication and discrimination, as well as evaluate the performance of this ET system on such application.

CHAPTER 3 EXPERIMENTAL

3 Experimental

3.1 Reagents and instruments

3.1.1 Chemicals and reagents

Chemical reagents used in researches presented are analytical grade, without any further purification. Solutions in the COD detection measurement were prepared using Milli-Q water filtered in a Milli-Q System (Millipore, Billerica, MA, USA). The cuvettes for colorimetric COD tests (LCK 514 for COD range 100~2000 mg/L O_2; LCK 1414 for COD range 5~60 mg/L O_2) were purchased from HACH company (HACH LANGE GMBH, Dusseldorf, Germany). In herbal products research, ultrapure water used for cleansing electrodes was prepared in Milli-Q plus 185 system (Millipore, Burlington, MA, USA). Natural mineral water was of brand *Ribes* purchased from local supermarket for brewing herbal medicinal products. Ethanol (96%) used for cleaning electrodes were acquired from Merck (Darmstadt, Germany). Alumina

powder, which was used for polishing the surface of copper block, was purchased from CH Instruments (Austin, TX, USA). Ferrocyanide redox pair was used as an electrochemical standard to study the behaviour of the prepared electrodes, which was prepared in the phosphate buffer solution containing 5.0 mM $K_3[Fe(CN)_6]/K_4[Fe(CN)_6]$ with pH 7. The information of reagents and their utilization are summarized in the Table 3.1.

Table 0.1 Summary of the reagents utilized in experiments.

Usage	Reagent	Manufacturer	Section
Electrode substrate	graphite powder (<50 μm)	BDH Laboratory supplies (Poole, UK)	Section 4.1 and 4.2
	epoxy resin kit	Resineco Green Composites (Barcelona, Spain)	Section 4.1 and 4.2
	H77 epoxy resin kit	Epoxy Technologies (Billerica, MA, USA)	Section 4.1 and 4.2
Electrochemical catalyst	Cu NPs (40~60 nm)	Sigma-Aldrich	Section 4.1 and 4.2
	CuO NPs (<50 nm)	Sigma-Aldrich	Section 4.1 and 4.2
	Ni NPs (<100 nm)	Sigma-Aldrich	Section 4.2 and 4.3
	Ni Cu alloy NPs (<80 nm)	Nanografi Nano Technology	Section 4.2, 4.2 and 4.3
	TiO_2 NPs (<25 nm)	Sigma-Aldrich	Section 4.3
	Glucose ($C_6H_{12}O_6$)	Sigma-Aldrich	Section 4.1 and

Analytes			4.2
	Glycine ($C_2H_5NO_2$)	Sigma-Aldrich	Section 4.1 and 4.2
	Ethylene glycol (CH_2OH)	Sigma-Aldrich	Section 4.1
	Potassium hydrogen phthalate (KHP, $C_8H_5O_4K$)	Sigma-Aldrich	Section 4.1
Buffer or electrolyte solution Electrolyte solutions	Potassium chloride (KCl)	ACROS Organics	Section 4.1 and 4.3
	Potassium hydroxide (KOH)	ACROS Organics	Section 4.3
	Sodium chloride (NaCl)	Sigma-Aldrich	Section 4.1 and 4.2
	Sodium hydroxide (NaOH)	Sigma-Aldrich	Section 4.1 and 4.2
	potassium hydrogen phosphate (K_2HPO_4)	Sigma-Aldrich	Section 4.1 and 4.3
	potassium dihydrogen phosphate (KH_2PO_4)	Sigma-Aldrich	Section 4.1 and 4.3
	potassium hexacyanoferrate (II) trihydrate $K_4[Fe(CN)_6]\cdot 3H_2O$	Panreac (Spain)	Section 4.1 and 4.3
	potassium hexacyanoferrate (III) $K_3[Fe(CN)_6]$	Panreac (Spain)	Section 4.1 and 4.3
Electrode coating	Nafion resin solution	Sigma	Section 4.1

material	N, N-Dimethylformamide (DMF)	Sigma-Aldrich	Section 4.1

3.1.2 Instruments

In COD related experiments, electrochemical measurements were carried out in a PGSTAT 30 Autolab potentiostat (EcoChemie, Netherlands) with GPES 4.7 version software (EcoChemie) with a conventional three-electrode cell configuration composed of prepared electrodes as the working electrodes, a metallic platinum electrode (Crison 5261, Barcelona, Spain) as the auxiliary electrode and a Ag/AgCl electrode as reference electrode. As for herbal medicinal products measurements, experiments were completed in a PGSTAT 12 Autolab multipotentiostat (EcoChemie, Netherlands) connected to a 663 VA stand (Metrohm Switzerland) and controlled by GPES software (version 4.9.007, Ecochemie), as well as the same auxiliary and reference electrodes as above mentioned.

The morphological characterization of the electrodes was conducted using scanning electron microscope (SEM) EVO®MA10. COD tests with HACH cuvettes were carried out with the DR3900 laboratory spectrophotometer (HACH).

3.1.3 Fabrication of graphite-epoxy composite electrodes

Due to the advantages of high electronic conductivity, good chemical stability, a relatively wide potential window in aqueous solutions, low background signal and fast electron transfer rates, carbon-based materials have a wide application in electrochemical analysis [1]. As a type of carbon-based material, graphite has been used in electrode fabrication for decades [2]. In researches presented here, graphite-epoxy composite (GEC) acts as the substrate for sensors and the preparation was according to previous

publication [3]. The composite was prepared by mixing graphite with epoxy, which played a role of binder. To develop the electrochemical properties, nanoparticles integrated with that composite as catalysts. The epoxy was used by combining the hardener and the resin in a ratio of 1/2 (w/w). As for bare GEC electrode, the composite was formed by mix graphite and epoxy at a ratio of 41/59 (w/w). As for nanoparticles modified electrodes, each one was prepared by blending graphite and epoxy with nanoparticles at a ratio of 54/41/5 (w/w/w).

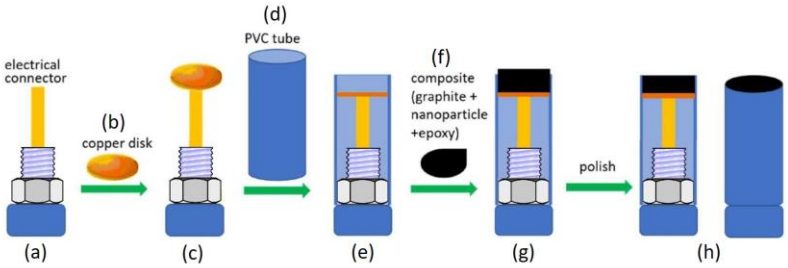

Figure 3.1 Schematic diagram explaining fabrication of GEC electrodes.

The procedure of assembling GEC electrodes is illustrated in Figure 3.1. The first step is to eliminate the oxidate layer at the copper disks by immersing them in hydrochloric acid aqueous solution. After that, a copper disk (b) with 5 mm diameter was soldered to an electrical connector (a), which was obtained as commercial product and put to use without any modification. Then the new-formed entirety (c) was inserted into a PVC tube (d) (diameter: 5 mm; length: 20 mm). Therefore, an interior cylinder cavity was formed up to the top of the tube (e). The composite (f) was blended thoroughly and inserted into the cavity, applying a heating procedure at 40 °C for 2 days (g). All electrodes were polished prior to utilization with emery papers of decreasing grain (400 to 1200 grit). Finally, electrodes with flat and glossy surfaces were ready for use (h). The prepared GEC electrodes modified with different nanoparticles and corresponding names presented in this text were summarized in Table 3.2 below.

Table 3.2 Summary of the electrodes' names and corresponding modifiers.

Nanoparticle	Electrode name	Section
Cu NPs （40~60 nm）	Cu NPs	Section 4.1 and 4.2
CuO NPs (<50 nm)	CuO NPs	Section 4.1 and 4.2
Ni NPs （<100 nm）	Ni NPs	Section 4.2
Ni Cu alloy NPs (<80 nm)	Ni-Cu NPs	Section 4.1, 4.2 and 4.3
TiO_2 NPs (<25 nm)	TiO_2 NPs	Section 4.3
--	GEC	Section 4.3

3.1.4 Fabrication of copper electrodes by electrochemical anodization procedure

There were two copper block-based electrodes being employed to COD determination fabricated according to procedures reported from literatures, including one filmed with Nafion (NfCuO/Cu, applied in Section 4.1) and one not (CuO/Cu, applied in Section 4.2) [4, 5]. These electrodes were fabricated by electrochemical anodization, as illustrated in Figure 3.2. A copper block (b), with 5 mm diameter and 4 mm length, was soldered to an electrical connector (a). Then, this couple (c) was inserted into a PVC tube (d), with length of 20 mm long and diameter of 5 mm. The cylindrical surface of the copper block was wrapped with H77 epoxy resin and cured for 24 h in an oven at 80 ℃ (e). Then, the surface of the electrode was polished with emery papers of decreasing grain size and alumina powder (1.0, 0.3 and 0.05 micron), obtaining a glossy and smooth surface. The surface was rinsed thoroughly using Milli-Q water. For the electrode CuO/Cu, the anodization was conducted in a solution of 0.05 mol/L NaOH solution using cyclic voltammetry technique, cycling potential from −0.1 to +0.8 V for 50 times at 100 mV/s (f). To modify surface of electrode NfCuO/Cu,

10 μL Nafion and 5 μL DMF was dropped on the surface and made solvent volatilized by keeping it in air for 48 h, followed by the same anodization procedure (g). Finally, dark CuO films formed on the electrodes' surfaces.

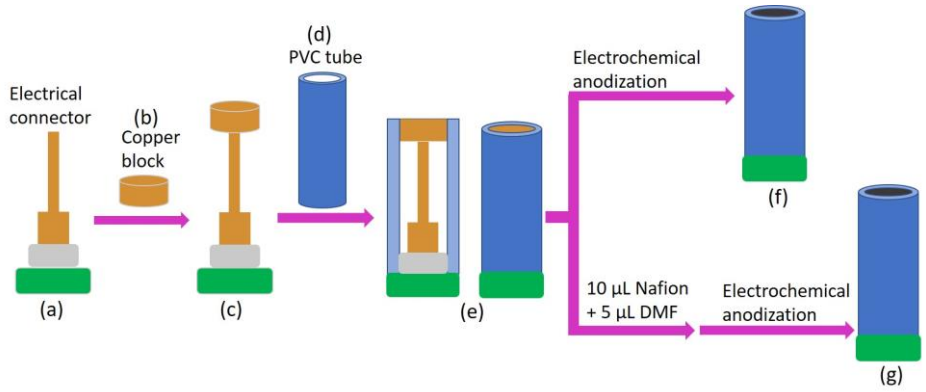

Figure 3.2 Schematic diagram illustrating fabrication of copper-based electrodes by electrochemical anodization procedure.

3.1.5 Construction of electronic tongues

Sensor arrays were established after primary analysis towards their response signals to analytes. Three sensor arrays were established and utilized for research in this text, as shown in Table 3.3:

Table 3.3 Summary of sensor arrays established in this text.

Sensor array	Electrode name	Section
Sensor array 1	Cu NPs CuO NPs NfCuO/Cu Ni-Cu NPs	Section 4.1
Sensor array 2	CuO/Cu Cu NPs CuO NPs Ni NPs Ni-Cu NPs	Section 4.2
Sensor array 3	TiO_2 NPs GEC Ni-Cu NPs	Section 4.3

3.2 Preparation of solutions of analytes and real samples

3.2.1 Solutions of analytes

In COD detection researches, glucose, glycine, ethylene glycol and KHP were used as COD standard substances on behalf of organic pollutants. Their solutions were used for voltammetric measurement for establishing ETs and ANN training and testing. NaOH and KOH were used to providing an alkaline condition for the purposed of enhancing ability of oxidizing organic compounds. KCl solution were used in research on herbal medical products for increasing the electronic conductivity of measuring samples. The summarised solutions of analytes or electrolytes and corresponding purposes in experiments were summarised in Table 3.4.

Table 3.4 Summary of the solutions prepared for analytes or electrolytes.

Usage	Reagent	Concentration /(mol/L)	Purpose	Section
COD standard solution	Glucose ($C_6H_{12}O_6$)	0.1	Voltammetric test and calibration plot, ANN training and testing	Section 4.1 and 4.2
	Glycine ($C_2H_5NO_2$)	0.1	Voltammetric test and calibration plot	Section 4.1 and 4.2
	Glycine ($C_2H_5NO_2$)	0.16	ANN training and testing	Section 4.2
	Ethylene glycol (CH_2OH)	0.1	Voltammetric test and calibration plot	Section 4.1

	Potassium hydrogen phthalate (KHP, $C_8H_5O_4K$)	0.05	Test and calibration plot	Section 4.1
Electrolyte	Sodium hydroxide (NaOH)	0.05	Alkaline condition	Section 4.1 and 4.2
Electrolyte	Potassium hydroxide (KOH)	0.05	Alkaline condition	Section 4.3
Electrolyte	Potassium chloride (KCl)	3.2	To increase conductivity	Section 4.3

3.2.2 Real samples

1) Wastewater and river water samples

In COD determination research, real water samples included pesticide polluted wastewater, river water and tap water samples that all from Catalonia (Spain). Information about these samples were summarised in Table 3.5. These river water samples were measured electrochemically after being mixed with NaOH electrolyte.

Table 3.5 Information of wastewater and river water samples.

Sample	River	Origin	Property	Study case
R1	River Llobregat	Gavà, Spain	Polluted by two kinds of pesticides (diuron and bentazon); COD value was determined as 1312 mg/L O_2 with HACH cuvette.	Section 4.1
R2	River Llobregat	Gavà, Spain	It was taken from effluent generated after washing agricultural equipment and machines after utilization and without any other treatment process. The determined COD was 2088 mg/L O_2 using HACH cuvette.	Section 4.1

R3	A stream alongside a farm	Lleida, Spain	It was obtained from the stream without any further process. The sample was clear and COD was determined as 11.7 mg/L O_2 with HACH cuvette.	Section 4.1 and 4.2
R4	A stream alongside a farm	Ripollet, Spain	It was obtained from the stream without any other process. The sample was clear and COD was determined as 12.1 mg/L O_2 with HACH cuvette.	Section 4.2
R5	A stream alongside a farm	Gavà, Spain	It was obtained from the stream without any other process. The sample was clear and COD value was determined as 15.1 mg/L O_2 with HACH cuvette.	Section 4.2
R6	A stream alongside a farm	Gavà, Spain	It was obtained from the stream without any other process. The sample was clear and COD value was determined as 9.21 mg/L O_2 with HACH cuvette.	Section 4.2
R7	A stream flowing through a town	Sant Boi de Llobregat, Spain	It was obtained from the stream without any other process. The sample was a little muddy and COD value was determined as 18.2 mg/L O_2 with HACH cuvette.	Section 4.2
R8	Tap water	Cerdanyola del Vallès, Spain	A normal tap water took from campus of university (Universitat Autònoma de Barcelona)	Section 4.1

2) Herbal medicinal samples

In experiments of research on herbal medicinal products, chamomile, passionflower, valerian and lavender were selected as four representative examples of anxiolytic herbs. Note that not all herb varieties could be found for all prepared forms of products. A total of 35 samples of various products of chamomile, passionflower, valerian and lavender were purchased in herbal health-care shops and supermarkets located in Barcelona (Spain). The information of brand and ingredients of considered samples was shown in Table 3.6. These products were stored in room temperature (20 °C) during the whole research work. All samples were put to electrochemical measurement after being brewed into infusion samples according to similar procedure. A kind of commercial mineral drinking water (brand: Ribes, Spain) was used for

brewing. Tea bags were treated by soaking each one in 250 mL boiling water for 5 min and then cooling in a water bath to room temperature. As for extracted liquids, 10 drops of each sample were mixed with 250 mL boiling water and put it into water bath. Loose plants, capsules and pills were smashed previously and 1.5 g of each sample was brewed by 250 mL boiling water for 5 min and followed by water bath after filtration with filtering paper. Finally, these prepared infusion samples were mixed with 3.15 mL KCl solution (3.2 mol/L) with the volume reaching 100 mL in a volumetric flask. All samples were analysed in quadruplicate to account for the possible variability during the experimental procedure. Therefore, a total of 140 testing samples were ready to measure.

Table 3.6 Information of collected herbal products in Article 3.

Sample	Brand	Type	Basic herb material (Content, property)	Other ingredients
1	Hornimans	Tea bag	Chamomile (85.5%, --)	Lavender flower (5%), aromatic spices
2	Pompadour	Tea bag	Valerian (20%, --)	Melissa, lime flower, lemon
3	Consum	Tea bag	Passionflower (25%, aerial part)	Melissa (40%), Hawthorne (25%), lavender (5%), vanilla aroma spice (5%)
4	Hornimans	Tea bag	Lavender (10%, flower)	Melissa (45%), passionflower (5%)
5	El Corte Inglés	Tea bag	Chamomile (100%, plant and flower)	--
6	Westminster	Tea bag	Chamomile (100%, --)	--
7	Hornimans	Tea bag	Valerian (<54%, --)	Green rooibos (36%), apple pieces (10%), spices
8	Soria natural	Liquid	Passionflower (18%, lyophilized extract of passionflower aerial part)	Glycerin, γ-cyclodextrins, α-cyclodextrins, flavonoids, water
9	Pompadour	Tea bag	Passionflower (10%, --)	Rooibos, melissa, honeybush, cinnamon

10	Arkopharma	Capsule	Passionflower (79.4%, aerial part)	--
11	Condis	Tea bag	Chamomile (100%, plant and flower)	--
12	Naturmil	Pill	Valerian (79.4%, root)	Bulking agent: modified corn starch, anticaking agent: calcium phosphate dibasic anhydrous, magnesium salts of fatty acids, silicon dioxide
13	Floralp's Natura	Tea bag	Valerian (100%, root)	--
14	Hacendado	Tea bag	Chamomile (100%, --)	--
15	Naturmil	Pill	Passionflower (80.6%, flower and leaf)	Fructooligosaccharide, bulking agent: microcrystalline cellulose, anticaking agent: magnesium stearate, silicon dioxide
16	Santiveri	Tea bag	Passionflower (100%, flowering aerial part)	--
17	Soria natural	Liquid	Valerian (around 18%, lyophilized extract of valerian root)	Glycerin, γ-cyclodextrins, α-cyclodextrins, valerianic acid, water
18	Kneipp	Pill	Valerian (40.4%, root)	Coating agent: sucrose, talc, shellac; bulking agent: lactose; microcrystalline cellulose and polyvinylpyrrolidone; anticaking agent: magnesium stearate, silicon dioxide
19	Sana Sana	Pill	Valerian (70%, root)	Bulking agent: microcrystalline cellulose; anticaking agent: magnesium stearate
20	Hornimans	Tea bag	Chamomile (100%, flower)	--
21	--	Loose plant	Chamomile (100%, plant and flower)	--
22	--	Loose plant	Passionflower (100%, aerial part)	--

23	--	Loose plant	Lavender (100%, flower)	--
24	--	Loose plant	Valerian (100%, root)	--
25	Arkopharma	Capsule	Valerian (82.9%, lyophilized root)	Capsule shell: hydroxypropyl methylcellulose
26	Soria Natural	Capsule (34-S)	Valerian (43.5%, lyophilized extract of root)	Stabilizer: microcrystalline cellulose; coating agent: neutral methacrylate copolymer
27	Soria Natural	Capsule (29-C)	Valerian (--%, dry extract of valerian root), passionflower (--%, dry extract of passionflower aerial part)	Dry extract of hawthorn, α-cyclodextrins, glazing agent: neutral methacrylate copolymer, lavender essential oil
28	Plantea	Pill	Passionflower (--%, --)	Microcrystalline cellulose, magnesium stearate
29	--	Loose plant	Chrysanthemum 1 (100%, flower)	--
30	--	Loose plant	Chrysanthemum 2 (100%, flower)	--
31	Consum	Tea bag	Chamomile (100%, plant and flower)	--
32	Carrefour	Tea bag	Chamomile (100%, plant and flower)	--
33	Eroski	Tea bag	Chamomile (100%, plant and flower)	--
34	Pompadour	Tea bag	Chamomile (100%, flower)	--
35	Hacendado	Tea bag	Valerian (94%, root)	Aromatic fruits

3.3 Electrochemical measurements

The electrochemical measurements in this text were carried out in a standard three-electrode cell at room temperature with electrochemical Autolab PGSTAT30 (COD research) or 12 (herb research), the equipment was shown in Figure 3.3. Aa metallic platinum electrode was used as the auxiliary

electrode and a Ag/AgCl electrode was used as reference electrode. The prepared electrodes were utilized as working electrodes.

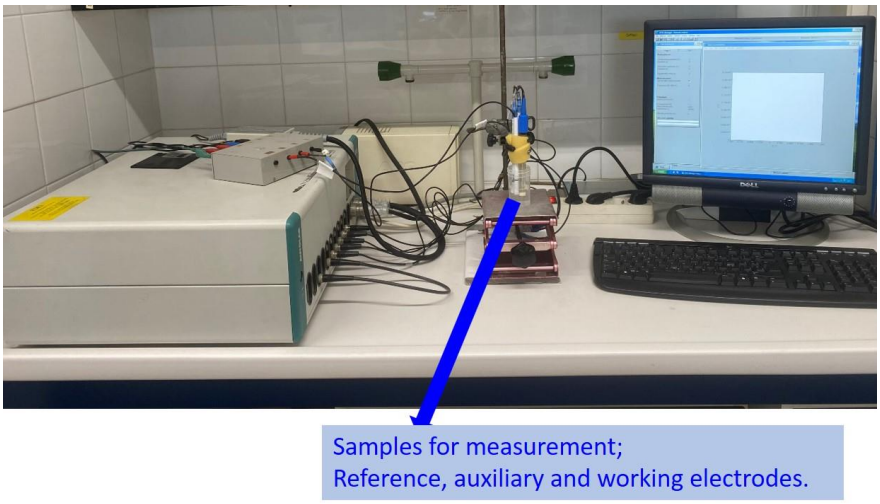

Figure 3.3 The equipment for electrochemical measurement.

For COD researches, the electrochemical voltammetric measurement towards standard and real samples with sensor arrays was carried out in 0.05 mol/L NaOH electrolyte. The cyclic voltammograms were recorded in a cycled potential range from 0 V to 1.0 V with a scan rate of 50 mV/s. The electrodeposition for modifying electrode surfaces was conducted in a solution of 0.05 mol/L NaOH solution with cycling potential from −0.1 to +0.8 V for 50 times.

As for research on herbal medicinal products, samples were measured in KCl medium (0.1 mol/L). Cyclic voltammograms were recorded for each sample by sweeping the potential between 0 V and +1.25 V, with a step potential of 0.01 V and a scan rate of 50 mV/s. The electrochemical cleaning procedure for eliminating unwanted effects was conducted by cycling the potential between 0 V and +1.30 V with a scan rate of 50 mV/s in 0.05 mol/L KOH solution.

The calculation of active area of electrodes' surfaces were carried out in a solution of 5 mM $K_3[Fe(CN)_6]/K_4[Fe(CN)_6]$ in PBS buffer in the potential range

from −0.2 V to +0.7 V by applying different cyclic voltammetry scan rates (10, 25, 50, 100, 200, 300 and 500 mV/s)

3.4 Repeatability test

Repeatability is a basic demand for an electrode used for the electronic tongue technique. Repetitive measurement is very critical in developing ET arrays for the reason that sensors need to withstand the larger number of measurements, which required to build the chemometric model. Bad repeatability can result in large inaccuracy to samples and models. Prepared electrodes were used as working electrodes in three-electrode system in 0.05 mol/L NaOH to test their stability and repeatability. For the sensor array 1 listed in Table 3.3, 10 groups cyclic voltammetric scan, which consists of two cyclic voltammograms responding to glucose (2.15 mmol/L) and blank electrolyte respectively, were recorded. As for sensor array 2, 10 consecutive measurements of cyclic voltammograms of prepared five electrodes towards a mixed solution of glucose and glycine (equivalent to a COD value of 300 mg/L O_2) were recorded, during which a blank electrolyte (0.05 mol/L NaOH) was also measured in between. In the case of electrodes of sensor array 3, sample 1 in Table 3.6 was treated and according to the protocol described in section 3.3.2 and its measuring solution was prepared firstly. 10 scans of CVs of electrodes to this sample were recorded by the electrode array in 0.1 KCl solution by cycling the potential between 0 and +1.2 V. Each scan was followed by a cyclic voltammetric scan between 0 and +1.3 V.

3.5 COD test using commercial cuvettes

COD test with HACH cuvettes were conducted according to the recommended procedure. In the very beginning, invert a few times to bring the

sediment into suspension. 2.0 mL of each sample was added into one cuvette using pipet. Closed the cuvettes and then inverted a few times. After being heated in a thermostat for 2 hours at 148 °C, these cuvettes were allowed to cool to room temperature. Then cleaned them thoroughly and inserted the cuvette into the cell holder of the spectrophotometer to read the COD values. Note that sediment must be completely settled before detection.

3.6 Data analysis

Voltammetric signals in the text were all recorded by Autolab and then were converted to excel files using Microsoft Excel 2019. The figures of CVs were prepared by OriginPro 8.5 (OriginLab Corporation, Northampton, MA, USA). The calibration plots in COD research and related analysis were carried out with this Origin programme. PCA procedure in COD research was carried out with web tool ClustVis for clustering samples (https://biit.cs.ut.ee/clustvis/) [6]. Orange open programming language (https://orangedatamining.com/, University of Ljubljana, Slovenia) were used to perform machine learning classification and analysis towards herbal medicinal products, such as PCA, *k*-NN, Random Forest, Naïve Bayes and SVM algorithms [7,8].

References

[1] A. Casanova, J. Iniesta, A. Gomis-Berenguer, Recent progress in the development of porous carbon-based electrodes for sensing applications, Analyst. 147 (2022) 767–783. https://doi.org/10.1039/D1AN01978C.

[2] D. Jariwala, V.K. Sangwan, L.J. Lauhon, T.J. Marks, M.C. Hersam, Carbon nanomaterials for electronics, optoelectronics, photovoltaics, and sensing, Chem Soc Rev. 42 (2013) 2824–2860. https://doi.org/10.1039/c2cs35335k.

[3] M. Sarma, M. del Valle, Improved Sensing of Capsaicin with TiO2 Nanoparticles Modified Epoxy Graphite Electrode, Electroanalysis. 32 (2020)

230–237. https://doi.org/10.1002/elan.201900400.

[4] T. Carchi, B. Lapo, J. Alvarado, P.J. Espinoza-Montero, J. Llorca, L. Fernández, A Nafion Film Cover to Enhance the Analytical Performance of the CuO/Cu Electrochemical Sensor for Determination of Chemical Oxygen Demand, Sensors. 19 (2019) 669. https://doi.org/10.3390/s19030669.

[5] C.R. Silva, C.D.C. Conceição, V.G. Bonifácio, O.F. Filho, M.F.S. Teixeira, Determination of the chemical oxygen demand (COD) using a copper electrode: a clean alternative method, J Solid State Electrochem. 13 (2009) 665–669. https://doi.org/COD.

[6] T. Metsalu, J. Vilo, ClustVis: a web tool for visualizing clustering of multivariate data using Principal Component Analysis and heatmap, Nucleic Acids Research. 43 (2015) W566–W570. https://doi.org/10.1093/nar/gkv468.

[7] A. Naik, L. Samant, Correlation Review of Classification Algorithm Using Data Mining Tool: WEKA, Rapidminer, Tanagra, Orange and Knime, Procedia Computer Science. 85 (2016). https://cyberleninka.org/article/n/608615 (accessed March 14, 2023).

[8] M. Peker, O. Özkaraca, A. Sasar, Use of Orange Data Mining Toolbox for Data Analysis in Clinical Decision Making: The Diagnosis of Diabetes Disease, in: Expert System Techniques in Biomedical Science Practice, 2018: pp. 143–167. https://doi.org/10.4018/978-1-5225-5149-2.ch007.

CHAPTER 4 RESULTS AND DISCUSSION

4 Results and Discussion

To achieve the objectives described in *Chapter 2*, research works were carried out according to the experiments as described in *Chapter 3*. Generally, studies presented here are related to development of ETs for the applications involving two topics, organic pollution analysis of wastewaters and authentication of herb varieties of herbal anxiolytic products. For the former topic, the work presented in this text could be divided into two parts. The first one was the primary test, which utilized single sensor to attain classic calibration equation for COD determination. This ET array was also helpful for evaluating the oxidation difficulties of the organic pollutants existing in water samples by PCA procedure, which can be related to the accuracy of detected COD values. This part was presented and discussed in Section 4.1. As for the latter one, it was the extension of the former one, optimization was involved according to previous experience, in terms of sensor fabrication and quantification methods. The ANN model was employed in this case for calculation of COD values. These works wee presented in Section 4.2. The third

part, which was for authentication and discrimination of herb varieties, as well as the evaluation to ingredients of herbal anxiolytic products, was presented in Section 4.3.

4.1 COD determination using sensors or sensor array modified with metal or metal oxide nanostructures

In recent years, nanomaterials have attracted lots of attention to modify electrochemical sensors because of their intriguing physicochemical properties, such as exceptional electrical and catalytic properties, large surface-to-volume ratio, as well as large number of active adsorption sites, which provide them advantages in analytical application [1]. As mentioned in *Chapter 1*, Cu-derived nanomaterials, such as Cu, CuO or Cu_2O, have obtained wide acceptance as a powerful electrocatalyst in electrochemical analytical research on organic compounds because of the efficient catalytic activity, such as organic compounds, i.e., glucose or phenolic substances. Due to the similar demanding of detecting and analysing organic species, Cu-derived nanomaterials have been attracted lots of effort to research on organic pollution in wastewater, such as COD determination [2–5]. CuO is one of the most extensively used metal oxide in electrochemical sensing applications. As for the preparation of CuO sensors, copper oxide nanoparticles can be immobilized directly at the surface of supporting material (e.g., glassy carbon). Some polymer binders, i.e., Nafion, was proposed to enhance the adhesion [6,7]. To fabricate COD electrochemical sensor, electrochemical oxidation (anodization) can be a promising strategy by generating the copper oxide layer on the copper surface directly.

Nafion is a cationic exchange polymer formed by perfluorosulfonate branches with sulfonic groups negatively charged at pH > 5. It can form a thin

film on electrode surface to avoid electrode passivation derived from adhesion of large contaminant particles on its surface by selection of contaminants based on their particle size. What's more, the Nafion is water insoluble and hydrophilic, which can be used on the electrode surface to enhance the chemical and mechanical endurance [2].

In this study case, three GEC-based electrodes were fabricated incorporating nanoparticle modifiers, Cu NPs, CuO NPs and Ni Cu alloy NPs. Inspired by the work reported by Carchi et al, Nafion was employed to protect the electrode surface from contamination by organic compounds [2]. In addition, a Cu-based electrode was also involved and modified by forming nanostructured CuO at its surface through an electrochemical anodization procedure, namely electrode NfCuO/Cu. The utilization of these four electrodes was inspired by the good performance of copper-based nanomaterials in electrochemical catalytic effects. Furthermore, the various nanomaterials involved, as well as different principles for electrode fabrication, were for the purpose of maximizing the differences in the voltammetric signals derived from different sensors to provide more useful information.

A calibration equation was obtained by electrode NfCuO/Cu based on cyclic voltammetric responses to glucose, which was used for simulating organic pollutants. In addition, the PCA technique was employed using cyclic voltammograms as inputs to evaluate the overall oxidation difficulties of organic pollutants existing in wastewater samples, which can help evaluate the organic pollution and accuracy of calculated COD values.

4.1.1 Electrochemical characterization of sensors

4.1.1.1 Electrochemical anodization

As section explained before, the Nafion film was covered on the Cu block electrode firstly. CuO nanostructure was then formed at the surface by the

electrochemical anodization procedure, which was conducted by employing cyclic voltammetry between the potential range between −1.0 and +0.8 V vs. Ag/AgCl in 0.05 M NaOH medium. Totally 50 scans were carried out in the anodization step. Some cyclic voltammograms during this procedure were recorded and illustrated in Figure 4.1.

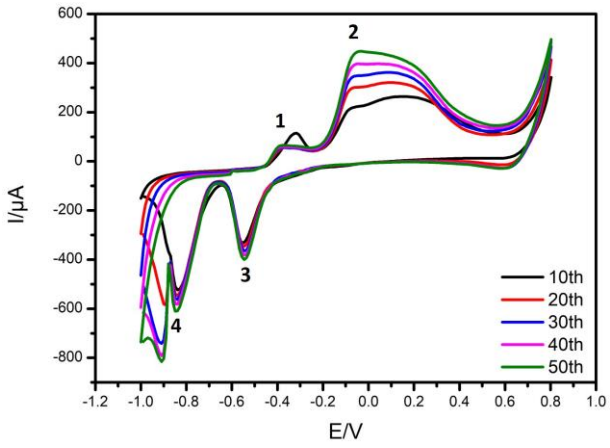

Figure 4.1 Cyclic voltammograms of the electrochemical anodization procedure on Nafion filmed Cu electrode at 100 mV/s in 0.05 M NaOH electrolyte solution.

The anodic peak 1 at around −0.4V corresponds to the formation of the first layer of Cu(I) oxide (Cu_2O), while the anodic peak 2 at around 0 V corresponds to the formation of the second mixed layer of Cu(II) oxide/Cu(II) hydroxide ($CuO/Cu(OH)_2$). As mentioned before, the stoichiometry of the formed oxide at copper surface is not fixed in anodization procedure, implying that Cu_2O, CuO, and $Cu(OH)_2$ may co-exist [8,9]. However, the formed $Cu(OH)_2$ deposit may transform into a soluble substances like $[Cu(OH)_4]^{2-}$ in an alkaline environment [8,10]. Therefore, the main component of the generated nanomaterials in the anodization at the electrode surface was CuO. The signals reaching +0.8 V indicated Cu(II)/Cu(III) oxidation. In the reverse scan, two cathodic peaks (3 and 4) were corresponding to the Cu(II)/Cu(I) (−0.54 V) and Cu(I)/Cu(0) (−0.84 V) reduction reactions, respectively [2,11].

4.1.1.2 Active surface areas of prepared electrodes

After the four electrodes, including GEC-based electrodes Cu NPs, CuO NPs and Ni-Cu NPs, as well as Cu-based NfCuO/Cu, were fabricated in the former section, the active surface areas were calculated. Randles–Sevcik Equation was employed in the calculation, which was shown as equation (12) [12,13].

$$Ip = 0.446 \cdot n \cdot F \cdot c \cdot A \cdot \sqrt{v} \cdot \sqrt{(\frac{nDF}{RT})} \qquad (12)$$

In this equation, n represents the electron number participated in the redox reaction. Ip is the peak current of the redox reaction in the voltammogram in unit A. F is the Faraday's constant (96,485 C·mol^{-1}). c is the concentration of the redox species (mol·cm^{-3}). A represents the surface area of the working electrode in cm^2. R is the Gas Constant (8.314 J·mol^{-1}·K^{-1}). T refers to the temperature in K, and D is the diffusion coefficient of the redox species in cm^2·s^{-1}. v is the scan rate in V·s^{-1}, which varied (0.01, 0.025, 0.05, 0.1, 0.2, 0.3 and 0.5 V·s^{-1}) in recording seven scans of cyclic voltammograms in experimental procedure. A three-electrode electrochemical system and 5 mmol·L^{-1} $[Fe(CN)_6]^{3-/4-}$ medium solution were used for measurement. The values of the active area of the electrodes could be calculated from the slope of the fitted line of $v^{1/2}$ vs. Ip/c graph. The calculated active areas were 139.23 mm^2 for NfCuO/Cu, 29.10 mm^2 for Cu NPs, 31.09 mm^2 for CuO NPs, and 35.65 mm^2 for Ni-Cu NPs, all of which were bigger than the geometric area (28.27 mm^2, 6 mm diameter). These results indicated the effective modification for the electrodes. Furthermore, the active area of electrode NfCuO/Cu was about five times that of other GEC electrodes, which implied a better function of anodic CuO nanostructure. It was predicted an improved performance for electrode NfCuO/Cu.

4.1.1.3 Repeatability test

In this step, the repeatability of the proposed four electrodes was completed according to the protocols described in section 3.5. The current

intensity at +0.70 V from CVs for electrodes NfCuO/Cu, Cu NPs, CuO NPs, and Ni-Cu NPs was recorded and displayed in Figure 4.2. As shown, the differences of current intensity between measurements are very small in cases of glucose solution and NaOH medium (blank). The relative standard deviation (RSD) values were calculated based on the CV data as listed in Table 4.1. The obtained RSD values of each electrode was lower than 5%, which indicates a good repeatability and stability, which gave them capability of building an ET array. These properties are essential for electrode members to conduct mass measurements without hysteresis or memory effects in ET research.

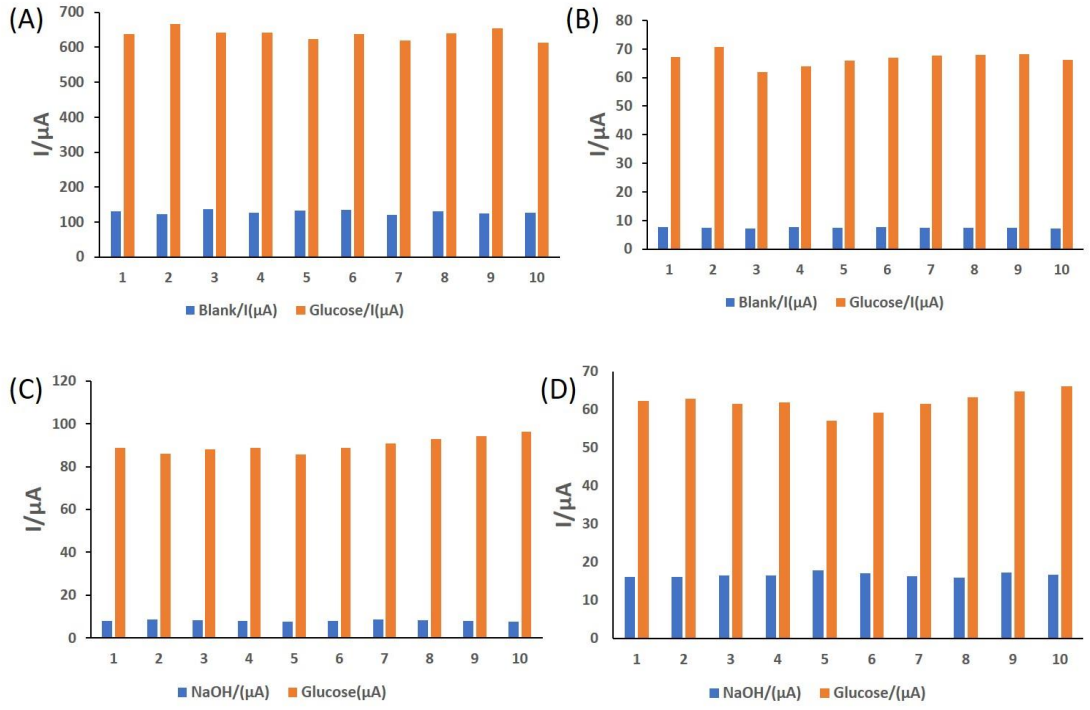

Figure 4.2 Current intensity at +0.70 V of oxidation in 10 cyclic voltammograms for electrodes NfCuO/Cu (A), Cu NPs (B), CuO NPs (C) and Ni-Cu NPs (D) responding to blank (blue) and 2.15 mmol/L glucose (orange) in 0.05 mol/L NaOH medium. Scan rate: 50 mV·s^{-1}.

Table 4.1. Relative standard deviation (RSD) values of electrodes NfCuO/Cu, Cu NPs, CuO NPs, and Ni-Cu NPs obtained in blank and glucose solutions.

	NfCuO/Cu	Cu NPs	CuO NPs	Ni-Cu NPs
Blank [1]	4.04%	3.07%	3.90%	3.44%
Glucose [2]	2.48%	3.57%	3.87%	4.14%

[1] 0.05 mol/L NaOH solution;

2 2.15 mmol/L glucose solution in 0.05 M NaOH medium.

4.1.1.4 Voltammetric responses to standard substances

In this step, the voltammetric responses of each sensor was measured according to the measuring condition in Section 3.4. Some commonly used COD standard organic compounds of different chemical structures and functional groups, glucose, glycine, ethylene glycol, and potassium hydrogen phthalate (KHP), that can show different activity in electrochemical reaction, were utilized as analytes for simulating organic pollutants. Among these substances, glucose is the one that is easier to be oxidized by electrochemical catalyst. Oppositely, KHP is the harder one. The prepared 4 electrodes, NfCuO/Cu, Cu NPs, CuO NPs and Ni-Cu NPs were used as working electrodes in this measurement.

Cyclic voltammetric responses of fabricated four electrodes toward four standard substances were checked in NaOH background electrolyte, which could provide an alkaline environment for redox reaction, according to the condition described in section 3.4. The concentration of NaOH was 0.05 mol/L, which was milder than of reported works, for the purpose of protecting the electrodes' surfaces [2,11,14]. Note that four organics were of same concentration, 2.15 mmol/L. The obtained oxidation parts of cyclic voltammograms were shown in Figures 4.3 and 4.4, which illustrated four organics obtained at one electrode and one organic obtained from four electrodes, respectively, for better comparison. As can be seen from Figures 4.3, it is obvious that the CV signals originated from each electrode were different from each other. As for each compound, different electrodes gave different oxidation curves. Note that, electrode NfCuO/Cu gave highest current intensity. Unfortunately, there was no obvious signal change indicating the oxidation of KHP, which indicated that it was very hard to be oxidized under the same condition. The result indicated that the diversity of the generated

signals was informative and rich enough to build an electronic tongue model. The responses of these electrodes to increasing concentration (0~3.6 mM) of these four standard substances were also measured, as shown in Figures 4.5~4.8.

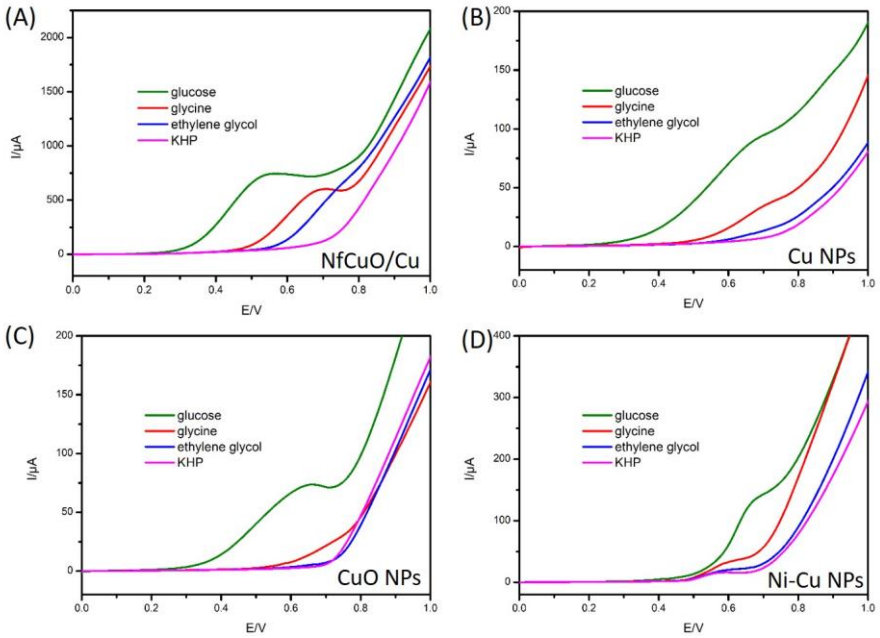

Figure 4.3 Oxidation curves of cyclic voltammograms obtained by electrodes NfCuO/Cu (A), Cu NPs (B), CuO NPs (C) and Ni-Cu NPs (D) responding to four organic substances: glucose, glycine, ethylene glycol and KHP in concentration 2.15 mmol/L. Electrolyte: 0.05 mol/L NaOH solution. Scan rate: 50 mV/s.

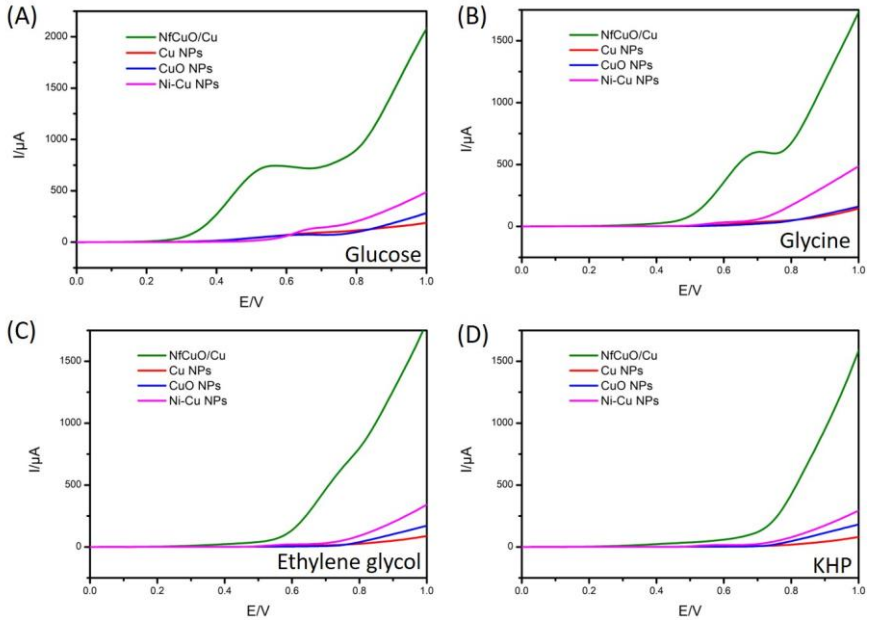

Figure 4.4 Oxidation curves of cyclic voltammograms obtained from electrodes NfCuO/Cu, Cu NPs, CuO NPs, and Ni-Cu NPs responding to four standard organic substances in concentration 2.15 mmol/L: glucose (A), glycine (B), ethylene glycol (C) and KHP (D). Scan rate: 50 mV/s.

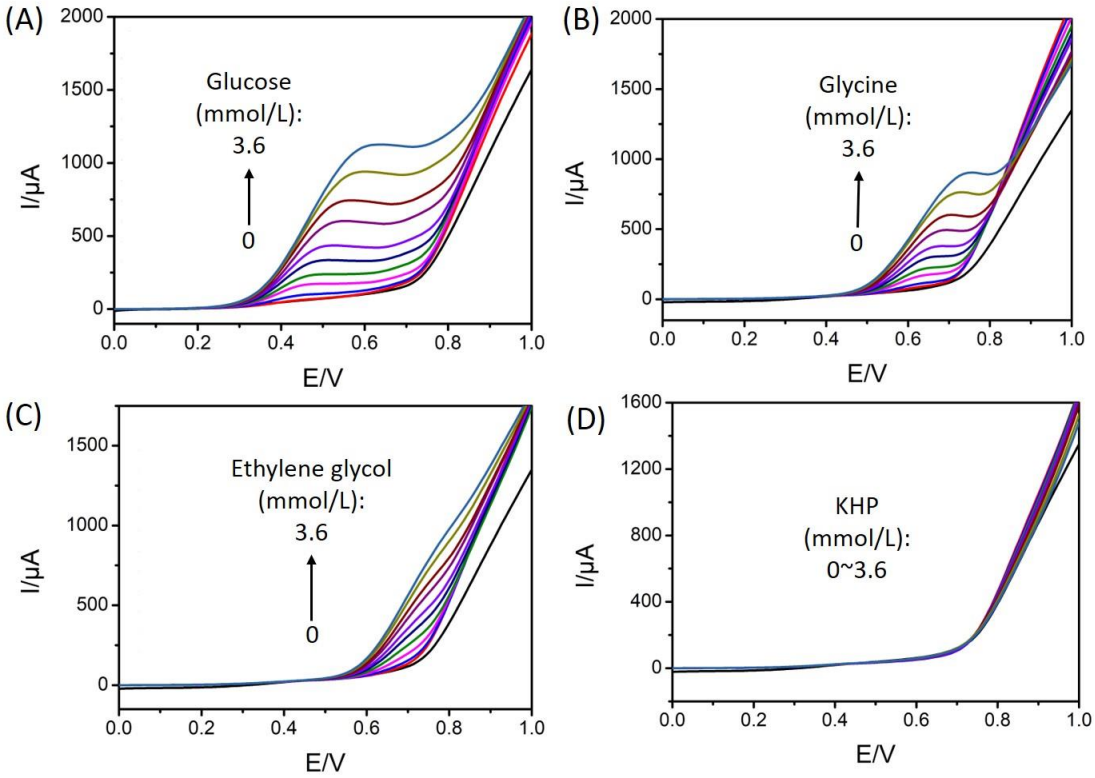

Figure 4.5 Oxidation curves of cyclic voltammograms of electrode NfCuO/Cu responding to glucose (A), glycine (B), ethylene glycol (C) and KHP (D) in concentration range 0~3.6 mmol/L in 0.05 M NaOH medium. Scan rate: 50 mV/s.

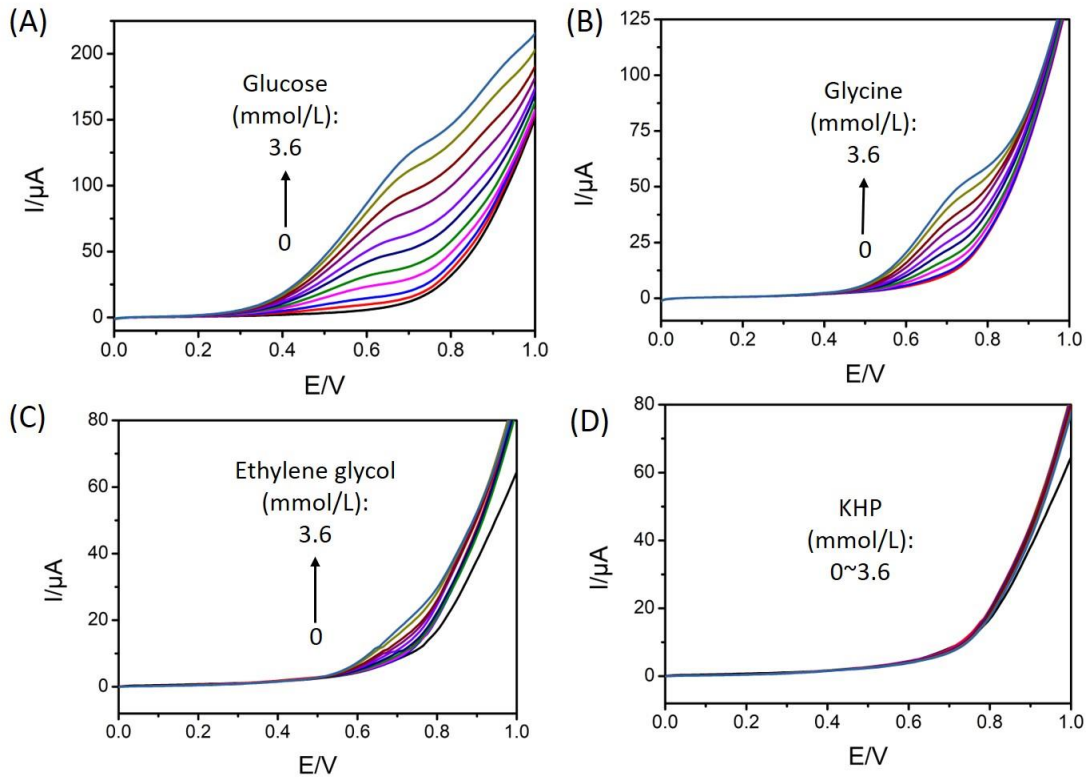

Figure 4.6 Oxidation curves of cyclic voltammograms of electrode Cu NPs responding to glucose (A), glycine (B), ethylene glycol (C) and KHP (D) in concentration range 0~3.6 mmol/L in 0.05 M NaOH medium. Scan rate: 50 mV/s.

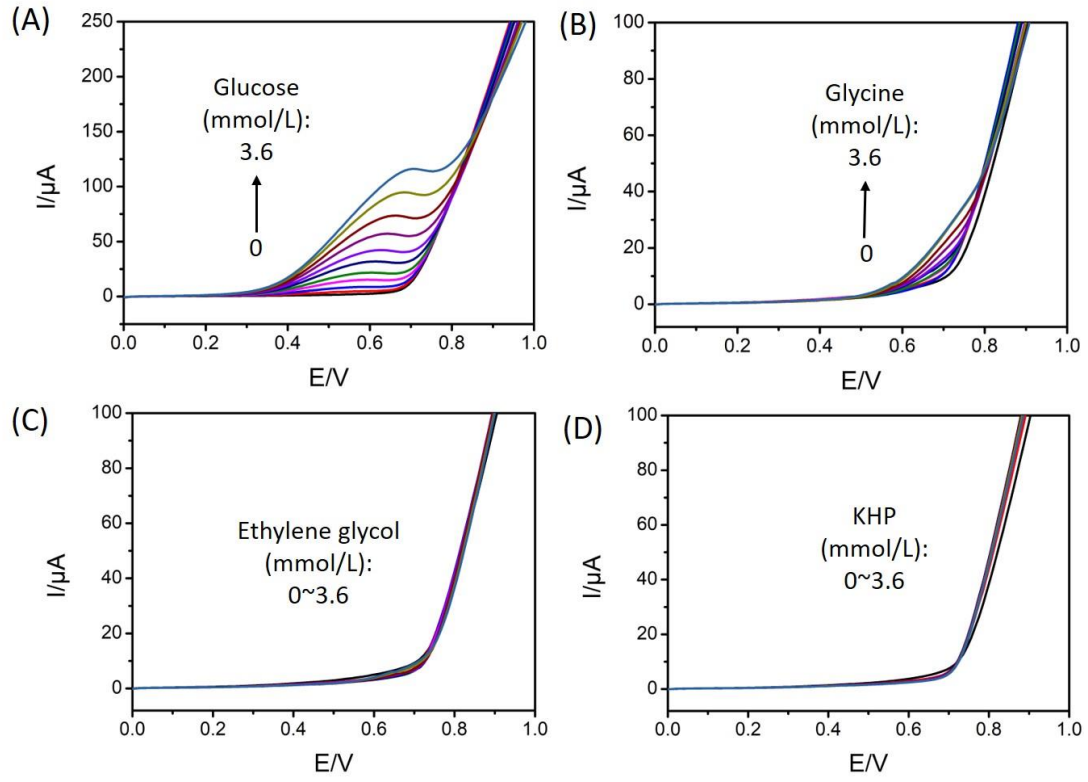

Figure 4.7 Oxidation curves of cyclic voltammograms of electrode CuO NPs responding to glucose (A), glycine (B), ethylene glycol (C) and KHP (D) in concentration range 0~3.6 mmol/L in 0.05 M NaOH medium. Scan rate: 50 mV/s.

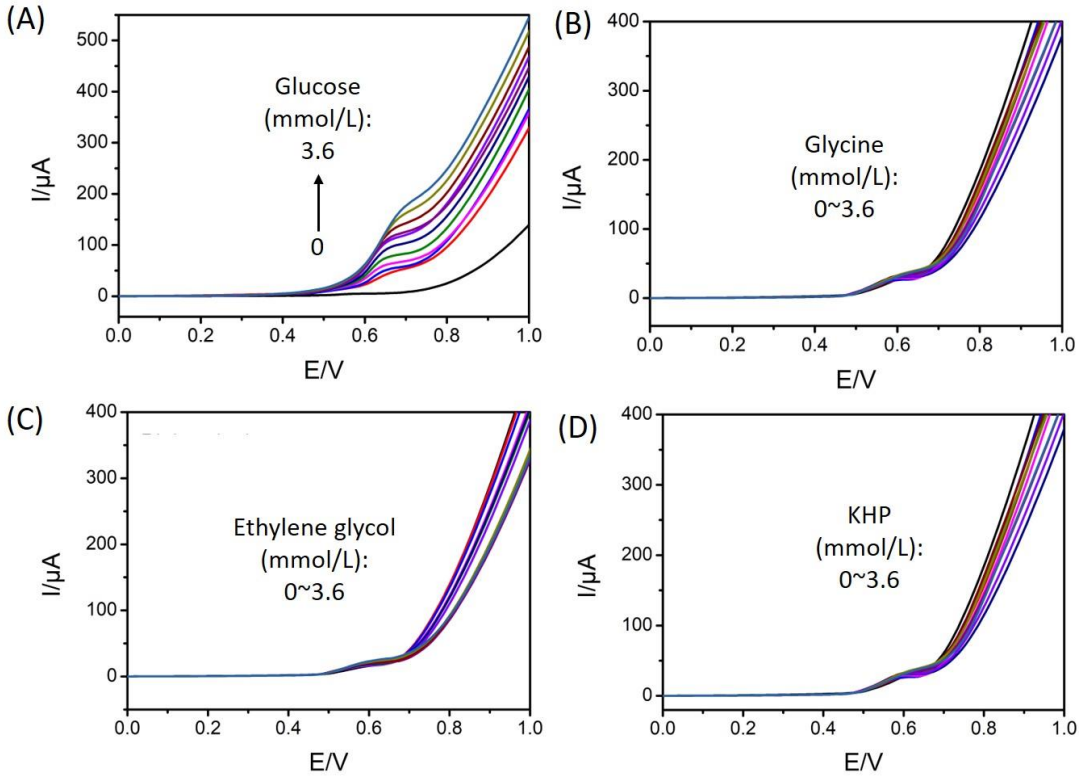

Figure 4.8 Oxidation curves of cyclic voltammograms of electrode Ni-Cu NPs responding to glucose (A), glycine (B), ethylene glycol (C) and KHP (D) in concentration range 0~3.6 mmol/L in 0.05 M NaOH medium. Scan rate: 50 mV/s.

4.1.2 Qualitative evaluation of standard and real samples using proposed ET array and PCA technique

Owing to the adequate diversity of CV signals derived from prepared four electrodes in former step, a clustering model would be established using PCA technique in here. To this aim, each standard substance was prepared in quadruplicate in concentration 2.15 mmol/L. Total 20 samples were measured and the obtained CV data were employed as inputs in PCA procedure. Electrochemical measurement was conducted in the same condition as the former step. The scores plot of the first two components resulted from PCA was shown in Figure 4.9. As observed, each standard organic substance was

clustered clearly, without overlap observed. Furthermore, glucose, a group that is easy to be oxidized, was located in the most left part and isolated from others. Whereas, KHP, which is hard to be oxidized, was in the righter position. To summarize, the PCA can discriminate different organics (the PC2 axis is mainly related to this), and indicate characterizations, such as the oxidation difficulties in this case, which can be differentiated by PC1 axis.

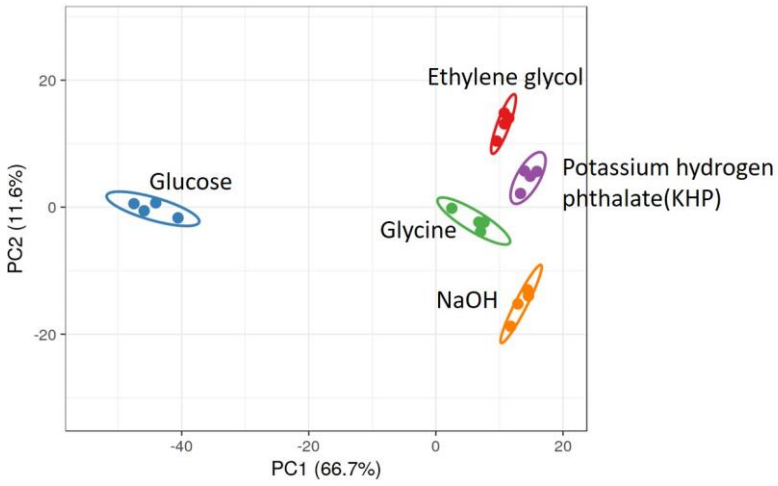

Figure 4.9 Score plot of the first two components obtained from PCA procedure. The clusters are glucose (blue), ethylene glycol (red), glycine (green), blank (orange) and potassium hydrogen phthalate (purple).

4.1.3 Calibration curve attained from electrode NfCuO/Cu for COD determination

As observed, electrode NfCuO/Cu responded to more substances than other electrodes and gave higher current signals to these substances, especially to glucose. Therefore, it was chosen for providing a classic protocol for COD determination using calibration curve. To achieve it, cyclic voltammetric responses of NfCuO/Cu to glucose in different concentration were recorded in previous condition, as shown in Figure 4.10 (A). Glucose was used as COD standard substances based on chemical equation, $C_6H_{12}O_6 + 6O_2 \rightarrow 6CO_2 + 6H_2O$, where 1 mol/L glucose equivalent to COD 192,000 mg/L O_2). It was found that the current intensity at around +0.70 V was proportion to the COD values over

the range from 19.20 to 905.5 mg/L O_2 (Figure 4.10 B). In addition, a regression equation I (μA) = 1.5281*COD+112.75 (R^2 = 0.9999) was fitted by least square. Limit of detection (LOD) value was calculated as 12.3 mg/L O_2 using the formula LOD = 3.3σ/S, where σ is the standard deviation of the response and S is the slope of the calibration curve. It is demonstrated that electrode NfCuO/Cu exhibits a good limit of detection, linear range, and high response signals, which can be verified from the comparison with some of the reported COD sensors in the literature, as shown in Table 4.2.

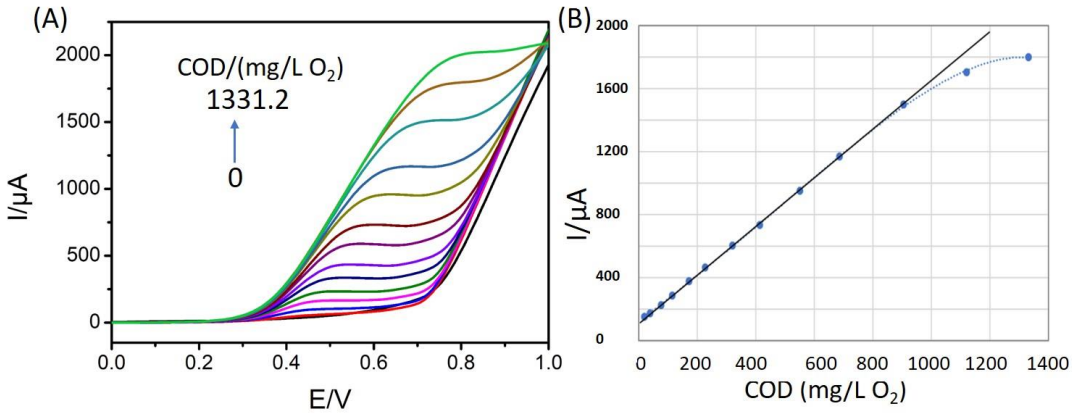

Figure 4.10 (A) Cyclic voltammetric responses of electrode NfCuO/Cu to glucose solutions that equivalent to COD range from 0 to 1331.2 mg/L O_2 in 0.05 M NaOH medium with scan rate 50 mV/s. (B) Calibration line fitted from COD values *vs.* current intensity at +0.70 V.

Table 4.2 Comparison of NfCuO/Cu with reported sensors of literature.

Sensor	Electrode Modifier	Standard Substance	LOD (mg/L O_2)	Linear Range (mg/L O_2)	Repeatability (RSD%)
CuO/AgO sensor [15]	CuO/AgO NPs	Glucose	28	106~1292	--
Boron doped diamond [16]	-	KHP, phenol	7.5	20~9000	1.9
Cobalt oxide/GCE [17]	Cobalt oxide film	Glycine	1.1	5.7~155.8	5.7
CuO/Cu disk [18]	Cu NPs	Glucose	1.07	2~595	
Ni Cu alloy/GCE [5]	Ni Cu alloy film	Glucose	1.0	10~1533	1.0
Ti/Sb-SnO_2/PbO_2 [19]	Sb-SnO_2/PbO_2	Glucose	0.3	0.5~200	<5%

CuO/Cu electrode [11]	CuO NPs	Glucose	20.3	53.0~2801.4	--
F-PbO_2 sensor [20]	Pb (II) particles	Glucose	15.5	100~1200	--
Nano-Ni/GCE [21]	Nano-Ni	Glucose	1.1	10~1533	4.7
This work	Nano-CuO	Glucose	12.3	19.2~905.5	2.48%

4.1.4 Analytical application of real samples

4.1.4.1 Spike-and-recovery assessment

To explore the potential of electrode NfCuO/Cu for practical application of analysing real wastewaters, sample R1, R2 and R3 listed in Table 3.5, section 3.3.2, were studied using it by spike-and-recovery experiment. To conduct this experiment, 10 mL of each sample was mixed with 10 mL 0.05 mol/L NaOH solution, following the cyclic voltammetric measurement using electrode NfCuO/Cu. CV measurement was repeated after spiking with 0.5 mmol/L glucose, which was equivalent to theoretical COD 96.0 mg/L O_2. The obtained voltametric oxidation curves were shown in Figure 4.11. The COD values were calculated based on current intensity at +0.70 V and calibration equation obtained above (I = 1.5281*COD + 112.75). These results were summarized in Table 4.3. Samples R1 and R2 were known that they had been polluted by pesticides, COD detected as 1312 and 2044 mg/L O_2 respectively by HACH cuvettes. While sample R3 was a relatively clean river water with COD 11.7 mg/L O_2. As shown from this data, the recovery yields of spiked glucose in measured samples were very near to 100%, which indicated that the electrode NfCuO/Cu has good performance in quantifying the organic compounds that are easy to be oxidized, such as glucose.

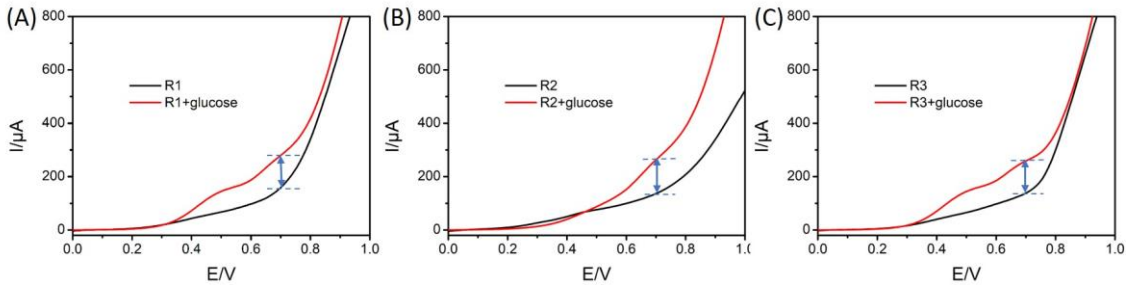

Figure 4.11. Oxidation of voltammetric responses of electrode NfCuO/Cu to samples R1~R3 before (black lines) and after (red lines) adding glucose (equivalent to COD 96.0 mg/L O_2). Scan rate: 50 mV/s.

Table 4.3 Recovery yield of spiked glucose found by electrode NfCuO/Cu.

Samples	Theoretical COD (mg/L O_2)*	COD found before spiking (mg/L O_2)	Added Glucose (mg/L O_2)	COD found after spiking (mg/L O_2)	Recovery yield (%)
Spiked R1	656	33.76	95.52	112.11	81.61%
Spiked R2	1044	17.10	95.52	101.64	88.06%
Spiked R3	5.85	18.56	95.52	97.37	82.09%

*Theoretical COD in measuring beaker after dilution.

4.1.4.2 Evaluation of polluted water using ET and PCA

In this step, the function of the sensor array would be explored combined with PCA technique. To prepare the measuring samples, 100 μL of each sample (R1, R2, R3 and R8) was added into 20 mL 0.05 mol/L NaOH medium to be a test solution. In addition, such test solutions of samples R1 and R2 were spiked with glucose respectively, which were measured and labelled as samples "Spiked R1" and "Spiked R2" after that. Each sample was prepared in quadruplicate. Voltammetric response of this sensor array to these samples plus a blank (0.05 mol/L NaOH solution prepared from Milli-Q water) and glucose solution (equivalent to COD 96 mg/L O_2) were measured electrochemically as done in previous step. The voltametric data was used as inputs for PCA procedure. The obtained PCA result was shown in Figure 4.12, where the numbers indicated theoretical COD values from calculation.

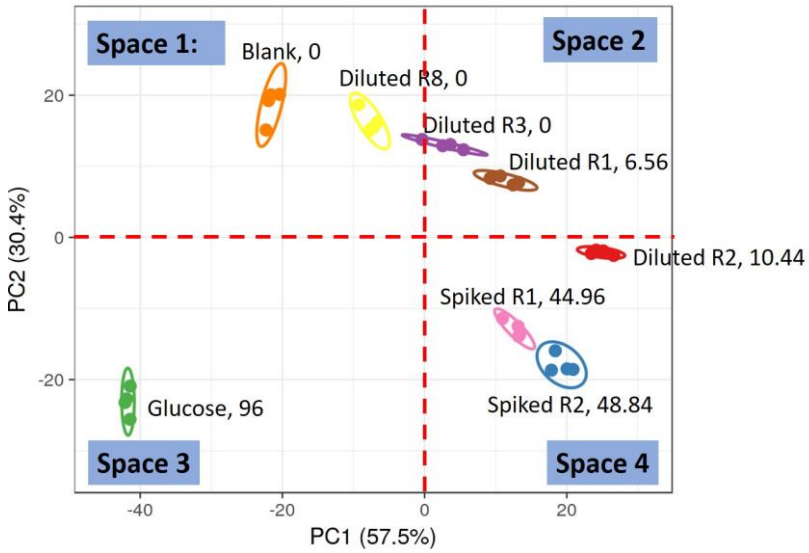

Figure 4.12 Score plot of the first two components resulted from PCA. Groups refers to glucose (green), blank (orange), diluted R8 (yellow), diluted R3 (purple), diluted R1 (brown), diluted R2 (red), glucose spiked R1 (pink) and glucose spiked sample R2 (blue).

As observed from this figure, the samples were clustered clearly. The entire PCA space in the figure could be divided into 4 spaces. The samples containing glucose tend to be in the inferior part, such as space 3 and 4. Oppositely, samples containing organic pollutants that are hard to be oxidized by the sensor array are located in superior parts, such as space 1 and 2. That was consistent with the shift of samples R1 and R2 after adding glucose. In addition, samples almost without any organic pollution were in superior part as well, which are related to their lower current intensity signals, like the case of high oxidation difficulty. However, the cleaner water samples, like blank and tap water R8, appeared in space 1, different from samples R1 or R2. The sample R3 was in the boundary of spaces 1 and 2, which is reasonable considering its property and lower COD. In addition, the samples with complex components are also discriminated, as shown by glucose and glucose-spiked samples, which were in space 3 and 4, respectively. Briefly, the space 1 samples show high possibility of clean water without much organic pollution. It is likely that Space 2 and Space 4 samples contain organic pollutants with high oxidation

difficulty. Space 3 are related to organic pollutants that are easy to oxidized and the COD values can be calculated accurately through electrochemical sensors, like proposed NfCuO/Cu.

Publication for Section 4.1:

Determination of Chemical Oxygen Demand (COD) Using Nanoparticle-Modified Voltammetric Sensors and Electronic Tongue Principles.

Qing Wang and Manel del Valle.

Chemosensors, **2021**, 9, 46.

https://doi.org/10.3390/chemosensors9030046.

4.2 Electronic tongue array combined with artificial neural network model for COD determination

As reported, many electrochemical sensors for COD determination were employed by plotting a calibration curve [2,5,21–26]. Nevertheless, wastewaters usually contain diverse organic compounds with complex structures, natures or concentration, which may result in low accuracy as mentioned in section 1.4.5. Therefore, sometimes electrochemical signals do not reflect the COD values because of the complexity and diversity of organic pollution in practical COD test. Basically, the COD value can be estimated precisely from the calibration curve only when the sample contains a single species.

In this direction, attempting the multi-determination of several standard substances and the use of multivariate data analysis might show better performance. Based on an array of electrochemical sensors that capture adequate signals derived by various organic species, plus a modelling tool for interpreting and extracting meaningful data, electronic tongue technique may provide help in such studies [27]. As a rapid, low-cost and simple tool, electronic tongues have been widely used for liquid analysis, which is done by treating the signal pattern with multivariate data analysis. It can generate an output pattern that reflects a synthesis of all the components and an overall outlook when analysing samples containing different compounds or analytes. This technique works based on the combination of collected information by several sensors which are likely to be of low specificity. Lots of efforts have been put into application of ETs in analytical field attracted by the advantages of simplicity and versatility, such as in food industry (wine, fish, meat, milk, beverage, etc.), water quality monitoring, environmental analysis, etc [28–32].

Whereas, very few studies have been carried out to explore the application of ETs in COD determination combined with artificial neural networks (ANNs). As shown from Section 4.1, a single electrochemical sensor can be limited in the complex system generated by organic compounds of various chemical structures and properties, which may increase the inaccuracy of COD values detected. As reported, it was revealed that some electrodes, such as glass carbon/Ni-Cu and boron-doped diamond (BDD), some tested organic compounds (e.g., glucose, glycine, phenol, ethanol, etc.) were fitted into the identical linear regression equation that showing the relationship of COD value and electrochemical signal [5,25]. In case of some other electrodes, it was found that hydroxyl radicals, which were responsible for the degradation of organic compounds, would show different rate constants for some organic compounds under the same conditions [25,33]. Therefore, COD calculation by combining signals derived from several sensors and standard substances can be helpful for collecting more information to increase accuracy. In this sense, electronic tongue technique is an ideal method for COD determination and organic pollution monitoring.

Voltammetry technology plays an important role in electroanalytical study by measuring the current as a function of the potential for generating information about one or more analytes. It is more versatile and robust because the voltammetric signals usually have a favourable signal to noise ratio, less influenced by electrical disturbances [24]. In this section, a voltammetric ET based on graphite, Cu and metallic nanomaterials were built for COD analysis. Similar to previous one, a Cu block electrode modified with CuO nanomaterial by electrochemical anodization procedure was employed, which was named as CuO/Cu. Different from that one, it was not filmed by Nafion. In addition, GEC-based electrodes incorporating Cu NPs, CuO NPs and Ni-Cu NPs were reused as members of this new ET array. Moreover, same electrode modified

with Ni NPs was involved as well in order to catching various voltammetric signals, named as Ni NPs in this text.

4.2.1 Preparation of sensors

4.2.1.1 Sensor fabrication

The electrochemical anodization procedure was carried out in a same way in Section 4.1. CuO nanostructure was formed at the Cu surface by cyclic voltammetry (50 scans) between the potential range −1.0~+0.8 V *vs.* Ag/AgCl in 0.05 M NaOH medium. Some cyclic voltammograms during this procedure were recorded, as illustrated in Figure 4.13. The surface of the Cu block electrode changed to dark from the initial glossy yellow because of the formation of copper oxide substance. GEC electrodes Cu NPs, CuO NPs, Ni NPs and Ni-Cu NPs were modified with corresponding nanoparticle according to the described procedure in section 3.2.1.

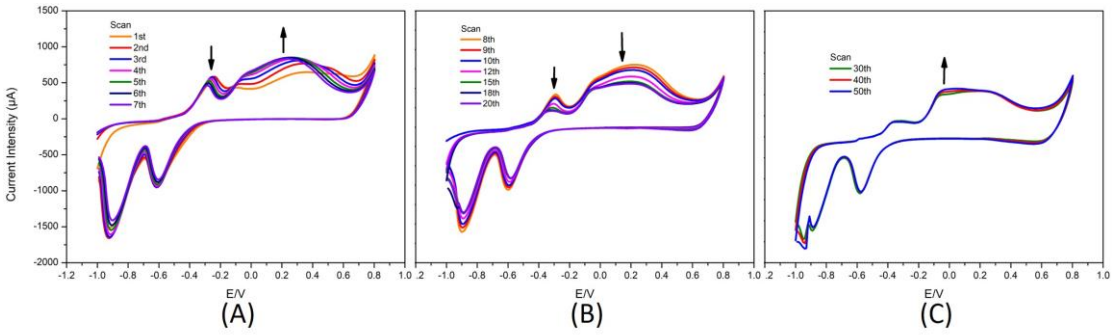

Figure 4.13 Some of cyclic voltammograms for electrochemical anodization of CuO NPs on the surface of Cu block in three different observed stages in 0.05 mol/L NaOH medium at scan rate 100 mV/s.

4.2.1.2 Morphological characterization

Scanning electron microscopy (SEM) images were taken to confirm the surface modification after completion of these electrodes, as shown in Figure 4.14. Therein, Figures (A) and (B) are Cu surface before and after the

electrochemical anodization. As observed, the surface look rougher and a layer of nanomaterial spreading over it contributed by the formation of CuO, which is helpful to enhance the electro-catalytic activity. The SEM images of other GEC electrodes were shown in Figures (C) Cu NPs, (D) CuO NPs, (E) Ni-Cu NPs and (F) Ni NPs.

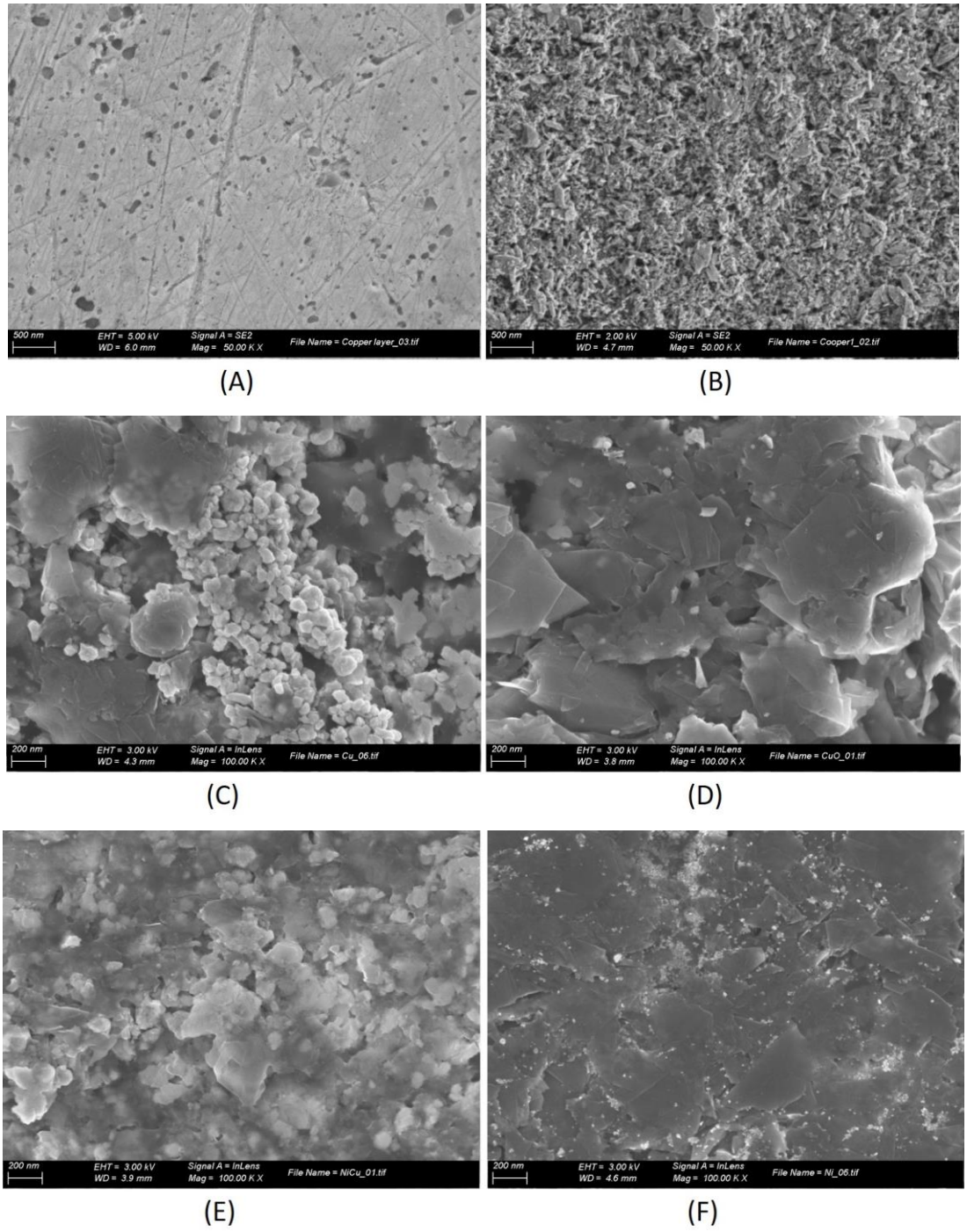

Figure 4.14 Scanning Electron Microscopy (SEM) images of surfaces of electrodes (A) bare Cu block, (B) electrode CuO/Cu after electrodeposition and GEC electrodes (C) Cu NPs, (D) CuO NPs, (E) Ni-Cu NPs and (F) Ni NPs.

4.2.2 Electrochemical performance of prepared sensors

4.2.2.1 Repeatability

Good repeatability is always important particularly for sensors used for developing ET applications because the sensors usually have to withstand the larger number of measurements required for building chemometric models compared with a classic univariate calibration model.

For this purpose, the repeatability of prepared electrodes was tested by checking their responses to of standard organic sample composed of glucose and glycine (equivalent to COD 300 mg/L O_2). The voltammetric responses were measured in 0.05 mol/L NaOH medium for 10 times, during which the blank electrolyte medium (0.05 mol/L NaOH) was also evaluated in between. The oxidation of obtained voltametric responses of these electrodes was shown in Figure 4.15, where the curves of same electrode were overlapped very well, which indicated the good repeatability. To prove it, the relative standard deviation (RSD) values over these 10-time measurement based on the current intensity at +0.6 V and +0.7 V were calculated, as listed in Table 4.5. RSD values were smaller than 5% in all the cases, which showed the good repeatability of the prepared sensors.

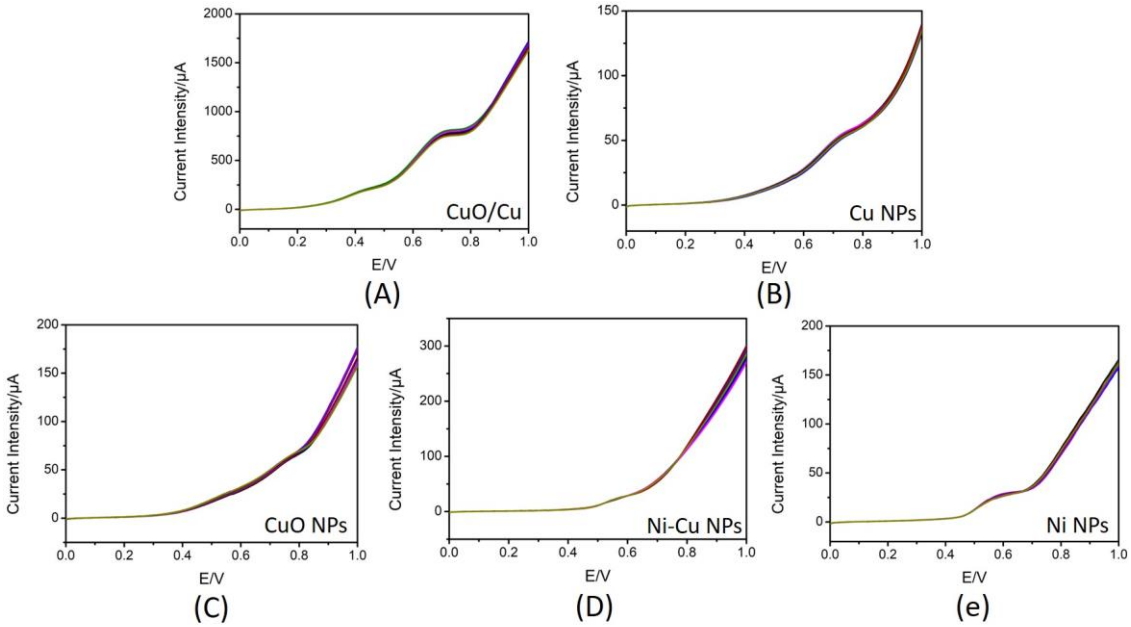

Figure 4.15 Oxidation of voltammetric responses for 10 times measured by electrodes (A) CuO/Cu, (B) Cu NPs, (C) CuO NPs, (D) Ni-Cu NPs and (E) Ni NPs to the mixture of glucose and glycine in 0.05 mol/L NaOH medium. Scan rate: 50 mV/s.

Table 4.5 RSD values calculated over these 10-time measurement for repeatability test based on the current intensity at +0.6 V and +0.7 V.

Sensor	RSD%[1]	RSD%[2]
CuO/Cu	2.91%	2.64%
Cu NPs	3.60%	2.21%
CuO NPs	3.95%	2.69%
Ni Cu NPs	0.69%	2.88%
Ni NPs	3.19%	2.80%

[1, 2] Calculated according to the current intensity at E=+0.6 V and E=+0.7 V, respectively.

4.2.2.2 Voltammetric responses to standard substances

The voltammetric responses of the prepared electrodes to glucose and glycine, who were used as COD standard substances, were estimated to check their potential of constituting an electronic tongue array. 0.05 mol/L NaOH solution was used as the medium in measurement to offer a mild alkaline condition. The voltametric signals derived from these sensors responding to glucose or glycine (equivalent to COD 400 mg/L O_2) were displayed in Figure 4.16.

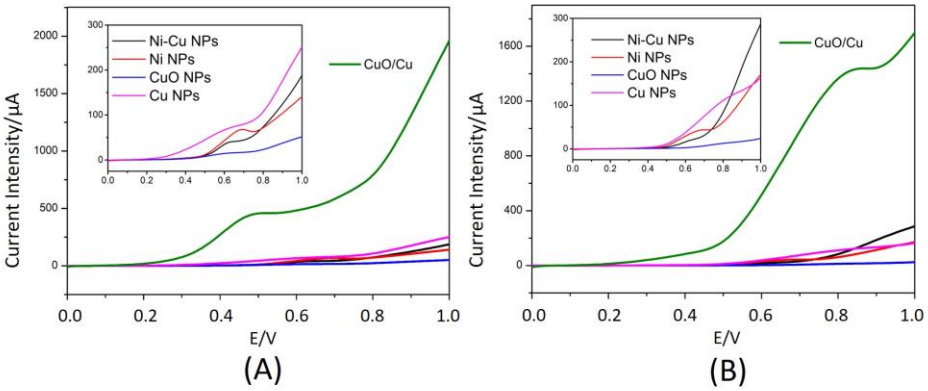

Figure 4.16 Oxidation of voltammetric responses of the prepared electrodes to glucose (A) and glycine (B) solutions with a theoretical COD value of 400 mg/L O_2 in 0.05 M NaOH medium. Scan rate: 50m V/s.

As illustrated, glucose and glycine were oxidized at the surfaces of five fabricated electrodes. What's more, the oxidation of these two compounds at different electrodes occurred at different potentials. For Ni NPs electrode, the oxidation of these two compounds occurred at between +0.6 and +0.7 V. While in the case of electrode CuO/Cu, the oxidation of glucose and glycine occurred at 0.5~0.6 V and 0.7~0.8 V, respectively. In addition, the current intensity for the CuO/Cu electrode are much higher than other sensors. It is worthy to note that, the different signals for different electrodes responding to these two analytes is desirable for developing ET arrays. Furthermore, voltammetric responses of the prepared electrodes to a series of concentrations of glucose and glycine were measured, as shown in Figures 4.17 and 4.18 respectively. The glucose was tested in concentrations equivalent to COD range from 0 to 1000 mg/L O_2. Glycine was measured with COD range 0~400 mg/L O_2. Table 4.6 summarized the fitted equations from the calibration lines obtained from electrode CuO/Cu, who gave the highest current signals.

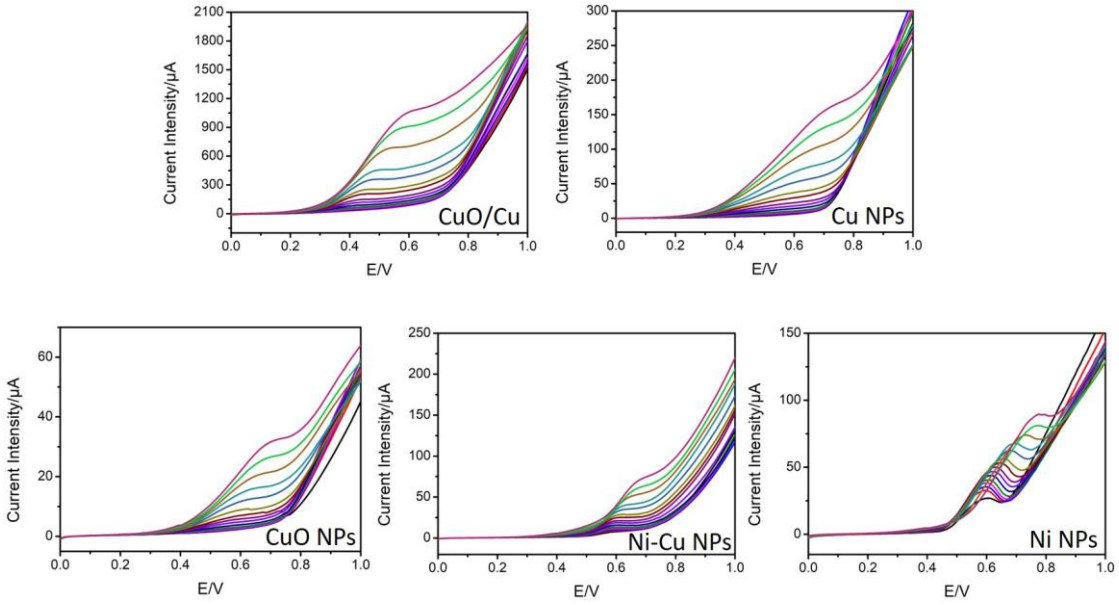

Figure 4.17 Oxidation of voltammetric responses of electrodes (A) CuO/Cu, (B) Cu NPs, (C) CuO NPs, (D) Ni-Cu NPs and (E) Ni NPs to glucose solutions in 0.05 mol/L NaOH medium with scan rate 50 mV/s. Equivalent theoretical COD values were from 0 to 1015 mg/L O_2.

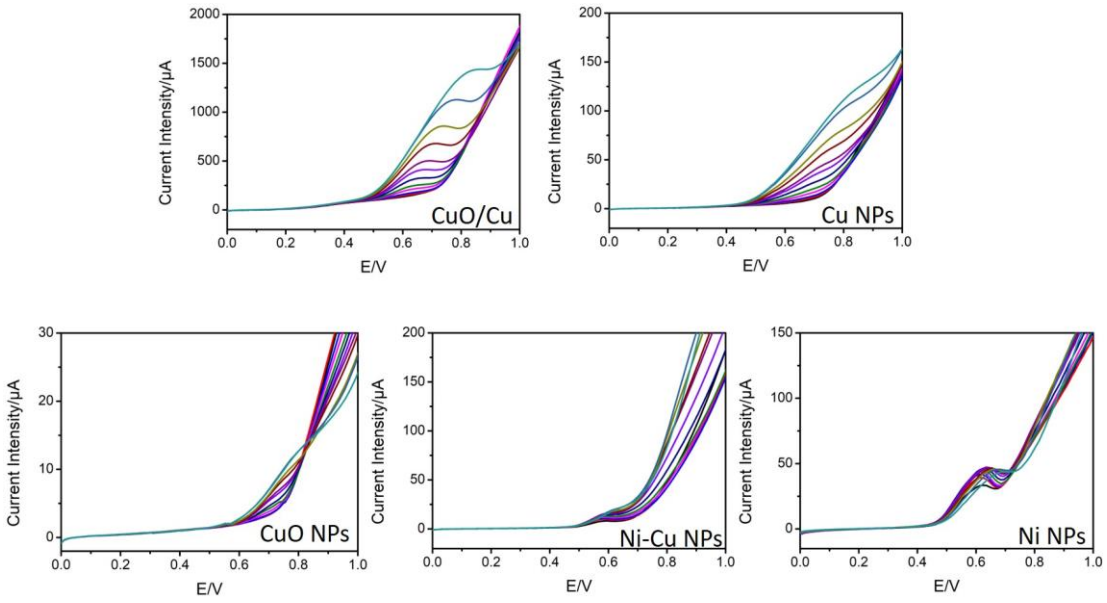

Figure 4.18 Oxidation of voltammetric responses of electrodes (A) CuO/Cu, (B) Cu NPs, (C) CuO NPs, (D) Ni-Cu NPs and (E) Ni NPs to glycine solutions in 0.05 mol/L NaOH medium with scan rate 50 mV/s. Equivalent theoretical COD values were from 0 to 400 mg/L O_2.

Table 4.6 Calibration equations derived from the oxidation current intensity at the fixed potentials of +0.6 and +0.7 V measured by electrode CuO/Cu responding to glucose and glycine, respectively.

Compound	Equation	Linear range (mg/L O_2)	Limit of detection (mg/L O_2)
Glucose	y = 1.0281x + 85.90, R^2 = 0.9996	30 ~ 800	15.7
Glycine	y = 3.3315x + 167.19, R^2 = 0.9991	10 ~ 180	4.6

4.2.2.3 Interference of chloride ions

As explained in section 1.4.3.1, chloride can cause serious interference on COD values due to the redox reaction with $Cr_2O_7^{2-}$ ions, which can lead to an overestimation of the COD value. Therefore, the interference of chloride to COD determination can't be ignored because of its common existence and high concentration in wastewater. Therefore, the test of chloride interference is an important factor to evaluate an electrochemical COD sensor. In this work, the experiments related to chloride interference test was investigated by recording voltammetric responses of each prepared electrodes towards some concentrations of NaCl in presence of glucose and glycine. The total concentration of glucose and glycine was equivalent to COD 300 mg/L O_2. The voltammetric oxidation signals were displayed in Figure 4.19. Fortunately, there were no much signal difference observed between scans, which implied there was no obvious influence arising from the presence of Cl^-. In addition, the RSD were also calculated as done in section 4.2.2.1. The values were listed in Table 4.7, with good behavior of the prepared electrodes indicated by low values.

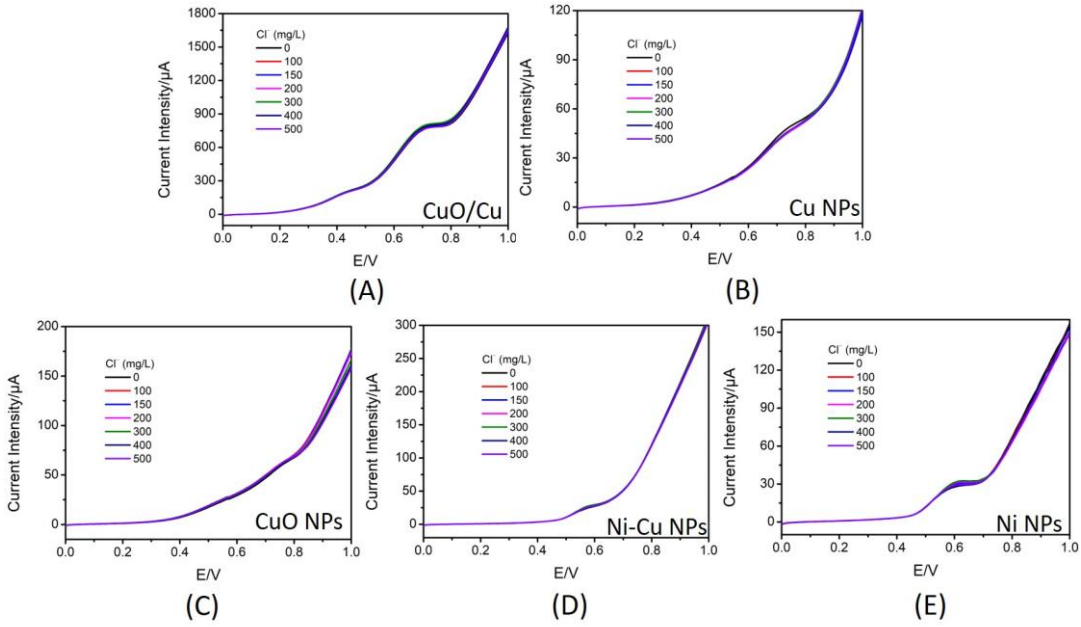

Figure 4.19 Voltammetric oxidation signals derived from electrodes (A) CuO/Cu, (B) Cu NPs, (C) CuO NPs, (D) Ni-Cu NPs and (E) Ni NPs responding to glucose and glycine in the presence of various concentrations of Cl^-. Medium: 0.05 mol/L NaOH. Scan rate: 50 mV/s.

Table 4.7 RSD values calculated from the voltammetric signals responding to glucose and glycine in the presence of various concentrations of Cl^- for each of the electrodes.

Sensor	RSD[1]	RSD[2]
CuO/Cu	1.82%	1.43%
Cu NPs	1.63%	2.22%
CuO NPs	2.84%	1.97%
Ni Cu NPs	2.94%	1.00%
Ni NPs	4.58%	1.55%

[1, 2] Calculation based on the current intensity of oxidation at +0.6 V and +0.7 V, respectively.

4.2.3 Optimization of methods for COD determination using individual sensor and electronic tongue array

4.2.3.1 Classic calibration curves for COD detection using sensor CuO/Cu

As shown section 4.2.2.2, calibration curves were fitted from the relationship between COD values and current intensity values directly obtained from electrochemical measurement using sensor CuO/Cu, as done by

some reported works [2,11,14]. However, in this case, large shift was occurred accompanied with the COD increase as shown in Figures 4.17 and 4.18, which could decrease the linear range and affect the sensor's performance. To dissolved this problem, the obtained voltammetric signals were treated by subtracting baseline utilizing Origin program. The baseline subtracted voltammetric signals were shown in Figure 4.20. Peak height values of them and corresponding COD values were plotted on graphs in Figure 4.20 and their relationships were shown by calibration equations fitted in Figure 4.21. The related analytical parameters were summarized in Table 4.8.

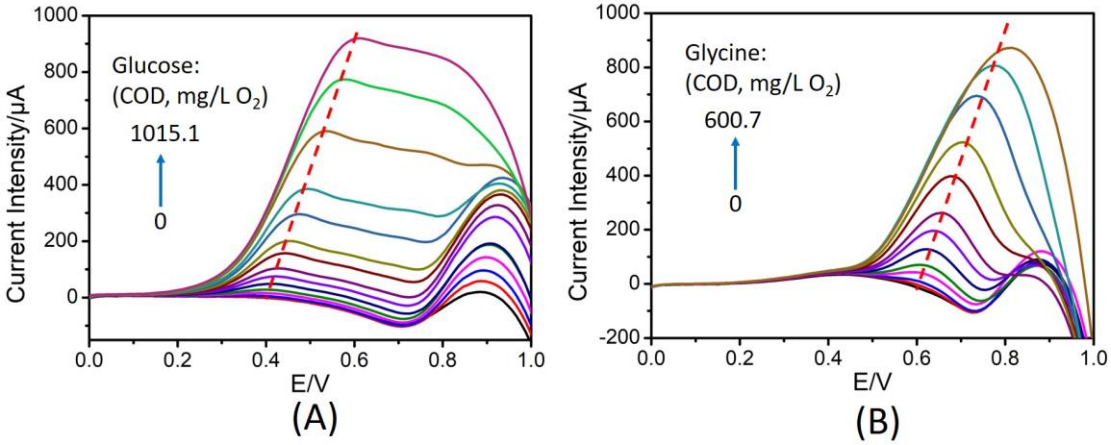

Figure 4.20 Baseline subtracted voltametric oxidation signals for (A) glucose and (B) for glycine.

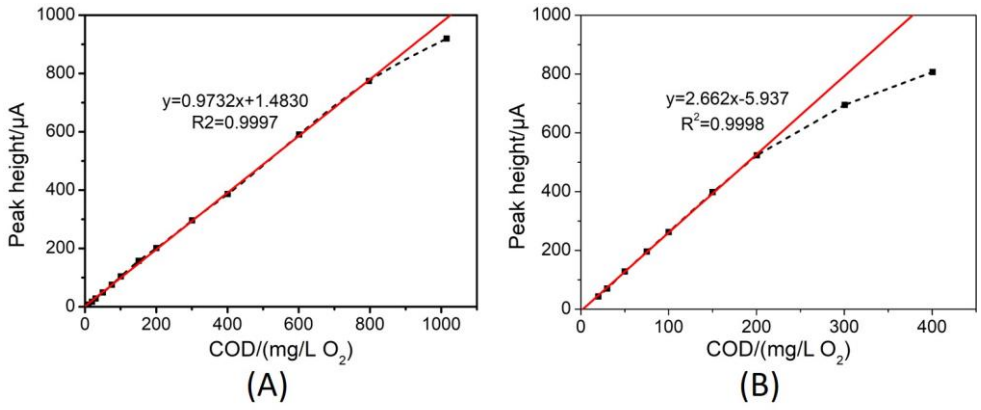

Figure 4.21. Calibration curves showing the relationship between COD values and peak height obtained from data of Figure 4.20, using glucose (A) and glycine (B) as standard analytes respectively, for sensor CuO/Cu.

Table 4.8 Analytical parameters of calibration curves showing the relationship between baseline subtracted voltammetric oxidation signals and COD values for sensor CuO/Cu.

Compound	Sensitivity (μA/mg/L O_2)	Intercept (μA)	R^2	Linear range (mg/L O_2)	LOD (mg/L O_2)
Glucose	0.9732	1.48	0.9997	20-800	13.6
Glycine	2.662	5.94	0.9998	20-200	4.1

4.2.3.2 ANN model for COD determination using ET sensor array

As seen from Figures 4.15 or 4.19, the oxidation of glucose and glycine were occurred at different potentials, as evidenced from two peaks at around +0.40 V and +0.70 V, which were corresponding to oxidation of glucose and glycine, respectively. Classic calibration method might be not suitable for this case because of these separated peaks. Therefore, the artificial intelligence response model, artificial neural network (ANN), would be built for the purpose of a better estimation for COD values based on quantification of glucose and glycine, as explained in Figure 4.22. This model would be able to combine the signals derived from several sensors and compensate the differences in the voltammetric signals captured for different compounds (e.g., sensitivity, peak position, etc.).

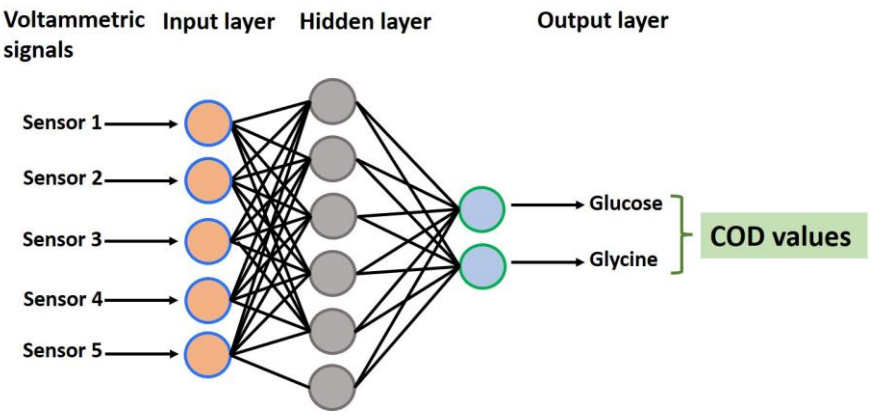

Figure 4.22 Graphic configuration of ANN model for COD determination based on standard substances glucose and glycine.

In this step, an ANN model was built involved in electronic tongue responses for the simultaneous determination of binary COD standard substances to seek for a method of estimating organic pollution more precisely. To this aim, a 4^2 tilted factorial design was proposed with 4 concentration levels and 2 factors, namely 2 analytes in this text. The concentration domains were decided by the voltammetric responses of electronic tongue array to each analyte, as shown in Figures 4.17 and 4.18. Two concentration ranges of 0.25~4.00 mM for glucose and 0.40~6.25 mM for glycine were chosen as the concentration domain for the purpose of the measurable voltammetric signals. As exemplified in the coordinate system in Figure 4.23, to obtain the ANN response model, a training subset composed of 16 samples (blue points) were prepared and a testing subset of 10 samples (red points) was chosen randomly to assess the performance of the model. The two axes represented the concentrations of two COD standard substances analytes to simulate organic pollutants with different electrochemical activity to be determined.

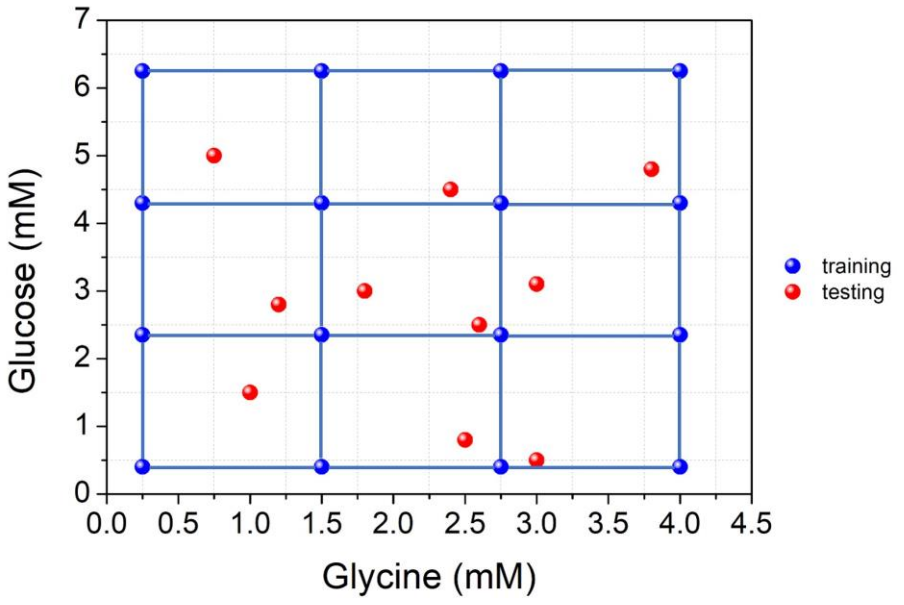

Figure 4.23 The coordinate system for illustrating the ANN model composed of training and testing subsets.

Firstly, the topology of the ANN model was optimized employing the data obtained from the training subset. The inputs were pruned with causal index (CI) analysis. The neurons and transfer functions were varied systematically to identify the configuration for the best performance. After the trial-and-error process, there were 91 neurons in the input layer (being fed with the voltammograms from the 5 sensors), 1 neuron and *purelin* transfer function in the output layer and 7 neurons and *logsig* transfer function in the hidden layer in the optimized ANN model. Next, the data of the testing subset were interpolated into the model. The graphs of illustrating the comparison between the predicted and expected COD values were shown in Figure 4.24. From these graphs, regression lines of both training and testing subsets were close to the ideal identity ones, which indicated a satisfactory performance. To explain the performance numerically, the regression parameters and the root mean square error (RMSE) of the fitting were calculated with results shown in Table 4.9. As observed, the slopes were near to 1 and intercept values were rather low. In addition, the coefficient of determination was close to 1 and the RMSE value was rather low. The good trend and performance of this model can be confirmed from these values.

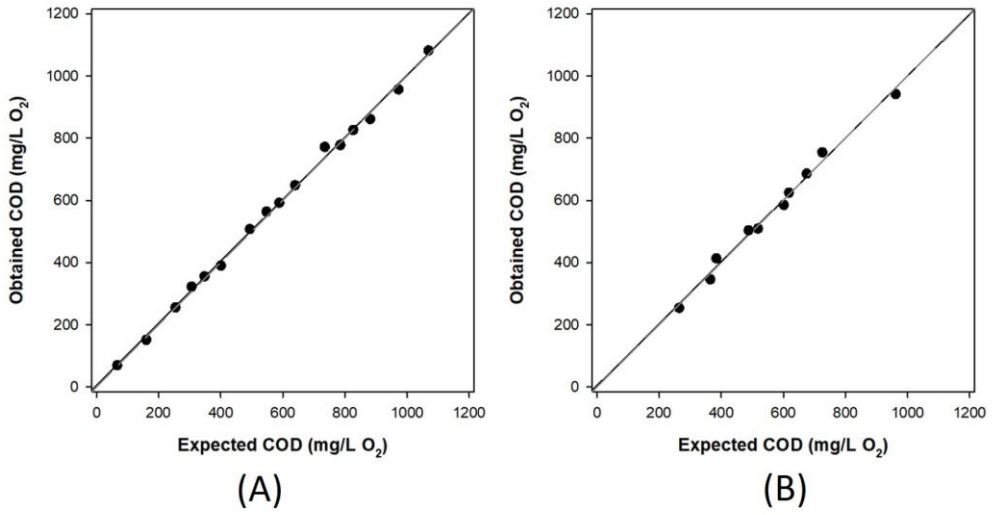

Figure 4.24 Graphs illustrating comparison between predicted *vs.* expected COD values for the training (A) and testing (B) subsets. The line refers to the ideal comparison line (y=x).

Table 4.9 Parameters of fitted regression lines for the comparison between obtained *vs.* expected values for the training and testing subsets.

Data set	Slope	Intercept (mg/L O_2)	R^2	RMSE (mg/L O_2)
Training	0.997 ± 0.027	6 ± 18	0.998	11.3
testing	0.996 ± 0.077	4 ± 45	0.991	16.6

4.2.4 Analysis on real samples using different methods

Several real river water samples (R3~R7, Table 3.5 in section 3.3.2) were analyzed after construction and validation of the ANN model using standard substances. These samples were firstly mixed with 0.1 mol/L NaOH solution (1:1, v/v) for an alkaline medium before the electrochemical measurements. Voltammetric responses of the ET array to these samples were measured in potential range from 0 V to +1.0 V with scan rate 50 mV/s. In addition to these five samples, five spiked samples based on them (labelled as S-R3~S-R7) were also analyzed by adding standard substances glucose and/or glycine, as information displayed in Table 4.10. Upon the voltammetric data attained, COD values were calculated in both approaches, ANN and classic calibration equations fitted by sensor CuO/Cu (Figure 4.21). For comparing the accuracy, commercial COD test cuvettes were utilized according to procedure described in section 3.6. The results achieved from these approaches were summarized in Table 4.10.

Table 4.10 Calculation results of river water and spiked samples from different approaches for COD determination.

Sample	**Spiked analytes** COD (mg/L O_2)	**y=0.9732x+ 1.4830** COD (mg/L O_2)	**y=2.662x- 5.937** COD (mg/L O_2)	**ANN** COD (mg/L O_2)	**Cuvette test** COD (mg/L O_2)

R3	--	105.6	44.18	--	11.70
R4	--	99.32	41.88	--	12.10
R5	--	102.7	43.12	--	15.10
R6	--	98.06	41.43	--	9.21
R7	--	100.8	42.43	--	5.24
S-R3	686.5 (glucose + glycine)	868.3	320.2	659.7	719.0
S-R4	187.3 (glycine)	481.8	178.9	141.9	216.0
S-R5	376.5 (glucose)	402.1	149.8	284.7	416.0
S-R6	320.0 (glucose + glycine)	361.1	134.8	286.7	342.0
S-R7	234.4 (glucose + glycine)	466.7	173.4	211.0	260.0

For comparing between these methods, exploratory analysis of the different methodologies was carried out by calculating the regression lines based on the results of each two methodologies, results were displayed in Table 4.11. The obtained results that were below the LOD values were discarded for avoiding bias in the low COD values. As seen from this table, the best linearity of the comparison, was the one of the cuvette test results *vs.* those of the ANN model method, which was also remarkably close to the identity line. As can be seen in Figure 4.25, the best comparison line, a good agreement was obtained between both values, which indicated the good suitability and potential in COD determination using ET arrays coupled with ANN models.

Table 4.11 Results obtained from the exploratory analysis on COD values calculated from different methodologies for river water and spiked samples.

Results compared	Comparison line	R^2 (n=5)
ET *vs.* Spiked	y = 1.0132 * x - 48.9	0.9383
Cuvette test *vs.* Spiked	y = 1.0134 * x + 24.8	0.9553
ET *vs.* Cuvette test	y = 0.9949 * x - 71.9	0.9723[c]

Equation 1[a] *vs.* Spiked	y= 0.8532 * x + 208	0.5384
Equation 2[b] *vs.* Spiked	y = 0.8701 * x + 240	0.7413
Equation 1[a] *vs.* Cuvette test	y = 0.3119 * x + 78.8	0.5385
Equation 2[b] *vs.* Cuvette test	y = 0.3181 * x + 90.7	0.7414

[a] Calibration equation fitted from the first oxidation peak. [b] Calibration equation fitted from the second oxidation peak. [c] The best determination coefficient.

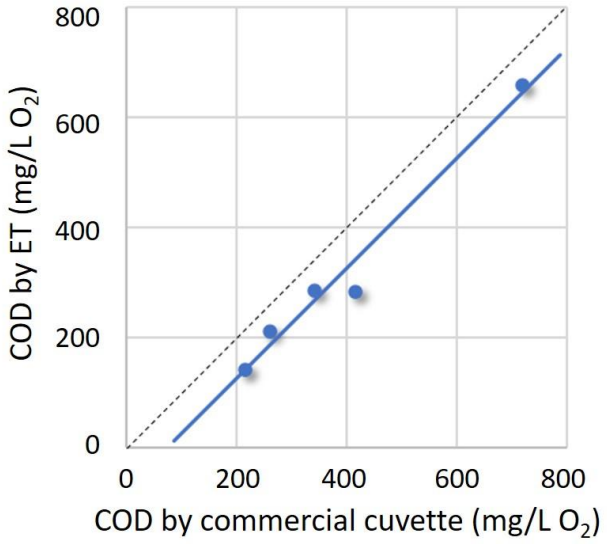

Figure 4.25 Graph illustrating the comparison between the results obtained from proposed ET-ANN approach and the commercial cuvette test.

It is worthy to note that, although electrochemical method has been accepted as a good approach due to many advantages, their quantification to COD values were always based on classic calibration curves and equations, as displayed in Table 4.12. The proposed ET combined with ANN model was an important and meaningful try in this field, which demonstrated the promising prospect. The ongoing work is to optimization and development of the application of ANN to COD determination.

Table 4.12 Comparison of reported approaches for COD determination based on electrochemical measurement.

Sensor	Standard Substance	LOD, linear range ($mg/L\ O_2$)	Determination approach	Electrochemical technology
Ni NPs/Glassy carbon [34]	Glycine	0.14, 0.24~480	Calibration curve	Amperometry

TiO_2/Ti [33]	KHP, phenol	--, 25~530	Calibration curve	Chronocoulometry
Nano-Cu/Cu [3]	Glucose, Glycine	8.90, 17.45~176	Calibration curve	Amperometry
Nano-Cu/graphite [3]	Glucose, Glycine	9.02, 32~256	Calibration curve	Amperometry
Cu NPs based C/SiO_2 [14]	Glucose	28, 53~670	Calibration curve	Chronoamperometry
CuO/AgO/ carbon nanotube-polystyrene composite [15]	Glucose	28, 106~1292	Calibration curve	Chronoamperometry
Ni Cu alloy NPs/ carbon nanotube-polystyrene composite [15]	Glucose	21, 106~1292	Calibration curve	Chronoamperometry
TiO_2/CuS/indium tin oxide electrode [35]	acetic acid, phenol, KHP, glucose,	0.017, 0.05~50	Calibration curve	Potentiometry
Nano-Cu/Cu-cable [18]	Glycine	2.4, 2~595	Calibration curve	Linear sweep voltammetry
CuO-Nafion film/Cu electrode [2]	Glucose	2.11, 50~1000	Calibration curve	Linear sweep voltammetry
NiCu film/Glassy carbon [5]	Phenol, lactose, glucose, glycine, ethanol, etc.	1.0, 10~1533	Calibration curve	Cyclic voltammetry
Boron-doped diamond (BDD) sensor [25]	Glucose, KHP, phenol, etc.	7.5, 20~9000	Calibration curve	Amperometry
This section [36]	Glucose, glycine	13.6*, 20-800*	Calibration curve, ANN model	Cyclic voltammetry

* Obtained from the calibration curve method using sensor CuO/Cu and glucose.

Publication for Section 4.2:

Quantitative Estimation of COD Values from an Array of Metal Nanoparticle Modified Electrodes and Artificial Neural Networks.

Qing Wang, Xavier Cetó and Manel del Valle.

Chemosensors, **2022**, 10, 504.

https://doi.org/10.3390/chemosensors10120504

4.3 Identification and discrimination of herbal calming products employing ET and machine learning algorithms

As introduced in Section 1.5, chamomile, passionflower, valerian and lavender were widely accepted as anxiolytic herbs for mental anxiety disorders treatment and prevention. Chamomile flowers are commonly used as infusions because of its widely-accepted smell and flavour. Chamomile can be used as mild sedatives in treating insomnia or other sleep complications by reducing nerves and anxiety. Passionflower and valerian roots are well used in aiding relaxation and treating insomnia by increasing γ-aminobutyric acid (GABA) levels in the brain [37,38]. Lavender tea and essential oils made of lavender flowers can be used for sleeping aids in traditional medicinal uses based on the property of calming nerves.

Herbal medicines should be always beneficial, well-qualified and safe for its good development and application as natural remedy. Therefore, quality control should be strictly-enforced during all the procedures, from the selection and storage of raw materials to manufacture process. Nevertheless, the existence of various forms of herbal medicinal products increases the complexity and difficulty in quality evaluation and control, which increase the possibility of adulteration or counterfeit. Therefore, the research and development to proper protocols for the application of identification characterization and evaluation of herbal medicinal products is an important subject. Thus, the work presented in this section was to develop a method for discrimination and characterization among anxiolytic products in various forms and preparation procedures. Herein, cyclic voltammograms of herbal products were employed as fingerprints acquired from the electrochemical reaction processes, which can provide lots of information both from oxidation

and reduction curves, based on the chemical properties of specific components. Furthermore, an array of electronic sensors was established for collecting information to build classification models for analysis on collected herbal calming products.

4.3.1 Preparation and selection of sensor array

For the purpose of building an ET array for herbal calming products analysis, four GEC-based electrodes were prepared initially according to the described procedure in section 3.2.1. These electrodes refer to bare GEC electrode (labelled as GEC in this text) and other three GEC-based electrodes incorporating different nanoparticles modifiers (Ni-Cu NPs, TiO_2 NPs and Ni NPs), for the sake of acquisition of broad and informative voltammetric signals. A chamomile tea bag product, sample 6 (Table 3.6, section 3.3.2) was treated as the method described in section 3.3.2, which was brewed in 250 mL boiling mineral water for 5 min and cooled to room temperature. Then the cyclic voltammograms were measured directly, without addition of any electrolyte medium, by prepared electrodes, as shown in Figure 4.26. As observed, electrodes Ni-Cu NPs, TiO_2 NPs and GEC showed more differences for voltammetric signals in terms of shapes, oxidation peaks and current intensities. Ni NPs electrode showed similar responses to GEC electrode. For ease the burden of data processing, three electrodes Ni-Cu NPs, TiO_2 NPs and GEC electrodes were selected to build a sensor array, which incorporate different nanoparticles as electrochemical catalysts for gathering wider electrochemical information. In the following measurement, sensor array composed of Ni-Cu NPs, TiO_2 NPs and GEC electrodes was used as the working electrodes in all electrochemical measurement.

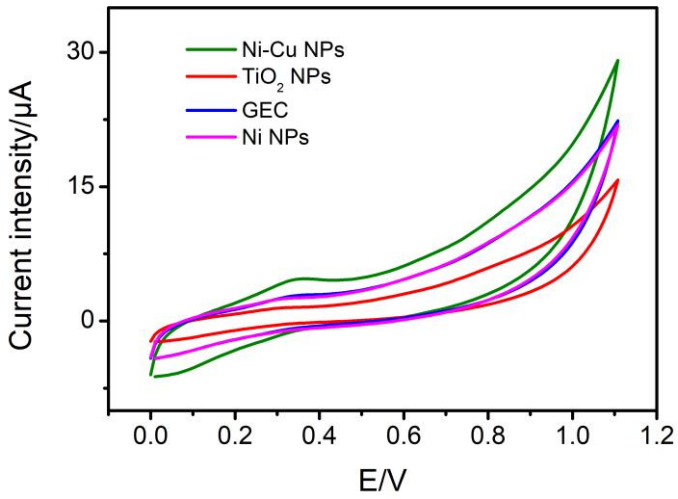

Figure 4.26 Voltammetric responses measured by electrodes Ni-Cu NPs, TiO_2 NPs, GEC and Ni NPs corresponding to sample 6 at scan rate 50 mV/s.

4.3.2 Repeatability test

Firstly, the repeatability test to the prepared electrodes was carried out. For this purpose, sample 1 (Table 3.6, section 3.3.2) was used as object and treated as the same way in the former step. Voltammetric responses were measured for 10 times using these electrodes in same condition, cycling the potential between 0 and +1.2 V at scan rate 50 mV/s. The obtained voltametric responses were shown in Figure 4.27. To keep the activity of electrodes in a mass of measurement, electrodes were rinsed using ethanol (96%) for 5 seconds and Milli-Q water after each measurement, following an electrochemical cleaning procedure. This cleaning step was carried out by cycling the potential between 0 V and +1.30 V at scan rate 50 mV/s in 0.05 mol/L KOH medium, as described in section 3.4. As observed in Figure 4.27, there were no typical differences on peak potential or peak height observed in these graphs. In addition, the RSD values were calculated based on these obtained current intensities at 0.45 V, where the oxidation occurred. These RSD values were calculated as 4.47%, 2.29% and 4.84%, corresponding to Ni-Cu NPs, TiO_2 NPs and GEC respectively, which were all smaller than 5%, indicating a good repeatability of the prepared sensors.

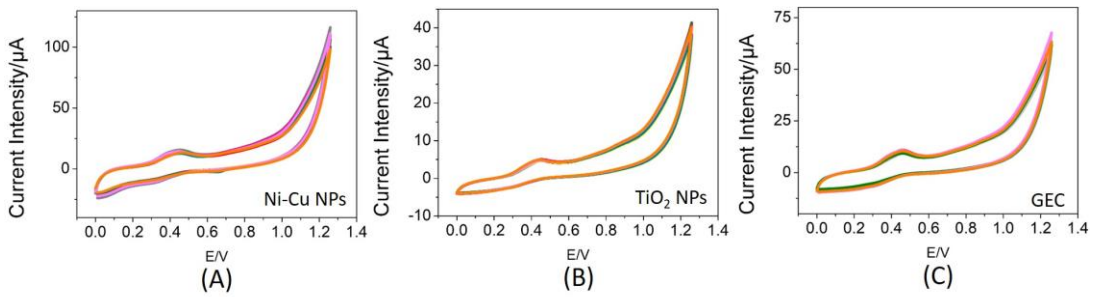

Figure 4.27 Voltammetric responses measured by electrodes Ni-Cu NPs (A), TiO_2 NPs (B) and GEC (C) to Sample 1 for 10 times at scan rate 50 mV/s.

4.3.3 Optimization of measuring condition

In this step, the medium for the electrochemical measurement was optimized. For simplicity and the sake of reflecting the nature properties of samples, the electrochemical measurement should be conducted in a convenient way, for example, using obtained infusion solution to do measurement directly. Sample 16 (Table 3.6, section 3.3.2) was treated in the same way and measured electrochemically, cycling the potential between 0 and +1.5 V at scan rate 50 mV/s, as shown in Figure 4.28 (black lines). It was observed that oxidation occurred at around +1.1 V at three electrodes with low current intensity, which could be explained by the low conductivity of the infusion solution. To improve this, this measurement was repeated after using 0.1 mol/L KCl electrolyte as medium, as shown Figure 4.28 (red lines). As can be seen, the current signals enhanced obviously and a bit of shift to lower potential occurred, which indicated an effective optimization. Note that no obvious oxidation appeared at higher potential range, from +1.25 V to +1.5 V. For saving time and protecting electrodes' lifetime by avoiding excessive currents at higher potentials, measurement would be carried out in the range from 0 to +1.25 V in 0.1 mol/L KCl medium in following measurement.

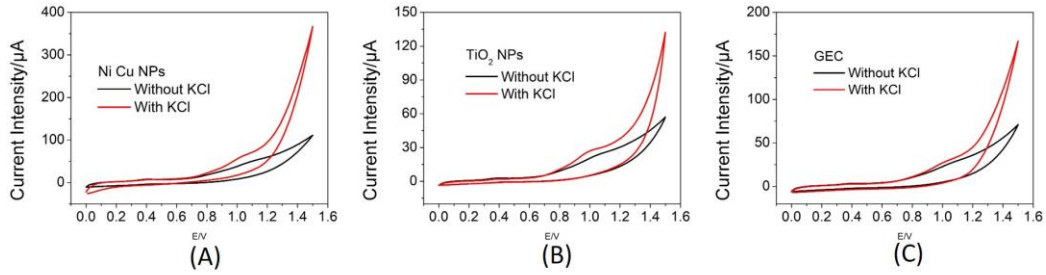

Figure 4.28 Voltammetric reponses measured by electrodes Ni-Cu NPs (A), TiO_2 NPs (B) and GEC (C) to Sample 16 with 0.1 mol/L KCl electrolyte (red lines) and without electrolyte (black lines) by cycling potential in range 0~+1.25 V. Scan rate: 50 mV/s.

4.3.4 Identification and Discrimination of herb varieties

4.3.4.1 Herbal products in same form

After the sensor array was established, its functionality was examined through the test of identifying the herb varieties of loose plant products, the products in same form and without any additive. Samples 21, 22, 23 and 24 in Table 3,6, corresponding to chamomile, passionflower, lavender and valerian plants, respectively, were smashed firstly. Then they were brewed in 250 mL boiling water and the obtained infusion solution was treated with 0.1 mol/L KCl medium for electrochemical measurement in quadruplicate. The voltammetric responses measured by the prepared electrodes were illustrated in Figure 4.29, in which the oxidation peaks of these four herbal plant products were displayed at around 0.05~0.45 V using Ni Cu NPs and GEC electrodes. In addition, oxidation and reduction processes occurred to chamomile, valerian and lavender samples could be observed in these graphs. As for the passionflower sample, there were no obvious peak signals observed. Furthermore, the oxidation signals of chamomile sample occurred at slightly higher potentials than the other herbs at Ni-Cu NPs and GEC electrodes, which may be related to flavonoids exist in chamomile of special chemical structures as antioxidants [39–41]. However, the voltammetric signals recorded by TiO_2 NPs electrode (Figure 4.29-B) showed different shapes and lower current

intensity as compared with other two electrodes.

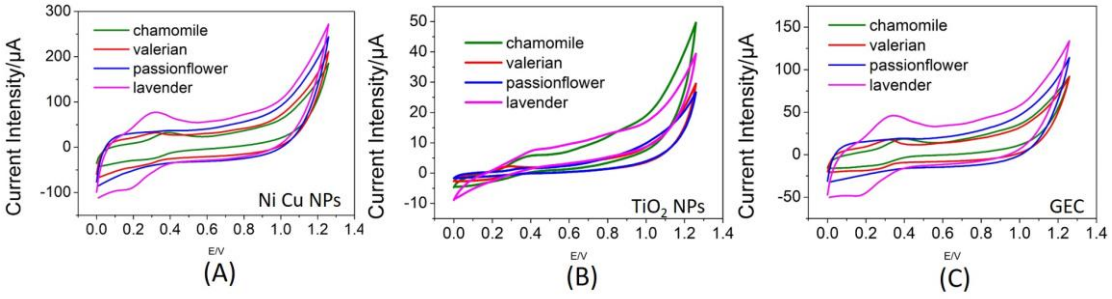

Figure 4.29 Voltammetric responses measured by electrodes Ni-Cu NPs (A), TiO_2 NPs (B) and GEC (C) to infusions of chamomile, valerian, passionflower and lavender loose plant samples in 0.1 mol/L KCl medium at scan rate 50 mV/s.

PCA was carried out using the voltammetric data as inputs, two outlier samples involved, loose plant samples of *Chrysanthemum* genus (Table 3.6, samples 29 and 30), herbs for ailments treatment in traditional Chinese therapies and also known as soothing medicinal plants [42,43]. The electrochemical measurement for these outlier samples were carried out under same condition, following the same smashing, brewing and testing sample preparation processes. The PCA result, score plot of the first two components, which explained 93% of the total variance, was shown in Figure 4.30. All samples involved were clustered in differentiated groups for each plant varieties as observed from this figure. In addition, each cluster showed compact appearance, which was contributed by satisfactory grouping and repeatability of the sensor array. As seen from the PC1 axis, the lavender class, which gave positive values, was isolated from other three herb classes. These three, chamomile, valerian and passionflower, were distinguished obviously by PC2 axis. It was worthy to note that, the outliers of chrysanthemum samples were isolated from other four groups and they were located nearly for the same variety, which means they were recognized by the electronic tongue. It was demonstrated that the prepared sensor array showed good performance in

identifying and discriminating herb varieties in same-form system, such as plant in this case, which indicated its potential application for further analysis.

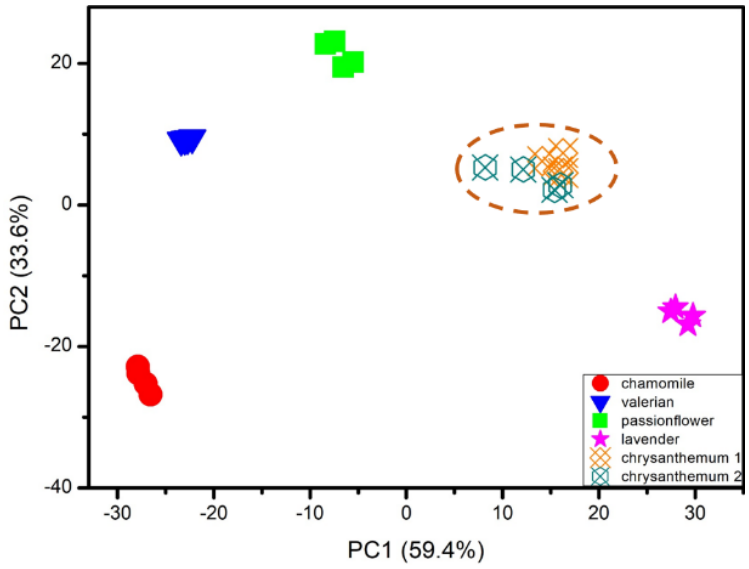

Figure 4.30 PCA result for loose plant samples of chamomile, valerian, passionflower, lavender and chrysanthemum using voltammetric data obtained by the electrode array as inputs.

4.3.4.2 Discrimination of products of different forms composed of single or complex ingredients

In the previous step, the herb varieties of those plant products (in same types) were identified and discriminated by the electronic tongue. In this step, to increase the degree of complexity, different forms of commercial products made of these four herb materials would be examined for identification. These forms considered were tea bag, loose plant, tablet, capsules and extracted liquid. Some of them were made of two or more herbs or added with some additives. 35 samples were treated and prepared for electrochemical measurement in quadruplicate and measured randomly. Voltammetric responses were measured for each sample in 0.1 mol/L KCl medium by cycling the potential between 0 V and +1.25 V at scan rate 50 mV/s. After each sample, electrochemical cleaning was conducted for eliminating pollution by sweeping the potential in range from 0 V to +1.30 V at scan rate 50 mV/s in 0.05 mol/L KOH solution. Voltammetric responses of these 35 samples obtained by the sensor array were displayed in Figure 4.31.

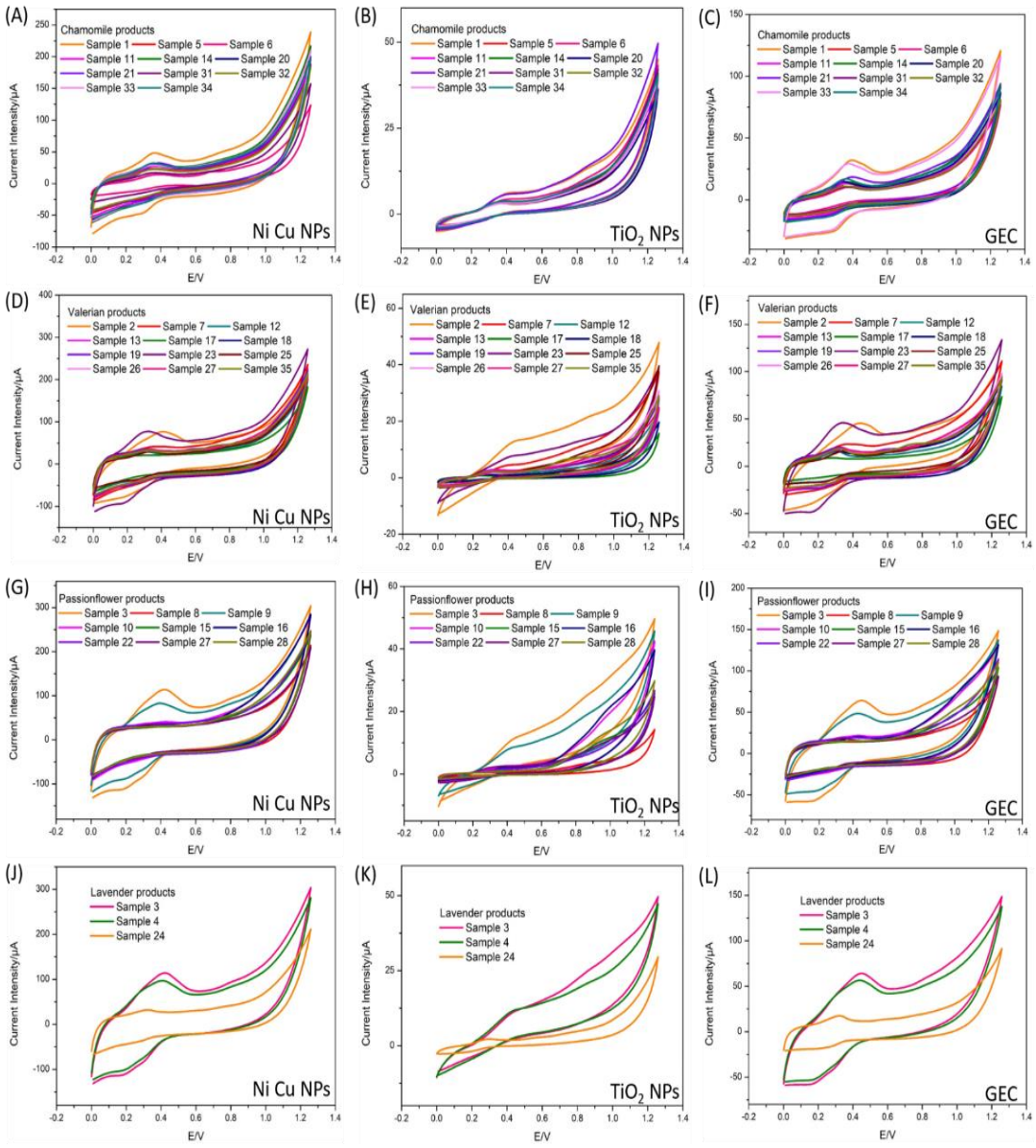

Figure 4.31 Voltammetric responses of 35 herbal products made of chamomile (A~C), valerian (D~F), passionflower (G~I) and lavender (J~L) measured by electrodes Ni-Cu NPs (A, D, G, J), TiO_2 NPs (B, E, H, K) and GEC (C, F, I, L) in 0.1 mol/L KCl medium at scan rate 50 mV/s.

Chamomile products, usually contain pure chamomile plant ingredient, are easily found in tea bag form sold in supermarkets and other shops. These chamomile tea bags can show a great variety of qualities and brands derived from their raw materials as seen from the wide range of prices. For these samples that contain pure chamomile, their voltammetric signals showed lots of similarity, e.g., shapes and oxidation peaks, which can be explained by the

similar ingredients which effected the electrochemical responses. However, sample 1, gave different signal because of the involvement of lavender and other aromatic spices (Figures 4.31 (A~C)). Furthermore, these differences in voltammetric responses derived from different brands were considered be related to the quality, origin or parts of raw herb materials (plant and/or flower). Valerian products, such as tablets and capsules, are more popular in pharmacies or healthcare product shops. Their infusion products were less than such medicinal forms. In addition, some valerian infusions were found combined with some other herbal plants or aromatic spices. As a result, the obtained electrochemical signals of those valerian-contained products gave lots of differences derived from the contents, parts and quality of plants, additives as well as brands. For example, because of the existence of melissa and other herbs, as seen from Figures 4.31 (D~F), oxidation peak of infusion sample 2 (tea bag) occurred at higher potential at these three electrodes. Similarly, oxidation occurred at around +0.4 V for passionflower samples 3 and 9 because of melissa and lavender, which were very different from that of other passionflower products, as shown in Figures 4.31 (G~I). Similar to valerian, passionflower products were easily found in tablets, capsules or extracted liquids made of its plant and/or root and their different forms contributed a lot to the differences of obtained signals. Less lavender products were found than the other three. Even some tea bags containing lavender were also combined with other herbs or additives, for example sample 3 and 4, which resulted in the signal differences from the pure lavender flowers, as shown in Figure 4.31 (J~L).

❖ Single-herb infusion products

Afterwards, PCA was employed to cluster the samples based on their main ingredients using voltametric data collected by the sensor array as inputs. To start from simplicity, infusion products (tea bags and loose plants) made of

only one herb were put to analysis firstly. A subset of voltammetric data of chamomile (10 samples), valerian (2 samples), passionflower (2 samples) and lavender (1 samples) samples were analysed by PCA, as shown in Figure 4.32, numbers in the figure representing samples corresponding to Table 3.6 in section 3.3.2. The first two principal components explained a total variance of 87.6% and these four herb varieties were clustered distinctively. The axis PC1 separated these herbs and axis PC2 discriminated the differences the interior of groups, which reflected the differences of raw materials. For instance, valerian sample 24 and 13, although in different forms, were classified into a group because of their same ingredient, valerian root. Although classified into almost sample variety according to the similar coordinate values of axis PC1, passionflower sample 22 and 16 were divided in two sub-classes by axis PC2, see those green squares in Figure 4.32, which could be explained by their different forms and/or utilization of passionflower raw materials. The discrimination for raw materials by axis PC2 was also shown in chamomile cluster, which showed a tendency that the samples made of only chamomile flower gave larger coordinate values, smaller values observed for those made of plant and flower. The four replicates of the unique lavender flower were well grouped on the very right position.

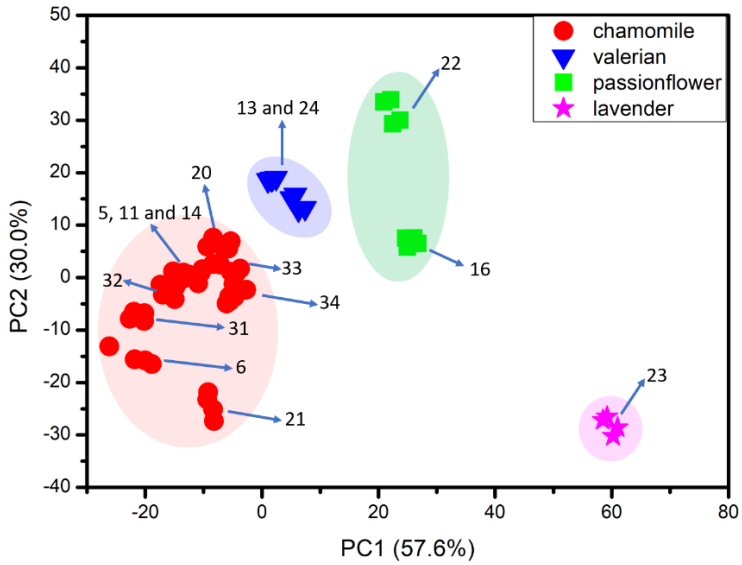

Figure 4.32 PCA result for single-herb infusion products using voltammetric signals measured by the proposed sensor array as inputs.

❖ Five forms and complex ingredients

Next, the PCA analysis was involved in more complex samples, which were in five forms, tea bag, loose plant, extracted liquid, tablet and capsule, as well as complex ingredients. Figure 4.33 displayed the score plot of the first two components, which explained 91.5% variance totally. As observed, almost all the samples were clustered correctly consistent with their main ingredient indicated by the product information although these products were in different forms. Some samples were not clustered properly because of the minority composition of the target ingredients. For instance, because of the considerable composition of melissa plant in samples 2, 3, 4 and 9, right-shift was observed compared with the original valerian, passionflower or lavender group, although such herbs could be found in their ingredients. As for sample 1, which was compose of chamomile (85.5%), lavender (5%) and some aromatic spices, was isolated from, but near to the chamomile group. Similarly, product 7 was also isolated from the valerian group because of the existence of other herb plants. In this case, the chrysanthemum was still distinguished and isolated from other four target herb groups as an outlier type, which indicated that this

electronic tongue has the ability of identifying and discriminating these target four herb varieties even in complex systems.

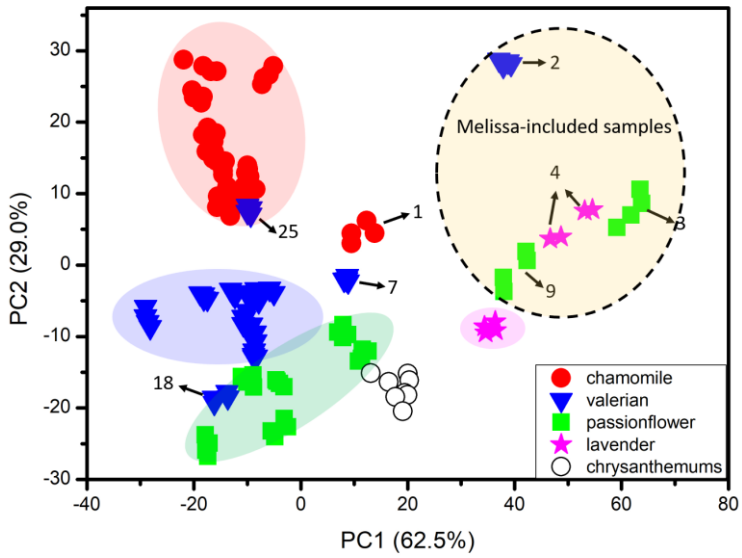

Figure 4.33 PCA result for products in five forms and of complex ingredients using the voltammetric responses measured by the proposed sensor array as inputs.

4.3.4.3 Identification of herb varieties using machine learning classification algorithms

In this step, four types of machine learning classifiers were employed, *k*-nearest neighbour (*k*-NN), support vector machine (SVM), Random Forest and Naïve Bayes, for herb variety identification in such multiclass system. In this analysis, samples 2, 3, 4 and 9 were not involved as the reason that subject herbs in these samples are of minority. Cyclic voltammograms of 31 samples were measured in quadruplicate. Therefore, a dataset composed of 124 voltammetric responses was employed as the inputs for the classifiers. The k-NN algorithm was used based on Euclidian distance for modelling. To optimize the *k* value, leave-one-out cross validation was carried out, obtained parameters were shown in Table 4.13, which indicated that *k* gave good accuracy from numbers 2~8. It was utilized as 3 in the following analysis and evaluation. To compare function of these models, their overall performance was evaluated according to

some metrics, e.g., classification accuracy, F1 score and area under the curve of receiver operating characteristic curve (AUC). The average values obtained from leave-one-out cross validation were shown in Table 4.14. As indicated, algorithms *k*-NN and SVM showed better performance on this classification system because of the higher metrics values than that of random forest or Naïve Bayes. Characteristics of each classified group, were calculated according to the confusion matrix results (Table 4.15~4.18), such as sensitivity and specificity, following equations (13) and (14), where TP, FP, TN, and FN refer to True Positive, False Positive, True Negative, and False Negative values, respectively. The calculated average values of specificity and sensitivity were shown in Table 4.14. Algorithms *k*-NN and SVM gave average values 1.000 and 1.000, respectively, which indicated their good specificity and sensitivity properties for those classified groups.

$$\text{Specificity} = \frac{\text{TN}}{\text{FP+TN}} \times 100 \quad (13)$$

$$\text{Sensitivity} = \frac{\text{TP}}{\text{TP+FN}} \times 100 \quad (14)$$

Table 4.13 Results of *k*-value optimization.

k-value	2~8	9	10	11	12
AUC	1.000	1.000	1.000	0.9997	0.9997
accuracy	1.000	0.9919	0.9758	0.9758	0.9758
F1-score	1.000	0.9919	0.9754	0.9754	0.9754

Table 4.14 Evaluation metrics obtained from leave-one-out cross validation.

models	AUC[a]	Accuracy[a]	F1 score[a]	Sensitivity[b]	Specificity[b]
k-NN (*k*=3)	1.000	1.000	1.000	1.000	1.000
SVM (linear)	1.000	1.000	1.000	1.000	1.000
Random Forest	0.9995	0.9919	0.9919	0.9943	0.9969
Naïve Bayes	--	0.7984	0.8291	0.8201	0.9411

a: Values obtained from Orange software;

b: Averages of values calculated separately for each class according to equations (13) and (14).

Table 4.15 Confusion matrix obtained from *k*-NN (*k*=3) in leave-one-out cross-validation.

		Predicted					
		Chamomile	**Valerian**	**Passionflower**	**Lavender**	**Outlier**	**∑**
Actual	**Chamomile**	44	0	0	0	0	44
	Valerian	0	44	0	0	0	44
	Passionflower	0	0	24	0	0	24
	Lavender	0	0	0	4	0	4
	Outlier	0	0	0	0	8	8
	∑	44	44	24	4	8	124

Table 4.16 Confusion matrix obtained from SVM in leave-one-out cross-validation.

		Predicted					
		Chamomile	**Valerian**	**Passionflower**	**Lavender**	**Outlier**	**∑**
Actual	**Chamomile**	44	0	0	0	0	44
	Valerian	0	44	0	0	0	44
	Passionflower	0	0	24	0	0	24
	Lavender	0	0	0	4	0	4
	Outlier	0	0	0	0	8	8
	∑	44	44	24	4	8	124

Table 4.17 Confusion matrix obtained from Random Forest in leave-one-out cross-validation.

		Predicted					
		Chamomile	**Valerian**	**Passionflower**	**Lavender**	**Outlier**	**∑**
Actual	**Chamomile**	43	1	0	0	0	44
	Valerian	0	44	0	0	0	44
	Passionflower	0	0	24	0	0	24
	Lavender	0	0	0	4	0	4
	Outlier	0	0	0	0	8	8
	∑	43	45	24	4	8	124

Table 4.18 Confusion matrix obtained from Naïve Bayes in leave-one-out cross-validation.

		Predicted					
		Chamomile	**Valerian**	**Passionflower**	**Lavender**	**Outlier**	**∑**

Actual							
	Chamomile	39	1	0	4	0	44
	Valerian	4	32	4	4	0	44
	Passionflower	0	0	16	8	0	24
	Lavender	0	0	0	4	0	4
	Outlier	0	0	0	0	8	8
	∑	43	33	20	20	8	124

4.3.5 Content evaluation for various products

Although these four are popular relaxing herbs, their products tend to be different forms on commercial market. From our observation, chamomiles flower, giving enjoyable flavour and taste, are very popular as tea bags without additives. On the contrary, lavender flowers are seldom used as infusion directly and usually need to be combined with other herbs, aromatic species or additives to adjust its flavour. Valerian and passionflower are commonly found in medicinal products, tablets, capsules and extracted liquids. Being mixed with other herbs or natural aromatic plants are common when they are used as infusion products. In this condition, the evaluation of the quality or content of such herbs used for production is harder owing to the complexity of the ingredients and forms. In this section, the content evaluation to valerian products in different forms was tried using PCA involved electronic tongue technique. 11 types of valerian mentally calming products were measured in quadruplicate and the obtained voltammetric data were employed as inputs in PCA procedure. The obtained score plot of the first two components, which explained 94.1% variance totally, were shown in Figure 4.34. Due to the involvement of various factors, e.g., different brands, different forms (capsule, tea bag, tablet, loose product and extracted liquid), raw materials (natural root, lyophilized extract of root, mixture of plant and root), different processing

methods, etc., these samples were quite dispersed on the coordinate system. Generally, axis PC1 identified the herb varieties and axis PC2 distinguished the differences among these products. As seen from PC1 axis, these products were divided into two categories by the PC1=0 line. At the left of this line, points were corresponding to products made of valerian root and those blended with other materials were on the right. From axis PC2, the detailed information on content were indicated. Central cluster was occupied by products with higher content of valerian root, such as samples 24, 13 and 35. In addition, containing similar material of lyophilized root extract, sample 26 (<43.5%) was closer to that centre than sample 17 (<18%), which could be explained by its higher content. It was demonstrated that this electronic tongue has the potential of the application of characterizing, evaluating and qualifying the properties of raw valerian material of these products.

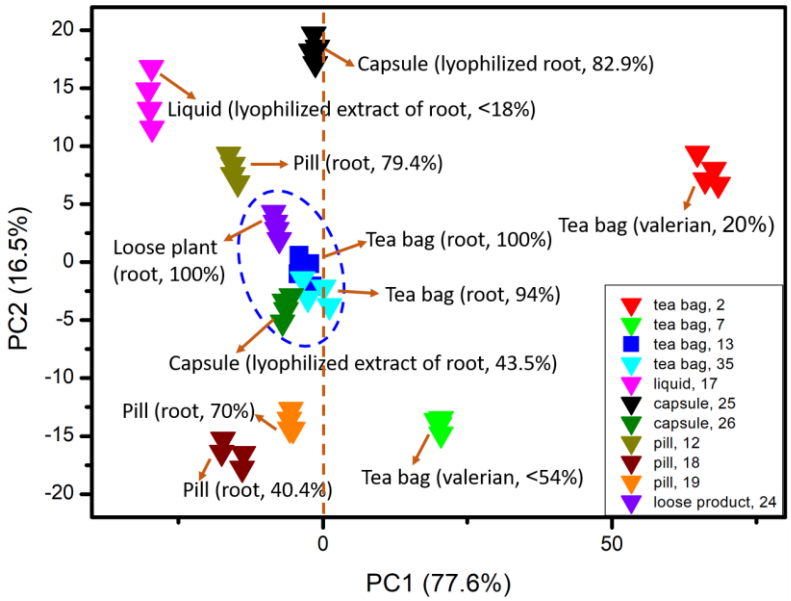

Figure 4.34 PCA result obtained from various valerian products.

Publication for Section 4.3:

Discrimination of calming herbs employing a voltammetric electronic tongue and machine learning algorithms.

Qing Wang, Clara Pérez-Ràfols, Núria Serrano, José Manuel Díaz-Cruz, Manel del Valle.

Journal of Food Engineering.

Submitted.

References

[1] F. Pena-Pereira, R.M.B.O. Duarte, A.C. Duarte, Immobilization strategies and analytical applications for metallic and metal-oxide nanomaterials on surfaces, TrAC Trends in Analytical Chemistry. 40 (2012) 90–105. https://doi.org/10.1016/j.trac.2012.07.015.

[2] T. Carchi, B. Lapo, J. Alvarado, P.J. Espinoza-Montero, J. Llorca, L. Fernández, A Nafion Film Cover to Enhance the Analytical Performance of the CuO/Cu Electrochemical Sensor for Determination of Chemical Oxygen Demand, Sensors. 19 (2019) 669. https://doi.org/10.3390/s19030669.

[3] Y. Diksy, I. Rahmawati, P.K. Jiwanti, T.A. Ivandini, Nano-Cu Modified Cu and Nano-Cu Modified Graphite Electrodes for Chemical Oxygen Demand Sensors, ANAL. SCI. 36 (2020) 1323–1327. https://doi.org/10.2116/analsci.20P069.

[4] X. Huang, Y. Zhu, W. Yang, A. Jiang, X. Jin, Y. Zhang, L. Yan, G. Zhang, Z. Liu, A Self-Supported CuO/Cu Nanowire Electrode as Highly Efficient Sensor for COD Measurement, Molecules. 24 (2019) 3132. https://doi.org/10.3390/molecules24173132.

[5] Y. Zhou, T. Jing, Q. Hao, Y. Zhou, S. Mei, A sensitive and environmentally friendly method for determination of chemical oxygen demand using NiCu alloy electrode, Electrochimica Acta. 74 (2012) 165–170. https://doi.org/10.1016/j.electacta.2012.04.048.

[6] A. Ashok, A. Kumar, F. Tarlochan, Highly efficient nonenzymatic glucose sensors based on CuO nanoparticles, Applied Surface Science. 481 (2019) 712–722. https://doi.org/10.1016/j.apsusc.2019.03.157.

[7] S.K. Meher, G.R. Rao, Archetypal sandwich-structured CuO for high performance non-enzymatic sensing of glucose, Nanoscale. 5 (2013) 2089–2099. https://doi.org/10.1039/C2NR33264G.

[8] W.J. Stepniowski, W.Z. Misiolek, Review of Fabrication Methods, Physical Properties, and Applications of Nanostructured Copper Oxides Formed via Electrochemical Oxidation, Nanomaterials. 8 (2018) 379. https://doi.org/10.3390/nano8060379.

[9] D. Giziński, A. Brudzisz, J.S. Santos, F. Trivinho-Strixino, W.J. Stępniowski, T. Czujko, Nanostructured Anodic Copper Oxides as Catalysts in Electrochemical and Photoelectrochemical Reactions, Catalysts. 10 (2020) 1338. https://doi.org/10.3390/catal10111338.

[10] J. Ambrose, R.G. Barradas, D.W. Shoesmith, Investigations of copper in aqueous alkaline solutions by cyclic voltammetry, Journal of Electroanalytical Chemistry and Interfacial Electrochemistry. 47 (1973) 47–64. https://doi.org/10.1016/S0022-0728(73)80344-4.

[11] C.R. Silva, C.D.C. Conceição, V.G. Bonifácio, O.F. Filho, M.F.S. Teixeira, Determination of the chemical oxygen demand (COD) using a copper electrode: a clean alternative method, J Solid State Electrochem. 13 (2009) 665–669. https://doi.org/COD.

[12] Understanding the Randles-Sevcik Equation: A Powerful Tool for Electrochemistry Research - Macias Sensors, (2023). https://maciassensors.com/the-randles-sevcik-equation/ (accessed July 6, 2023).

[13] M. Bonet-San-Emeterio, A. González-Calabuig, M. del Valle, Artificial Neural Networks for the Resolution of Dopamine and Serotonin Complex Mixtures

Using a Graphene-Modified Carbon Electrode, Electroanalysis. 31 (2019) 390–397. https://doi.org/10.1002/elan.201800525.

[14] W. Duan, M. Gunes, A. Baldi, M. Gich, C. Fernández-Sánchez, Compact fluidic electrochemical sensor platform for on-line monitoring of chemical oxygen demand in urban wastewater, Chemical Engineering Journal. 449 (2022) 137837. https://doi.org/10.1016/j.cej.2022.137837.

[15] M. Gutiérrez-Capitán, A. Baldi, R. Gómez, V. García, C. Jiménez-Jorquera, C. Fernández-Sánchez, Electrochemical Nanocomposite-Derived Sensor for the Analysis of Chemical Oxygen Demand in Urban Wastewaters, Anal. Chem. 87 (2015) 2152–2160. https://doi.org/10.1021/ac503329a.

[16] H. Yu, C. Ma, X. Quan, S. Chen, H. Zhao, Flow Injection Analysis of Chemical Oxygen Demand (COD) by Using a Boron-Doped Diamond (BDD) Electrode, Environ. Sci. Technol. 43 (2009) 1935–1939. https://doi.org/10.1021/es8033878.

[17] J. Wang, C. Wu, K. Wu, Q. Cheng, Y. Zhou, Electrochemical sensing chemical oxygen demand based on the catalytic activity of cobalt oxide film, Analytica Chimica Acta. 736 (2012) 55–61. https://doi.org/10.1016/j.aca.2012.05.046.

[18] H.H. Hassan, I.H.A. Badr, H.T.M. Abdel-Fatah, E.M.S. Elfeky, A.M. Abdel-Aziz, Low cost chemical oxygen demand sensor based on electrodeposited nano-copper film, Arabian Journal of Chemistry. 11 (2018) 171–180. https://doi.org/10.1016/j.arabjc.2015.07.001.

[19] C. Ma, F. Tan, H. Zhao, S. Chen, X. Quan, Sensitive amperometric determination of chemical oxygen demand using Ti/Sb–SnO2/PbO2 composite electrode, Sensors and Actuators B: Chemical. 155 (2011) 114–119. https://doi.org/10.1016/j.snb.2010.11.033.

[20] J. Li, L. Li, L. Zheng, Y. Xian, S. Ai, L. Jin, Amperometric determination of chemical oxygen demand with flow injection analysis using F-PbO2 modified electrode, Analytica Chimica Acta. 548 (2005) 199–204. https://doi.org/10.1016/j.aca.2005.05.068.

[21] T. Jing, Y. Zhou, Q. Hao, Y. Zhou, S. Mei, A nano-nickel electrochemical sensor for sensitive determination of chemical oxygen demand, Anal. Methods. 4 (2012) 1155–1159. https://doi.org/10.1039/C2AY05631C.

[22] Y.-C. Kim, S. Sasaki, K. Yano, K. Ikebukuro, K. Hashimoto, I. Karube, A Flow Method with Photocatalytic Oxidation of Dissolved Organic Matter Using a Solid-Phase (TiO2) Reactor Followed by Amperometric Detection of Consumed Oxygen, Anal. Chem. 74 (2002) 3858–3864. https://doi.org/10.1021/ac015678r.

[23] E.T.D. Nóbrega, I.T.G. de Oliveira, A.D. Viana, L.H. da S. Gasparotto, E.P. Moraes, A low-cost sensor based on silver nanoparticles for determining chemical oxygen demand in wastewater via image processing analysis, Anal. Methods. 11 (2019) 5577–5583. https://doi.org/10.1039/C9AY01755K.

[24] I. Campos, M. Alcañiz, D. Aguado, R. Barat, J. Ferrer, L. Gil, M. Marrakchi, R. Martínez-Mañez, J. Soto, J.-L. Vivancos, A voltammetric electronic tongue as tool for water quality monitoring in wastewater treatment plants, Water Research. 46 (2012) 2605–2614. https://doi.org/10.1016/j.watres.2012.02.029.

[25] H. Yu, H. Wang, X. Quan, S. Chen, Y. Zhang, Amperometric determination of chemical oxygen demand using boron-doped diamond (BDD) sensor, Electrochemistry Communications. 9 (2007) 2280–2285. https://doi.org/10.1016/j.elecom.2007.06.037.

[26] D. Dan, F. Dou, D. Xiu, Y. Qin, Chemical oxygen demand determination in environmental waters by mixed-acid digestion and single sweep polarography,

Analytica Chimica Acta. 420 (2000) 39–44. https://doi.org/10.1016/S0003-2670(00)00969-7.

[27] M. Wang, X. Cetó, M. del Valle, A novel electronic tongue using electropolymerized molecularly imprinted polymers for the simultaneous determination of active pharmaceutical ingredients, Biosensors and Bioelectronics. 198 (2022) 113807. https://doi.org/10.1016/j.bios.2021.113807.

[28] X. Cetó, M. Llobet, J. Marco, M. del Valle, Application of an electronic tongue towards the analysis of brandies, Anal. Methods. 5 (2013) 1120–1129. https://doi.org/10.1039/C2AY26066B.

[29] M. Gutiérrez-Capitán, J.-L. Santiago, J. Vila-Planas, A. Llobera, S. Boso, P. Gago, M.-C. Martínez, C. Jiménez-Jorquera, Classification and Characterization of Different White Grape Juices by Using a Hybrid Electronic Tongue, J. Agric. Food Chem. 61 (2013) 9325–9332. https://doi.org/10.1021/jf402960q.

[30] P. Ciosek, W. Wróblewski, Sensor arrays for liquid sensing--electronic tongue systems, Analyst. 132 (2007) 963–978. https://doi.org/10.1039/b705107g.

[31] M. Valle, Sensor Arrays and Electronic Tongue Systems, International Journal of Electrochemistry. 2012 (2012) 986025. https://doi.org/10.1155/2012/986025.

[32] X. Cetó, M. del Valle, Electronic tongue applications for wastewater and soil analysis, IScience. 25 (2022) 104304. https://doi.org/10.1016/j.isci.2022.104304.

[33] College of Sciences, Northeastern University, Shenyang 110819, China, Y. Ge, Electrochemical Determination of Chemical Oxygen Demand Using Ti/TiO2 Electrode, Int. J. Electrochem. Sci. (2016) 9812–9821. https://doi.org/10.20964/2016.12.05.

[34] Q. Cheng, C. Wu, J. Chen, Y. Zhou, K. Wu, Electrochemical Tuning the Activity of Nickel Nanoparticle and Application in Sensitive Detection of Chemical Oxygen Demand, J. Phys. Chem. C. 115 (2011) 22845–22850. https://doi.org/10.1021/jp207442u.

[35] N. Hao, Z. Dai, M. Xiong, X. Han, Y. Zuo, J. Qian, K. Wang, Rapid Potentiometric Detection of Chemical Oxygen Demand Using a Portable Self-Powered Sensor Chip, Anal. Chem. 93 (2021) 8393–8398. https://doi.org/10.1021/acs.analchem.1c01863.

[36] Q. Wang, X. Cetó, M. del Valle, Quantitative Estimation of COD Values from an Array of Metal Nanoparticle Modified Electrodes and Artificial Neural Networks, Chemosensors. 10 (2022) 504. https://doi.org/10.3390/chemosensors10120504.

[37] D. Benke, A. Barberis, S. Kopp, K.-H. Altmann, M. Schubiger, K.E. Vogt, U. Rudolph, H. Möhler, GABAA receptors as in vivo substrate for the anxiolytic action of valerenic acid, a major constituent of valerian root extracts, Neuropharmacology. 56 (2009) 174–181. https://doi.org/10.1016/j.neuropharm.2008.06.013.

[38] S. Akhondzadeh, H.R. Naghavi, M. Vazirian, A. Shayeganpour, H. Rashidi, M. Khani, Passionflower in the treatment of generalized anxiety: a pilot double-blind randomized controlled trial with oxazepam, Journal of Clinical Pharmacy and Therapeutics. 26 (2001) 363–367. https://doi.org/10.1046/j.1365-2710.2001.00367.x.

[39] A.N. Panche, A.D. Diwan, S.R. Chandra, Flavonoids: an overview, Journal of Nutritional Science. 5 (2016) e47. https://doi.org/10.1017/jns.2016.41.

[40] A. Marino, M. Battaglini, N. Moles, G. Ciofani, Natural Antioxidant Compounds as Potential Pharmaceutical Tools against Neurodegenerative Diseases, ACS Omega. 7 (2022) 25974–25990. https://doi.org/10.1021/acsomega.2c03291.

[41] X. Zhang, C. Wu, In Silico, In Vitro, and In Vivo Evaluation of the Developmental Toxicity, Estrogenic Activity, and Mutagenicity of Four Natural Phenolic Flavonoids at Low Exposure Levels, ACS Omega. 7 (2022) 4757–4768. https://doi.org/10.1021/acsomega.1c04239.

[42] D.-C. Hao, Y. Song, P. Xiao, Y. Zhong, P. Wu, L. Xu, The genus Chrysanthemum: Phylogeny, biodiversity, phytometabolites, and chemodiversity, Front Plant Sci. 13 (2022) 973197. https://doi.org/10.3389/fpls.2022.973197.

[43] C. Meneses, M. Valdes-Gonzalez, B.B. Garrido-Suárez, G. Garrido, Systematic review on the anxiolytic and hypnotic effects of flower extracts in in vivo pre-clinical studies published from 2010 to 2020, Phytother Res. 37 (2023) 2144–2167. https://doi.org/10.1002/ptr.7830.

CHAPTER 5 CONCLUSIONS AND PROSPECTS

5 Conclusions and prospects

5.1 Conclusions

In this thesis, three voltammetric ETs were established aiming at applications of COD determination or analysis of anxiolytic herbal medicinal products. Sensors utilized for constructing these ETs were fabricated in laboratory and were classified as two categories. One was fabricated using graphite as substrate and metallic nanoparticles were involved into the composite combined with epoxy. The nanoparticles were Ni-Cu alloy, Ni, Cu, CuO and TiO_2, which were used as catalysts for electrochemical reaction occurred between the electrodes and research targets. The other one was composed of two electrodes based on Cu block, which was modified at the surface by filming nano CuO through an electrodeposition procedure. The copper-based electrode was chosen for COD determination because its powerful electrocatalyst function in alkaline media for oxidizing some organic substances. Two ETs were established in the researched on the analysis of

organic pollution in wastewater, one carried out measurement from qualitative evaluation to organic pollutants and the other one was tried to determinate COD values through a novel way, artificial neural network model. The promoted performance of the proposed ET combined with ANN model compared with classic calibration line method presented in this text demonstrated its feasibility and promising prospect in this field. In addition, an ET array constructed by three graphite-based electrodes was devoted to the analysis of anxiolytic medicinal products, such as pills, capsules, tea bags, loose plants and extracted liquids, which were made of herbs chamomile, passionflower, valerian and lavender. This ET showed good applicability in distinguishing herb varieties among products in same forms. What's more, the evaluation to the content of raw herb materials and the herb discrimination could be achieved with this ET even in complex sample system. In the former chapters, the experiments and results were illustrated briefly, some more specific and conclusive points would be summarized in terms of these two topics as following.

- **Topic 1, Organic pollution evaluation and COD determination utilizing ETs combined with PCA and ANN algorithms.**

  I. Electrochemical deposition method was demonstrated useful for surface modification at copper-based sensors, which showed good electrochemical activity in alkaline condition for analyzing some organic substances based on voltammetric techniques. The electrodes prepared according to this method devoted good detection limit and linear range when employed for COD value determination by classic calibration line method.

  II. Electrodes prepared, graphite-epoxy composite (GEC) electrodes and electrodeposited copper-based electrodes, showed good

repeatability and stability, which could afford all the measurement carried out during the research.

III. The first electronic tongue array was constructed by GEC-based electrodes Cu NPs, CuO NPs, Ni-Cu NPs and electrodeposited copper-based electrode NfCuO/Cu. This ET involved PCA procedure using voltammetric signals as inputs collected by the members in the array responding to COD standard substances of different difficulty levels of degradation in electrochemical procedure, which could help evaluate the levels of organic pollution and the accuracy of the COD values calculated based on the calibration equation obtained by electrode NfCuO/Cu individually.

IV. The second electronic tongue array was constructed by five electrodes, GEC-based electrodes Cu NPs, CuO NPs, Ni-Cu NPs, Ni NPs and electrodeposited copper-based electrode CuO/Cu. An artificial neural network model was built using two COD substances, glucose and glycine, as analytes simulating the organic pollutants. The ET combined with ANN method showed positive promotion compared with classic calibration equation method and the detected COD values were assessed with reference method, which employed commercial COD test reagent.

☞ **Topic 2, discrimination and identification of anxiolytic herbal medicinal products in various forms.**

I. A bare GEC electrode and nanoparticles modified GEC-based electrodes Ni-Cu NPs and TiO_2 NPs were demonstrated good repeatability and stability and the measuring condition were optimized by employing 0.1 mol/L KCl solution as the medium for

cyclic voltammetric measurement.

II. The electronic tongue array constructed these three electrodes was able to discriminate herbs of chamomile, valerian, passionflower, lavender and outliers (chrysanthemum) among their loose plant products from PCA procedure using cyclic voltammetric responses to these sensors as the inputs.

III. In addition, ingredients of products in various forms could be identified based on this ET and PCA even in complex systems composed of five forms of products, such as pills, capsules, loose plants, tea bags and extracted liquids.

IV. The automated machine learning algorithms, k-NN and SVM showed good performance for the classification to these multiform products using CVs as the dataset.

V. This electronic tongue was demonstrated good behaviour for qualification, characterization and evaluation of valerian raw material in analysing various valerian products, indicating its good potential in the application of aiding quality control.

5.2 Prospects

As discussed above, many profitable merits were achieved from the research and results presented. The ET combined with ANN technique provides us a novel idea in analysing organic pollution in wastewater. The voltammetric ET was able to identify the herb varieties as well as aid the quality evaluation of commercial products. Nevertheless, these achievements are little steps in their fields. Lots of difficulties need to be overcome to get efficient improvement and development. Some ideas would appear upon looking back and rethinking on these experiments. Herein, some points of view for prospective development based on these years' experiences were described.

Although the advantages such as easy operation, rapidness and environment friendliness, electrochemical methods of COD determination are facing some challenges. The most important one is the achievement of full oxidation of organic pollutants. Because of the unknown complexity of components and contents of organic pollution, the truth of whether the sensors could response to all of them can affect the accuracy of found COD values, which are usually calculated based on the collected signals in electrochemical procedure. The efficiency of electrochemical oxidation of organics were not explored or tested for their application into more complex wastewater systems containing organic pollutants that hard to be oxidized. In addition, the reaction mechanism and resulting reaction products can depend on the sensor material and its structure in practical application. Therefore, the selection of base material, the electro-catalyst and the fabrication method can have a significant impact on the construction of an electrochemical COD sensor. In this sense, some materials or catalysts with powerful electro-catalytic activity are more prospective in terms of larger efficiency of electrochemical oxidation of organics. In our ongoing research, some novel nanomaterials, such as nanocubes composed of copper or palladium nanoparticles as well as gold nanoparticles are involved in sensors construction. In addition, the electrochemical anodization method is a cheap and efficient way of modify sensors. The optimization of anodization procedure and characterization of formed nanostructures are interesting topic for further function improvement.

PCA can be used for evaluating organic pollution towards wastewaters. More wastewater samples need to be measured to get more specific and detailed information from PCA model to provide complementary and useful information for practical pollution evaluation. ANN model is a good candidate approach for COD determination, which should be improved by involving more standard substances to meet the demand of complex organic pollution.

The electronic tongue technique showed good potential in authentication and evaluation of anxiolytic herbal products made of ingredients of chamomile, valerian, passionflower or lavender. In addition, some extra information targeting the quality or origin of herb raw material can be captured in further experiments by managing the samples and optimizing electrochemical measurement.

ANNEX: PUBLICATIONS